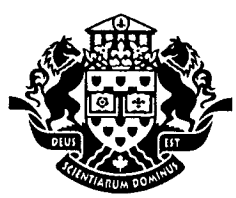

Université d'Ottawa · University of Ottawa

Université d'Ottawa · University of Ottawa

FACULTÉ DES ÉTUDES SUPÉRIEURES ET POSTDOCTORALES

FACULTY OF GRADUATE AND POSTDOCTORAL STUDIES

Marie-Soleil GIGUÈRE

AUTEUR DE LA THÈSE - AUTHOR OF THESIS

M.Sc. (Chemistry)

GRADE - DEGREE

Department of Chemistry

FACULTÉ, ÉCOLE, DÉPARTEMENT - FACULTY, SCHOOL, DEPARTMENT

TITRE DE LA THÈSE - TITLE OF THE THESIS

Sequencing Synthetic Copolymers Using Electrospray Ionization Mass Spectrometry

P. Mayer

DIRECTEUR DE LA THÈSE - THESIS SUPERVISOR

M. Dubé

CO-DIRECTEUR DE LA THÈSE - THESIS CO-SUPERVISOR

EXAMINATEURS DE LA THÈSE - THESIS EXAMINERS

P. Sundararajan

D. Fogg

J.-M. De Koninck, Ph.D.

LE DOYEN DE LA FACULTÉ DES ÉTUDES SUPÉRIEURES ET POSTDOCTORALES

SIGNATURE

DEAN OF THE FACULTY OF GRADUATE AND POSTDOCTORAL STUDIES

SEQUENCING SYNTHETIC COPOLYMERS USING ELECTROSPRAY IONIZATION MASS SPECTROMETRY

Marie-Soleil Giguère

Thesis submitted to the
School of Graduate Studies and Research
University of Ottawa
In partial fulfillment of the requirements for the
M.Sc. degree in the

Ottawa-Carleton Chemistry Institute

Thèse soumise à
L'École des études supérieures et de la recherche
Université d'Ottawa
En vue de l'obtention de la maîtrise ès sciences à

L'Institut de chimie d'Ottawa-Carleton

July 2003

Candidate	Supervisor
Marie-Soleil Giguère	Paul M. Mayer
	Marc A. Dubé

Your file Votre référence
ISBN: 0-612-90074-6
Our file Notre référence
ISBN: 0-612-90074-6

«L'essentiel est invisible pour les yeux,
On ne voit bien qu'avec le cœur»

Antoine de Saint-Exupéry, Le Petit Prince.

Abstract

The dissociation of gas-phase synthetic homopolymers poly(butyl acrylate) (PBA), poly(methyl methacrylate) (PMMA) and poly(vinyl acetate) (PVAc) ionized by Li^+ or Na^+ was investigated by electrospray-ionization tandem mass spectrometry. Based on these results it was possible to use tandem mass spectrometry to sequence three copolymers produced by free radical polymerization (PBA/PVAc, PBA/PMMA and PMMA/PVAc). In the case of PVAc containing copolymers, tandem mass spectrometry yielded partial sequence information including the number of VAc monomers and consecutive BA or MMA monomers while the complete sequence (and mixture of sequences) could be deduced for PBA/PMMA.

The poly(vinyl acetate) ions lose acetic acid molecules from the polymer side chain, and ultimately metal acetate, to form a polyene with a positive charge on the carbon backbone while PBA and PMMA fragment along the polymer backbone. An extensive study was made of the dissociation characteristic of PVAc. Collision-induced dissociation (CID) was performed at different center-of-mass collision energies to study the sequential appearance of the fragment ions. Molecular mechanics/molecular dynamics (MM/MD), Hartree-Fock, semi-empirical and density functional calculations were employed to model the lowest energy dissociation processes.

Acknowledgements

Je remercie du fond du cœur mon superviseur Prof. Paul Mayer pour son appui, son enthousiasme et la confiance qu'il m'a accordé. Grâce à sa patience et ses conseils j'ai pu mener à bien ce projet.

Merci à « big Clem » pour son aide avec l'électrospray, à Prof. Holmes et Sander pour le partage de leurs connaissances. Merci à mes collègues de travail, par leur présence ils ont fait de mes études de maîtrise une expérience très agréable. Merci à « petit Clem » et à Darren pour les discussions intéressantes. J'ai vraiment apprécié le temps passé avec les filles : Julie, Janeen, Emma, Xian, Erica, Danielle et Mélanie.

Merci à mon cosuperviseur Prof. Marc Dubé et à ces étudiants Renata et Hong pour leur collaboration. Les Profs. St-Amant et Barriault ainsi que leur groupe respectif (principalement Delphine, Étienne, Danny, Ross et Louis) ont toujours été disponibles et sympathiques, merci pour leurs conseils et leur amitié.

Finalement, merci infiniment à ma famille, spécialement à ma mère et mon père, bien que je les aie parfois délaissés durant les deux dernières années, j'ai toujours eu conscience de l'appui qu'ils me donnaient. Merci à mes amis Julie, Patrick et Ghislain pour m'avoir aidé à garder le sourire. Merci surtout à Louis pour son amour et sa tendresse, sans toi rien ne serait pareil.

Table of Contents

List of Figures

List of Tables

List of Abbreviations

AcH	Acetic acid
AcLi	Acetic lithium
AcNa	Acetic sodium
AIBN	Azodiisobutyronitrile
AM1	Austin Model 1
B3-LYP	Becke-style three parameter density functional theory using the Lee, Yang and Parr correlation function
BA	n-Butyl acrylate
Bu	Butene
CI	Chemical ionization
CID	Collision-induced dissociation
CTA	Chain transfer agent
Da	Dalton
DC	Direct current
DFT	Density functional theory
EI	Electron impact
ESI-MS	Electrospray ionization mass spectrometry
ESI-MS/MS	Electrospray ionization tandem mass spectrometry
FAB	Fast atom bombardment
GPC	Gel permeation chromatography
GTO	Gaussian type orbitals

HF	Hartree theory
IH	Isobutyronitrile
In	Initiator
IR	Infra-red spectroscopy
KS	Kohn-Sham
LC-MS	Liquid chromatography mass spectrometry
LS	Light scattering
m/z	Mass-to-charge ratio
MALDI	Matrix assisted laser desorption-ionization
MM/MD	Molecular mechanics/molecular dynamics
MMA	Methyl methacrylate
$\overline{M}_n$	Number-average molecular weight
$\overline{M}_w$	Weight-average molecular weight
NMR	Nuclear magnetic resonance
NVT	Mole, volume and temperature
PBA	Poly(n-butyl acrylate)
PD	Polydispersity
PEG	Poly(ethylene glycol)
PMMA	Poly(methyl methacrylate)
PPG	Poly(propylene glycol)
PS	Poly(styrene)
PVAc	Poly(vinyl acetate)
Py/GCMS	Pyrolysis gas chromatography mass spectrometry

RF	Radio frequency
SCF	Self-consistent field method
SIMS	Secondary ions mass spectrometry
STO	Slater type orbitals
TOF	Time-of-flight
U	Direct current
UV	Ultraviolet
VAc	Vinyl acetate

Chapter One

INTRODUCTION TO THE CHARACTERIZATION OF SYNTHETIC POLYMERS

A polymer is a molecule of large molecular weight built up by the repetition of small units (monomers). The chain can be linear or branched to form a three-dimensional network. Random and block copolymers are common materials and millions of tons are produced every year around the world. A large variety of polymers are produced by nature. Rubber is a natural polymer which is a high molecular weight polyisoprene with a *cis*1,4-configuration as shown in Figure 1.1. Natural rubber is obtained from a latex contained in the tree *Hevea*. Other examples of natural polymers are cellulose (poly[(1-4)-β-D-glucose) (Figure 1.2) and biopolymers like proteins and DNA.

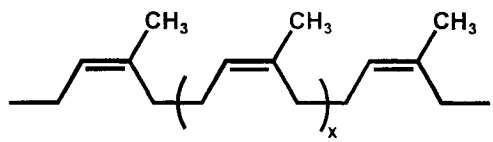

Figure 1.1 Structure of natural rubber.

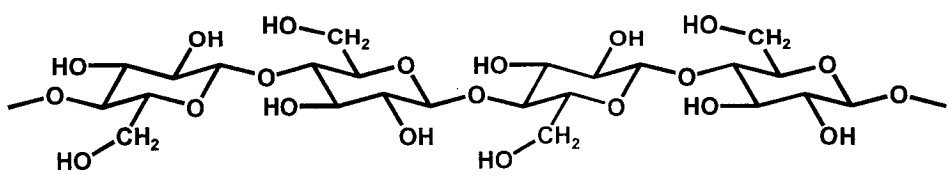

Figure 1.2 Structure of cellulose.

Synthetic polymers represent a large commercial interest. They are typically mixtures of oligomers having a variety of chain-lengths and chemical compositions. This range of chemical compositions (including chain end groups) and dispersity of chain-lengths are responsible for the final material properties. By copolymerization it is possible to produce a material with adjustable mechanical properties. By adding a second monomer to a polymer, it is possible to convert a rigid material to an elastic and rubbery product. It is possible to control the degree of crytallinity of the new material in order to adjust its toughness.

1.1 Techniques for polymer characterization[1]

The characterization of homopolymers and copolymers is composed of several aspects:

- molecular weight and polydispersity (PD),
- configuration and conformation of the repeat units (monomers)
- identification of the chain end groups
- chain branching
- molar fraction of each component (in the case of copolymers)
- identification of the variation of the copolymer composition as the chain grows (also call composition drift)

The average molecular weight and the molecular weight distribution are usually determined using light scattering (LS) or gel permeation chromatography (GPC). The average molecular weight of polymer is defined by two variables, the number-average molecular weight ($\overline{M}_n$) and the weight-average molecular weight ($\overline{M}_w$):

$$\overline{M}_n = N_i M_i / N_i \qquad \overline{M}_w = N_i M_i^2 / N_i M_i \qquad 1.1$$

where M_i is the molecular weight of a chain of length i monomers units and N_i is the number of moles of a chain of length i monomers units.

LS has been used to determined molecular weights from 10 000 to 10 000 000 Da by measuring the scattered light from a polymer solution. The intensity of the scattering depends on the mass of the particles. In GPC, individual polymer molecules are separated according to their hydrodynamic volumes. With the appropriate calibration, GPC can be used to determine the molecular weight of a polymer ($\overline{M}_n$ and $\overline{M}_w$) according to the retention time of the compounds. The traditional detection technique for GPC is refractive index detection but it does not give information related to the sequence of copolymers and their chemical composition.

For structural analysis of polymer samples (determination of the repeat units), nuclear magnetic resonance (NMR) and infrared spectroscopy (IR) are common tools. Knowing the characteristic chemical shifts or absorption band for monomers, the chemical composition of the polymer can be identified. Van den Eynde et al.[2] studied the

composition of random poly(methyl methacrylate/styrene) copolymer by X-ray photoelectron spectroscopy and secondary ion mass spectrometry.

Pyrolysis gas chromatography mass spectrometry (PyGC/MS) is used to determine the composition of a polymer. The first work on off-line PyGC of polymer was presented by Davison in 1954.[3] The application of on-line PyGC to polymers came in 1959 by three different groups.[4-6] PyGC/MS consist of a pyrolyzer where 10 to 100 μg of polymer are pyrolysed at 400-600 °C using a catalytic or reactive reagent with an inert carrier gas. The pyrolyzer is connected to a gas chromatograph coupled with a quadrupole mass filter with either an electron impact or chemical ionization source. Typical problems observed by PyGC are: difficult specific pyrolysis, poor chromatographic separation of the degradation product and difficulties in the identification and interpretation of the pyrolysis products. The improvement of GC columns and the coupling with a mass spectrometer partially solved these problems. PyGC/MS has a disadvantage over GPC, LS, IR and NMR in that it is a destructive analytical technique requiring relatively large amounts of sample.

1.2 Review of the mass spectrometry of polymers

Mass spectrometry represents a growing technique in polymer characterization because of the information that can be obtained by recording both the polymer mass

spectrum and the tandem mass spectrum. An excellent review of the analytical tools for the analysis of copolymers by mass spectrometry has been presented by Montaudo.[7] Scrivens and Jackson[8] and Murgasova and Hercules[9] have also published reviews of polymer analysis by mass spectrometry.

Different mass spectrometric techniques have been applied to polymer analysis with more or less success. Electron impact (EI) and chemical ionization (CI) mass spectrometry generally do not provide molecular weight information about the polymer due to thermal decomposition when the sample is heated. Softer ionization techniques that do not require thermal volatilization such as secondary ion mass spectrometry (SIMS) and fast atom bombardment (FAB) were the first widely successful methods applied to polymer analysis. The development of matrix assisted laser desorption-ionization (MALDI)[10, 11] in 1988 was a major step forward for the implementation of polymer analysis by mass spectrometry. Because of the pulse nature of laser desorption-ionization, MALDI is normally coupled with a time-of-flight (TOF) mass analyser. TOF has in theory no upper mass limit so it is possible to analyse molecular ions of 300 kDa using MALDI/TOF.[12] The development of electrospray ionization (ESI)[13-15] in 1984 was also an improvement in this field because ESI represents an interface for the coupling of liquid chromatography and mass spectrometry (LC-MS) which allow direct coupling of GPC and MS for on-line analysis. Another advantage of ESI is the production of multiply charged ions; it allows the analysis of largest species because of the small mass-to-charge ratio (m/z) obtained. ESI is normally coupled with a conventional mass

analyser such as quadrupole filter or ion trap. ESI will be discussed in more detail in Chapter 3.

When the polydispersity ($\overline{M}w / \overline{M}n$) of the sample is larger than 1.2 the molecular weight obtained by MALDI[8, 16] and ESI[16, 17] tend to be lower than the GPC value. GPC has been coupled with mass spectrometry in order to accurately determine the molecular weight distribution without calibration of the liquid chromatography system, and in this case, the relatively narrow distributions of polymers from GPC can be accurately analysed by mass spectrometry.

1.3 Sequencing efforts

The determination of the sequence of copolymers is important since it can affect the final properties of the material. The solubility of a random copolymer may be low in a solvent that can dissolve one of the constituent homopolymers but can be increased when a mixture of two solvents is used. The solubility of a block copolymer may be very high, especially when the two components have different polarities. By example, a block copolymer of poly(styrene) and poly(vinyl alcohol) is soluble in water, acetone and benzene.[1]

As mentioned earlier, ^{1}H and ^{13}C NMR can be used to characterize the chemical structure of the repeat units of a polymer and the short range tacticity. However, it is only able to yield average results for an entire polydisperse mixture. Short sequences of

monomers in a copolymer can be obtained by NMR from a monodisperse sample with constant composition.

The fragmentation pattern of homopolymers must be studied in order to sequence copolymers by mass spectrometry. Collision-induced dissociation (CID) mass spectrometry permits the structure or the sequence of the polymer to be determined. The fragmentation patterns for a variety of polymers have been studied and are often assigned to backbone cleavage along the polymer chain.

Jackson and Scrivens studied the high energy collision-induced dissociation of poly(methyl methacrylate) (PMMA)[18-22] generated by matrix-assisted laser desorption/ionization-time of flight (MALDI-TOF). They observed two main progressions of distonic ions formed by homolytic cleavage of the polymer backbone from both ends of the polymer. As shown in Scheme 1.1, cleavage occurs next to the tertiary carbon of the polymer backbone. The resulting fragment ion m/z depends on which fragment retains the cation. Minor products due to 1,5 hydrogen rearrangements were also observed to occur from both ends of the polymer. Proposed mechanisms for homolytic cleavage and 1,5 hydrogen rearrangement are shown in Figures 1.3 and 1.4.

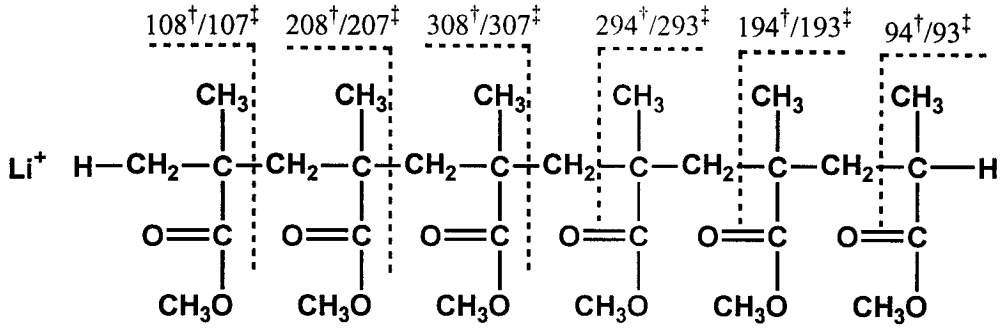

Scheme 1.1: CID fragmentation pattern of poly(methyl methacrylate) Li^+. "†" is formed by homolytic cleavage, "‡" is formed by 1,5 hydrogen rearrangement.

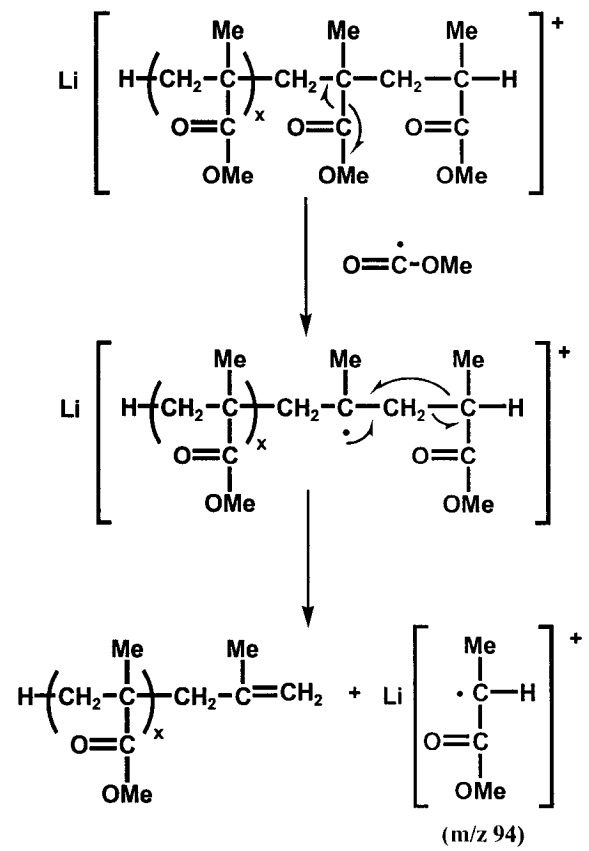

Figure 1.3: Proposed fragmentation mechanism for homolytic cleavage of PMMA.

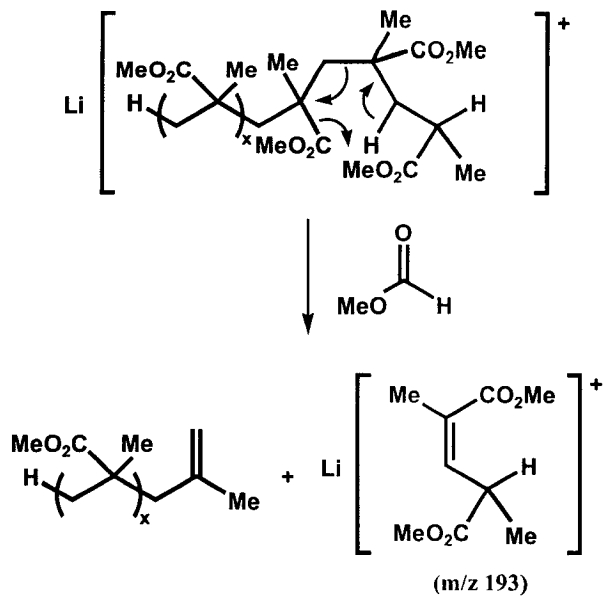

Figure 1.4: Proposed fragmentation mechanism for the 1,5 hydrogen rearrangement in PMMA.

Molecular modeling of the gas phase structure of PMMA ionized with Na^+ showed that the oligomers adopt a closed-loop shape with the ester side chains of the polymer complexing the metal cation.[22] The analysis of PMMA shows that the loss of the metal cation and backbone fragmentation are in competition during the fragmentation. For smaller metal cations, the loss of the cation is not significant for either large and small oligomer chains. When the size of the metal cation increases, the bare cation becomes the most abundant fragment ion. This is related to the binding energy of the cation to PMMA. Cs^+ is bounded by a lower energy to PMMA than Li^+ so the loss of Cs^+ is more energetically possible. Bowers et al.[23] explained the importance of small oligomer fragments by backbone fragmentation. Assuming a quasi-cyclic structure (from molecular modeling) they proposed two mechanisms. In the first one (Figure 1.5), after the activation, the quasi-cycle opens by dissociation of one end of the oligomer chain

from the metal ion. Then, dissociation of the cation or backbone cleavage may occur. In the second mechanism, the quasi-cycle opens by dissociation in the oligomer chain (Figure 1.6).

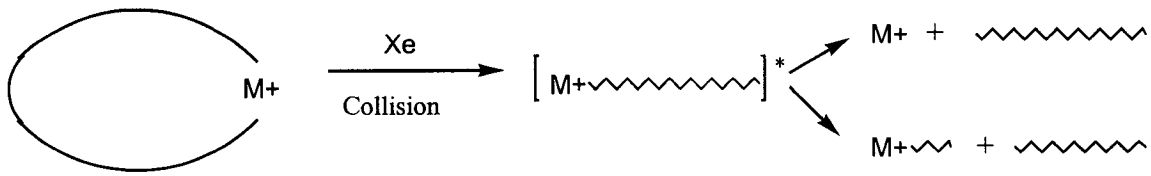

Figure 1.5: First mechanism for the loss of metal ion and backbone fragmentation

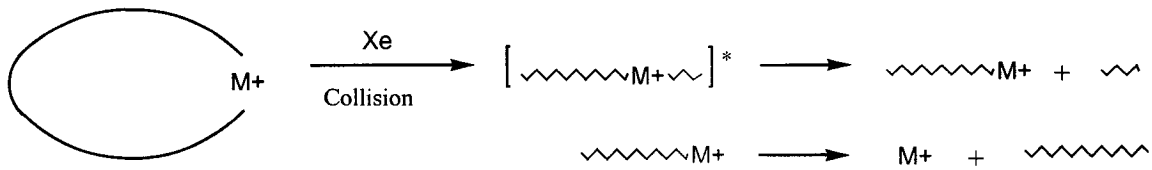

Figure 1.6: Second mechanism for the loss of metal ion and backbone fragmentation

The second mechanism is unlikely to happen. M^+ is formed by a two step process composed of the loss of a neutral fragment and dissociation of M^+. Usually sequential processes give minor products and from the spectral data, M^+ loss is a major fragmentation pathway. The second mechanism does not explain the formation of small oligomer fragments. For energetic reasons the metal ion should remain with the longer chain. With the first mechanism, after the opening of the cycle losses of M^+ or of metal ion bounded to oligomer are in competition. To explain the importance of small oligomer fragments observed experimentally, it was proposed that the dissociation by backbone cleavage happens close to the metal ion in the chain.

Scrivens and Jackson also studied the fragmentation of ionized poly(styrene) (PS)[21, 24-26] and its gas phase conformation.[27] Closely related mechanisms have been proposed for its fragmentation with polymer backbone fragmentation observed to occur by homolytic cleavage and 1,5 hydrogen rearrangements. The gas phase structure of the PS ion shows coordination of the metal by the phenyl rings on the side chain of the polymer. Unlike ionized PMMA, the structure of ionized PS is close to linear with the metal cation lying between two phenyl rings in the middle of the polymer backbone.

This trend in fragmentation along the polymer backbone extends to more polar polymers such as poly(3-hydroxybutanoic acid) ionized with a potassium or sodium cation[28] and polyols such as poly(ethylene oxide) and poly(propylene oxide) ionized with silver.[29] Selby et al.[30] have shown that low energy CID of poly(ethylene glycol) (PEG) ionized with an alkali metal cation yields metal cations and small fragments from H rearrangement reactions. At higher collision energies, 1,4-H_2 eliminations are observed producing two types of unsaturated fragment ions along with some homolytic cleavages at either end of the polymer (Figure 1.7). Bottrill et al.[31] and Jackson et al.[21] also observed the presence of these three progressions. Gidden et al.[32] modeled the gas phase conformation of PEG and poly(propylene glycol) (PPG) and as it was observed for PMMA the polymer surrounds the metal allowing the oxygen atoms on the backbone to coordinate the cation.

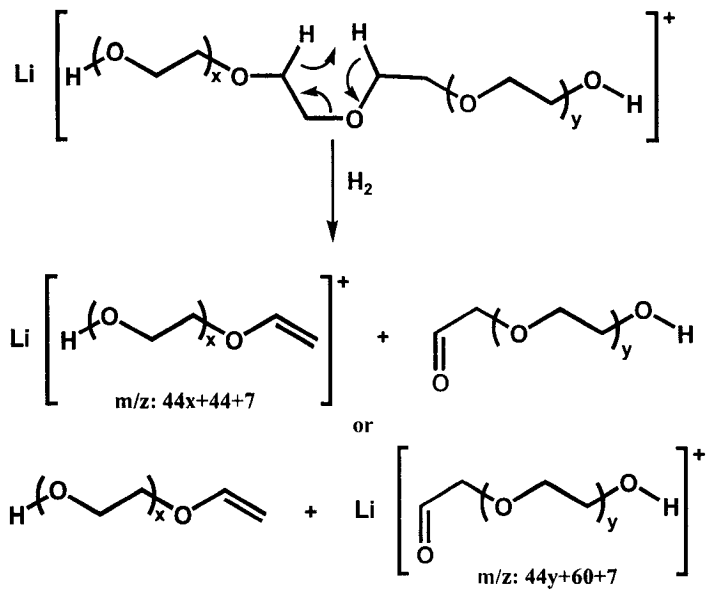

Figure 1.7: Proposed fragmentation mechanism for 1,4-H_2 elimination in PEG.

Sequencing of commercial diblock and triblock copolymers of poly(ethylene glycol) and poly(propylene glycol) has been done by Cerda et al.[33] The polar copolymers were ionized by protonation and fragmented by collisional-induced dissociation and electron capture dissociation. The authors studied polymers of low molecular weight and they were able to identify the complete sequence of the polymer.

Sequencing of proteins by mass spectrometry is usually preceded by cutting the protein backbone at specific places using various enzymes for digestion into peptides. The same approach can be applied to polymer sequencing using saponification, aminolysis, hydrolysis and pyrolysis of the polymer in order to reduce the chain lengths.[7]

In this study the fragmentation of ionized PMMA, poly(butyl acrylate) (PBA) and poly(vinyl acetate) (PVAc) from ESI-MS and ESI-MS/MS was investigated in order to

use tandem mass spectrometry to sequence three copolymers produced by free radical polymerization (PBA/PVAc, PBA/PMMA and PMMA/PVAc). Butyl acrylate and vinyl acetate are copolymerized for the fabrication of adhesives and sealants related to the paper, textile and wood industry. Methyl methacrylate is a component of acrylic latex paint and lubricating oil. It is also used in the fabrication of shatterproof glass and contact lenses because of its light transmission and biocompatibility properties.

References

(1)Billmeyer, F. W., Jr. *Textbook of Polymer Science*, 3rd ed.; John Wiley & Sons: New York, 1984.

(2)Van den Eynde, X.; Bertrand, P.; Penelle, J. *Macromolecules* **200**, *33*, 5624.

(3)Davison, W. H. T.; Slaney, S.; Wragg, A. L. *Chem. Ind.* **1954**, 1356.

(4)Lehrle, R. S.; Robb, J. C. *Nature* **1959**, *183*, 1671.

(5)Radell, E. A.; Strutz, H. C. *Anal. Chem.* **1959**, *31*, 1890.

(6)Martin, S. B. *J. Chromatogr.* **1959**, *2*, 272.

(7)Montaudo, M. S. *Mass. Spec. Rev.* **2002**, *21*, 108.

(8)Scrivens, J. H.; Jackson, A. T. *Int. J. Mass Spectrom.* **2000**, *200*, 261.

(9)Murgasova, R.; Hercules, D. M. *Int. J. Mass Spectrom.* **2003**, *226*, 151.

(10)Karas, M.; Bachmann, D.; Bahr, U.; Hillenkamp, F. *Int. J. Mass Spectrom.* **1987**, *78*, 53.

(11)Busch, K. L. *Int. J. Mass Spectrom.* **1995**, *30*, 233.

(12)Imrie, D. C.; Pentney, J. M.; Cottrell, J. S. *Rapid Commun. Mass Spectrom.* **1995**, *9*, 1293.

(13)Fenn, J. B.; Mann, M.; Meng, C. K.; Wong, S. F. *Mass Spec. Rev.* **1990**, *9*, 37.

(14)Kebarle, P.; Tang, L. *Anal. Chem.* **1993**, *65*, 972.

(15)Gaskell, S. J. *Int. J. Mass Spectrom.* **1997**, *32*, 677.

(16)Montaudo, G.; Lattimer, R. P. *Mass Spectrometry of Polymers*; CRC Press: Boca Raton, 2002.

(17)Hunt, S. M.; Sheil, M. M.; Belov, M.; Deerick, P. J. *Anal. Chem.* **1998**, *70*, 1812.

(18)Jackson, A. T.; Jennings, K. R.; Scrivens, J. H. *J. Am. Soc. Mass Spectrom.* **1997**, *8*, 76.

(19)Jackson, A. T.; Yates, H. T.; Scrivens, J. H.; Green, M. R.; Bateman, R. H. *J. Am. Soc. Mass Spectrom.* **1997**, *8*, 1206.

(20)Scrivens, J. H.; Jackson, A. T.; Yates, H. T.; Green, M. R.; Critchley, G.; Brown, J.; Bateman, R. H.; Bowers, M. T.; Gidden, J. *Int. J. Mass Spectrom.* **1997**, *165/166*, 363.

(21)Jackson, A. T.; Yates, H. T.; Scrivens, J. H.; Critchley, G.; Brown, J.; Green, M. R.; Bateman, R. H. *Rapid Commun. Mass Spectrom.* **1996**, *10*, 1668.

(22)Gidden, J.; Jackson, A. T.; Scrivens, J. H.; Bowers, M. T. *Int. J. Mass Spectrom.* **1999**, *188*, 121.

(23)Bowers, M. T.; Gidden, J.; Wyttenbach, T.; Batka, J. J.; Weis, P.; Jackson, A. T.; Scrivens, J. H. *J. Am. Chem. Soc.* **1998**, *121*, 1421.

(24)Deery, M. J.; Jennings, K. R.; Jasieczek, C. B.; Haddleton, D. M.; Jackson, A. T.; Yates, H. T.; Scrivens, J. H. *Rapid Commun. Mass Spectrom.* **1997**, *11*, 57.

(25)Jackson, A. T.; Yates, H. T.; Scrivens, J. H.; Green, M. R.; Bateman, R. H. *J. Am. Soc. Mass Spectrom.* **1998**, *9*, 269.

(26)Jackson, A. T.; Bunn, A.; Hutchings, L. R.; Kiff, F. T.; Richards, R. W.; Williams, J.; Green, M. R.; Bateman, R. H. *Polymer* **2000**, *41*, 7437.

(27)Gidden, J.; Bowers, M. T.; Jackson, A. T.; Scrivens, J. H. *J. Am. Soc. Mass Spectrom.* **2002**, *13*, 499.

(28)Jedlinski, Z.; Adamus, G.; Kowalczul, M.; Schubert, R.; Szewczuk, Z.; Stefanowicz, P. *Rapid Commun. Mass Spectrom.* **1998**, *12*, 357.

(29)Chen, R.; Tseng, A. M.; Ushing, M.; Li, L. *J. Am. Soc. Mass Spectrom.* **2001**, *12*, 55.

(30)Selby, T. L.; Wesdemiotis, C.; Lattimer, R. P. *J. Am. Soc. Mass Spectrom.* **1994**, *5*, 1081.

(31)Bottrill, A. R.; Giannakopulos, A. E.; Waterson, C.; Haddleton, D. M.; Lee, K. S.; Derrick, P. J. *Anal. Chem.* **1999**, *71*, 3637.

(32)Gidden, J.; Wyttenbach, T.; Jackson, A. T.; Scrivens, J. H.; Bowers, M. J. *J. Am. Chem. Soc.* **2000**, *122*, 4692.

(33)Cerda, B. A.; Horn, D. M.; Breuker, K.; McLafferty, F. W. *J. Am. Chem. Soc.* **2002**, *124*, 9287.

Chapter Two

FREE RADICAL POLYMERIZATION

Staudinger proposed in 1920[1] that vinyl polymerization (involving unsaturated monomers) occurs by a chain mechanism where there is no intermediate species between monomers and polymers. The chain mechanism incorporates three steps (as proposed by Flory in 1937[2]): initiation, propagation and termination. In free radical polymerization, a radical attacks the carbon-carbon double bound of the monomer resulting in a new radical to propagate the chain reaction. The steps of free radical polymerization will be described in detail below.[3, 4]

2.1 Free radical polymerization mechanism

2.1.1 Initiation

An initiator is used to generate radicals. The initiator has a weak bond that can be broken by providing the required homolytic bond dissociation energy by thermolysis, photolysis, radiolysis or sonolysis. Thermolysis and photolysis will be discussed in detail below.

During thermolysis, the initiator is heated to a temperature from 50°C to 150 °C in order to break bonds with dissociation energy ranging from 125 to 165 kJ/mol.

Carbon-hydrogen and carbon-carbon bonds are too strong to be broken by this technique and so, molecules with a heteroatom-carbon or heteroatom-heteroatom bond are normally chosen. Peroxide and azo compounds are common thermal initiators, especially benzoyl peroxide and azodiisobutyronitrile (shown in Figure 2.1).

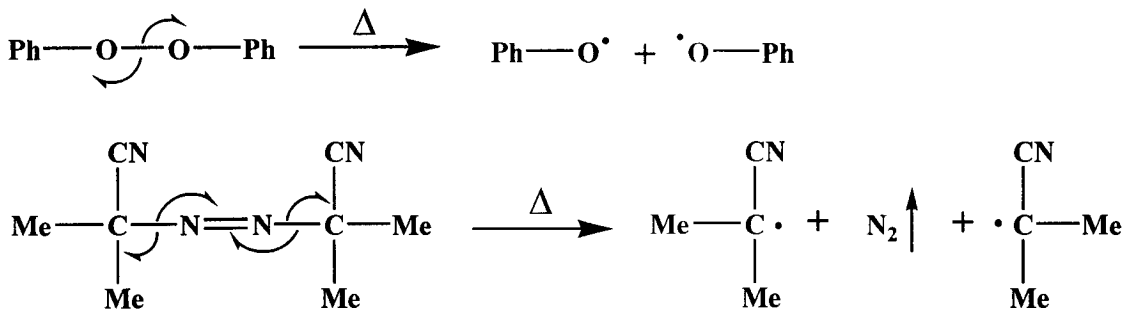

Figure 2.1: Initiation reactions in free radical polymerization.

For benzoyl peroxide, an oxygen-oxygen bond with dissociation energy of about 150 kJ/mol is broken. In the case of azo compounds, two carbon-nitrogen bonds are broken and a dinitrogen molecule is formed with a strong nitrogen-nitrogen triple bound (945 kJ/mol). For AIBN, two tertiary radicals are formed, which are stabilized by delocalization of the radical in the π bond of the nitrile.

In photolysis, UV and visible light can be used to cleave bonds. Peroxides and azo compounds can absorb a photon to promote either a low-bonding or non-bonding electron to an anti-bonding orbital. In the case of peroxides, UV light is required to initiate the radical formation. For azo compounds, light from the near-UV and UV region will break the carbon-nitrogen bound. Photolysis can also be applied to halogens, nitrites and organometallic compounds. Care should be taken to protect the reaction mixture

from light in order to control the initiation of the polymerization. Photoinitiation can be controlled perfectly by adjusting the light intensity, as opposed to thermal initiation where the generation of the radical is not rapidly controlled because of the heat capacity of the system.

2.1.2 Propagation

During the propagation stage of the polymer synthesis the radicals will react with unsaturated monomer (vinyl compounds) in order to break a π bond and form a σ bond. The radical can attack the more or less substituted side of the alkene to form a primary or secondary radical. Steric factors tend to control the selectivity of the reaction rather than the stability of the radical product. Therefore, the less substituted carbon of an alkene will typically be attacked to form a secondary radical as shown in Figure 2.2. The radical formed will add successively to monomers to propagate the polymerization.

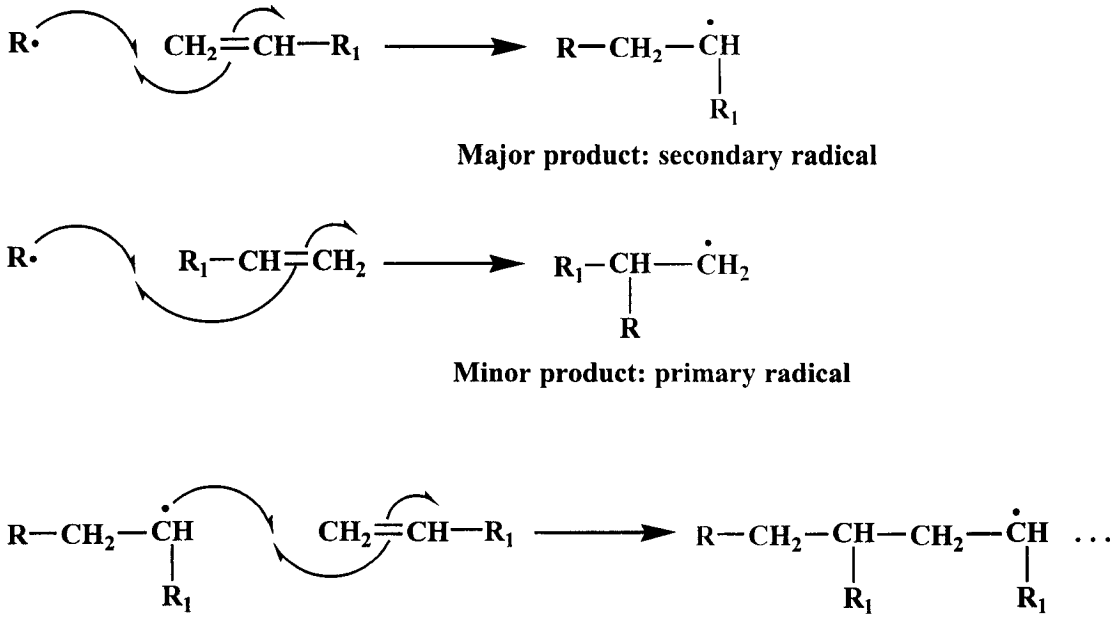

Figure 2.2: Propagation reactions in free radical polymerization.

2.1.3 Termination

During the termination step non-radical species are formed. Two mechanisms are possible, combination and disproportionation.

Two radicals will couple to form a two-electron covalent bond. Combination can happen between two growing polymer chains but also between the radicals produced during the initiation step (between two isobutyronitrile radicals for example). A solvent cage can surround the two radicals after their formation and if the solvent is viscous, the radicals cannot diffuse and they recombine. Examples of the final products from combination are shown in Figure 2.3.

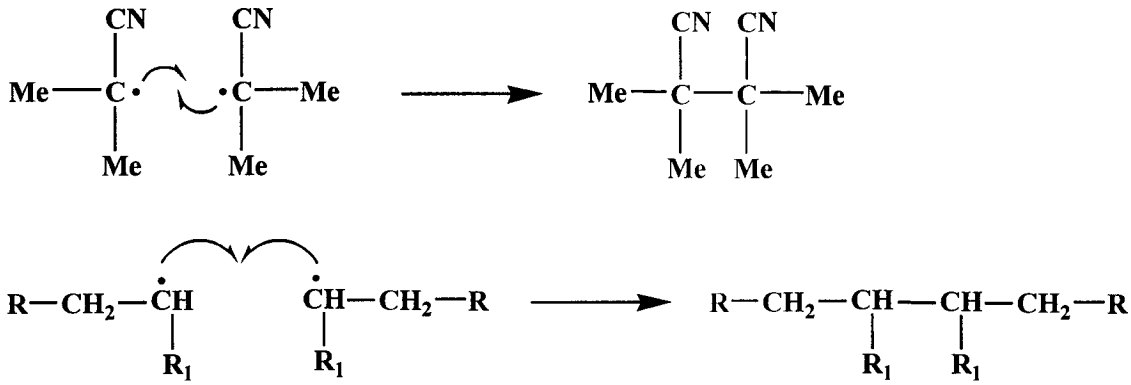

Figure 2.3: Termination by combination.

Two radicals can react together by hydrogen abstraction to form a saturated and an unsaturated polymer. A hydrogen atom is transferred from the carbon beta to the radical site to an other growing chain as shown in Figure 2.4.

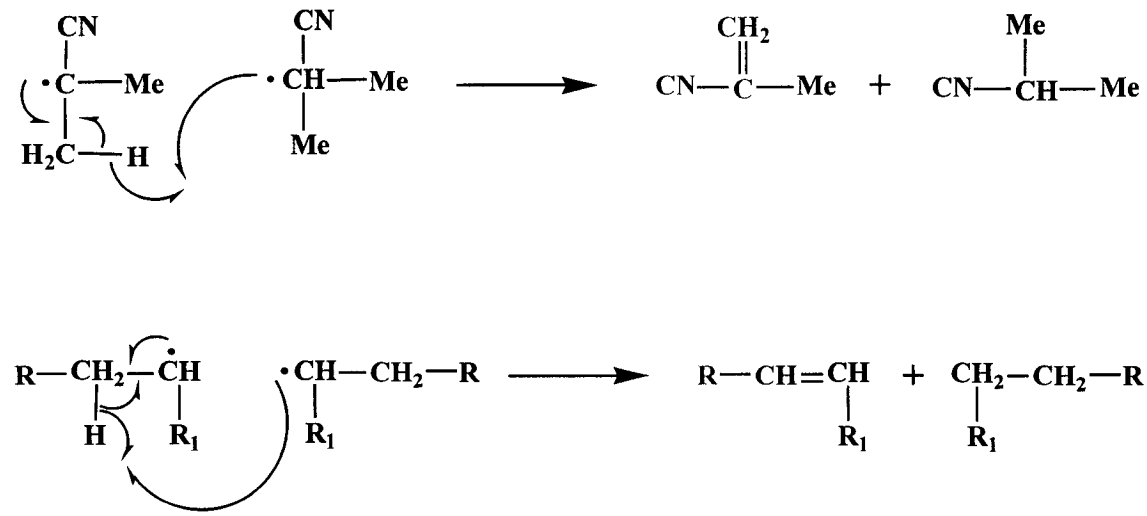

Figure 2.4: Termination by disproportionation.

2.2 Reaction conditions

In the present study, free radical polymerization was used to produce three types of homopolymers: poly(methyl methacrylate) (PMMA), poly(n-butyl acrylate) (PBA) (referred to as butyl acrylate throughout the thesis) and poly(vinyl acetate) (PVAc) and three copolymers using the same vinyl monomers: Poly(butyl acrylate/vinyl acetate), poly(butyl acrylate/methyl methacrylate) and poly(methyl methacrylate/vinyl acetate). The monomers were purchased from Aldrich. BA and MMA were washed three times with NaOH 10% (w/w) using equal volumes of monomer and sodium hydroxide solution. The monomers were then extracted three times with deionized water and dried on calcium chloride. The washed monomers (BA and MMA) and VAc were purified by distillation under vacuum with a rotary evaporator. The water bath temperature and the pressure used for the distillation are listed in Table 2.1.

Table 2.1 Distillation conditions.

Monomers	Water bath temperature (°C)	Vacuum pressure*
BA	30 to 35	Full vacuum
MMA	25 to 30	30 to 50 mmHg
VAc	25 to 30	50 to 70 mmHg

* Reading on the pressure gauge of the rotary evaporator system.

The initiator used to start the polymerization is azodiisobutyronitrile (AIBN); graduate students in the group of Professor Marc A. Dubé recrystallized it three times in methanol. A chain-transfer agent (CTA) was added to the reaction mixture in order to control the molecular weight of the polymer sample. The CTA reacts with the growing

polymer to stop polymerization by hydrogen atom transfer. Chain transfer to polymer or monomer can happen leading to the formation of branched polymers with a broad molecular weight distribution, change transfer to solvent can also happen. Dodecanethiol or butanethiol (Aldrich) were used as CTA and toluene (BDH Ltd.) as solvent without further purification. AIBN was always added last to the reaction mixture to prevent the initiation of polymerization by light or room temperature. Once the initiator was in the solution, it was kept in a freezer until needed. Exactly 2 mL of the reaction mixture dissolved in toluene was pipetted into glass ampoules. The ampoules and their fabrication will be described in more detail in section 2.3. The composition of reaction mixtures for the homo and copolymerizations are shown in Table 2.2.

Table 2.2 Reaction conditions.

Monomers	Percentage (w/w)	CTA (mol/L)	AIBN (mol/L)
BA	4	0.02*	0.02
	4	0	0.02
	7	0.02	0.02
	7	0.02	0
	10	0.02	0.02
MMA	3	0	0.03
	4	0.02	0.03
VAc	8	0.02	0.2
	8	0	0.2
	17	0.02	0.2
BA/MMA	5/5	0.02*	0.03
BA/VAc	7/17	0.02*	0.12
	11/11	0.02	0.12
MMA/VAc	7/7	0.02	0.05

* Butanethiol and dodecane thiol were use as CTA.

The reaction conditions were adjusted to the desired molecular weight using a JAVA™-based program (*Impress v0.2*) for the simulation of free-radical polymerization developed by Badeen and Dubé.[5] *Impress* can model free radical polymerization of acrylonitrile, alpha-methyl styrene, butyl acrylate, methyl methacrylate, styrene and vinyl acetate. It can be used to predict homopolymerization and copolymerization of two or three monomers at different temperatures. Only AIBN and dodecanethiol can be used as initiator and CTA respectively in the model. As output, *Impress* gives:

- the time,
- the mass conversion,
- the accumulated average molecular weight in number and in weight ($\overline{M}_n$ and $\overline{M}_w$),
- the volume,
- the temperature of the reaction mixture,
- the polymerization rate,
- the initiator radical concentration,
- the propagation and termination rate constants (k_p, k_t),
- the instantaneous and cumulative polymer compositions.

The reaction conditions were adjusted in order to produce oligomers with an accumulated average molecular weight lower than 4000 Da.

The ampoules were fixed to a vacuum system (shown in Figure 2.5) using "Cajon" ultra-torr unions. Four ampoules at a time were frozen in liquid nitrogen for two minutes before the vacuum valve was opened. After fifteen minutes under vacuum (200

millitorr), the valve was closed and the ampoules were thawed using ethanol. In total, four freeze-pump-thaw cycles were performed to remove air from the reaction mixture. As shown in Figure 2.6 oxygen can interfere with the polymerization reaction.[6] After the freeze-pump-thaw cycles, the ampoules were sealed (Figure 2.7) and heated at 60°C in paraffin using a hot plate (the sealed ampoules could be kept in the freezer or in an ice bath before the polymerization). The ampoules were transferred to an ice bath to stop the reaction at various reaction times in order to study the composition of the polymer mixture over the course of the reaction. Reaction times were chosen that were evenly spaced along the theoretical conversion versus time data from *Impress.* Solvent was evaporated at room temperature and atmospheric pressure until the polymer had the appearance of oil, then it was dried under vacuum overnight. The resulting polymer samples were dissolved in acetone: water 9:1 for analysis by ESI-MS.

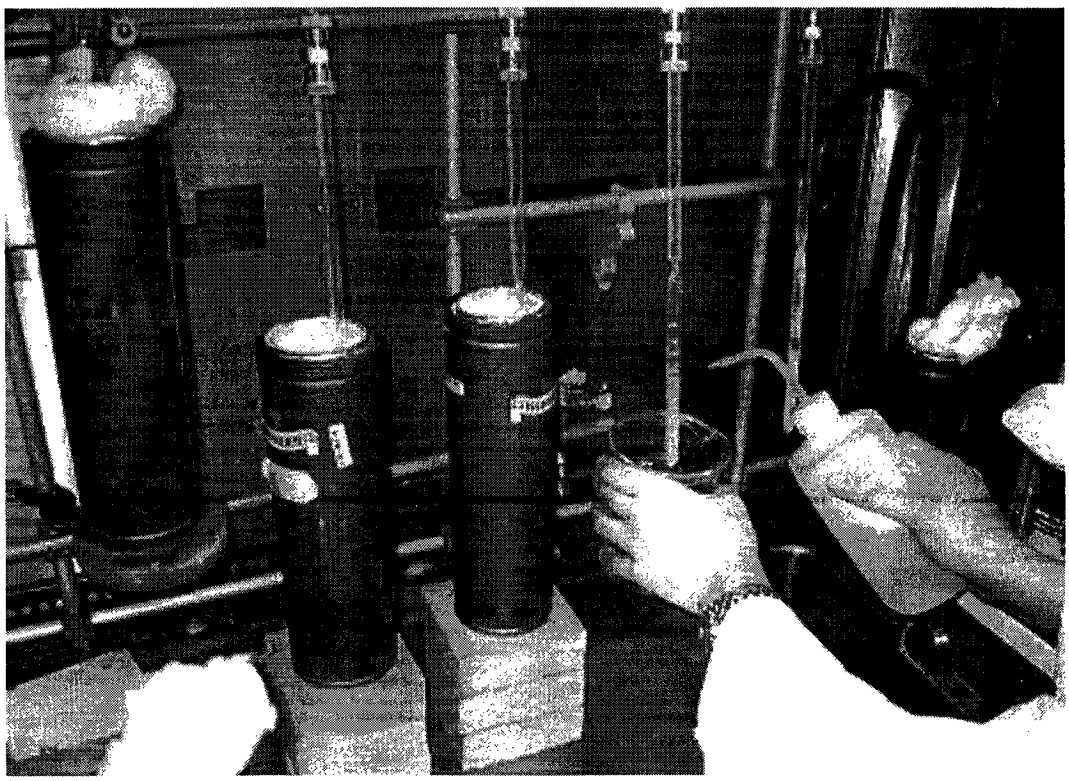

Figure 2.5: Freeze-pump-thaw system.

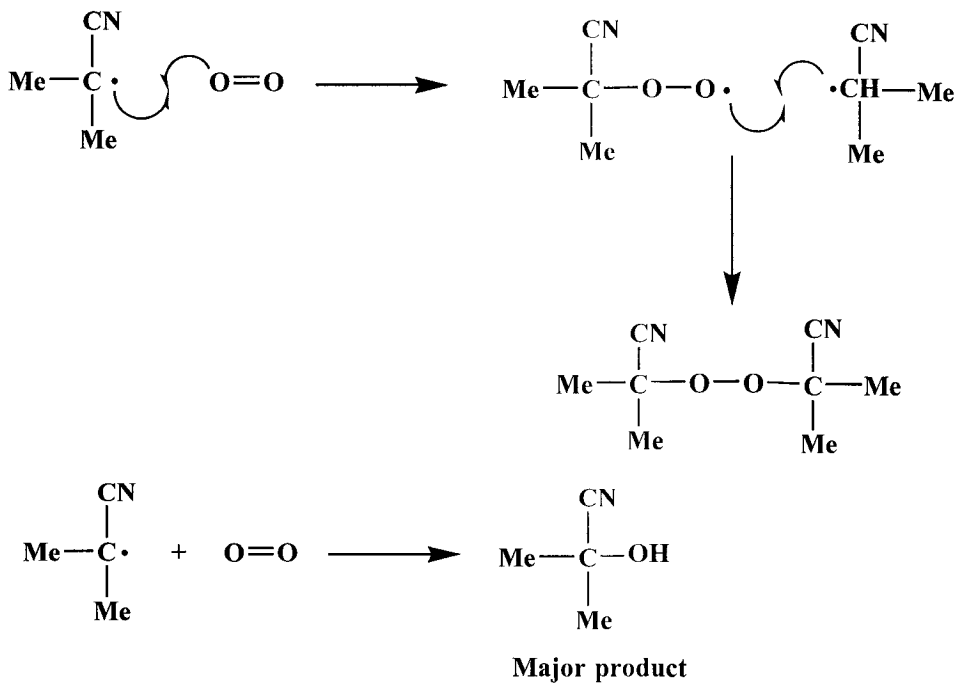

Figure 2.6: Interference of oxygen in free radical polymerization.

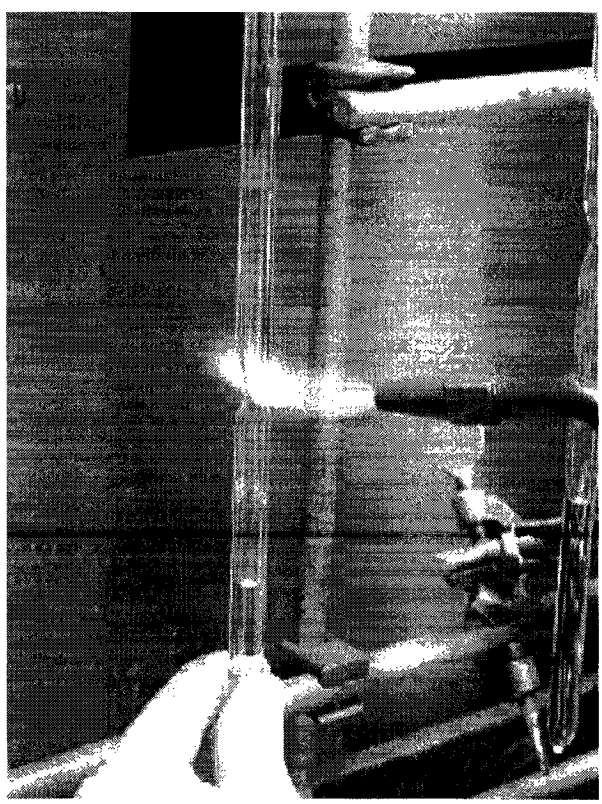

Figure 2.7: Sealing of an ampoule using an oxygen/natural gas flame.

The glass ampoules were weighed empty and with the reaction mixture in order to calculate the mass conversion (C) of the polymer from equation 2.1.

$$C(\%) = \frac{w_{polymer}\ (g)}{\left[(w_{ampoule+reaction\ mixture} - w_{ampoule})\ (g) \times \text{weight fraction of monomer in the reaction mixture} \right]} \times 100 \qquad 2.1$$

The conversion was also calculated from the volume of the reaction mixture used for the polymerization as shown in equation 2.2.

$$C\ (\%) = \frac{w_{polymer}\ (g)}{\left[V_{ampoule}\ (ml) \times \text{monomer concentration of the reaction mixture (g/ml)} \right]} \times 100 \qquad 2.2$$

2.3 Ampoule fabrication

Glass tubes with an external diameter of 9.5 mm and heavy wall were used to prepare the ampoules. Each tube was cut into four 31 cm long pieces. One end was melted closed and the other was molded to round the end (to preserve the seal of the Cajon union) using an oxygen/natural gas flame. At a distance of 15 cm from the open end, a narrow neck was made on the ampoule in order to make the seal step easier. The tube was heated and the two ends were pulled apart to reduce the external diameter to about 4 mm. The tube was then heated with a natural gas flame to prevent the breakage of the glass during the freeze-pump-thaw cycle. Prior to the reaction, the tubes were washed three times with acetone and dried to remove the solvent.

References

(1)Staudinger, H. *Ber. Dtsch. Chem. Ges. B.* **1920**, *53*, 1073.

(2)Flory, P. J. *J. Am. Chem. Soc.* **1937**, *59*, 241.

(3)Billmeyer, F. W., Jr. *Textbook of Polymer Science*, 3rd ed.; John Wiley & Sons: New York, 1984.

(4)Parsons, A. F. *An Introduction to Free Radical Chemistry*; Blackwell Science Ltd: Oxford, 2000.

(5)Badeen, C.; Dubé, M. A. *Polym. React. Eng.* **2003**, *11*, 53.

(6)Bevington, J. C. *J. Polym. Mater.* **1993**, *10*, 195.

Chapter three

MASS SPECTROMETRY

3.1 Electrospray ionization mass spectrometry (ESI-MS):

Yamashita and Fenn[1] demonstrated the potential of electrospray as a mass spectrometric technique in 1984 by developing electrospray ionization mass spectrometry (ESI-MS). ESI is an atmospheric pressure ionization technique that can easily couple liquid chromatography and mass spectrometry. Atmospheric pressure ionization is a good interface between high-pressure chromatography and the low-pressure mass spectrometer. During the desolvation process, the solvent is evaporated without using heat preventing thermal degradation of unstable compounds. ESI is a soft ionization technique meaning it primarily produces an intact molecular ion from nonvolatile samples.

The goal of the technique is to transfer ionized species from the liquid phase to the gas phase. The samples are ionized in solution by acidification or salt adduct formation. The electrospray process is divided into three steps. First, charged solvent droplets are produced, followed by solvent evaporation to reduce the size of the droplet. As the droplets get smaller, fission finally occurs due to charge repulsion to produce smaller highly charged droplets that eventually produce solvent-free gas phase ions. The

mechanism of the production of gas-phase ions for small and highly charged droplets is not well understood.[2]

The production of charged droplets occurs at the capillary tip (Figure 3.1). The sample passes through a metal capillary with an internal diameter of about 100 μm. A high voltage is applied to the tip (2 to 5 kV), which is located two or three centimeters from a counter electrode leading to the high vacuum of the mass spectrometer. The electric field created at the capillary tip is very high due to the narrow radius of the capillary. As shown in Figure 3.1b, in positive ion mode, the potential of the capillary is positive and so positive ions in solution will drift toward the liquid surface and negative ions will drift toward the capillary. An accumulation of positive charge destabilizes the surface, leading to the formation of a Taylor-cone (Figure 3.1c). At sufficiently high field, the cone is not stable and a fine liquid filament composed of positive ions is emitted in a process called budding[3] (Figure 3.1d). The filament forms droplets with high positively charged surfaces.

The droplet will shrink by solvent evaporation. The evaporation happens while the droplets traverse a pressure and potential gradient toward the mass spectrometer. During this non-ergotic process, the droplets cool, but collisional warming prevents them from freezing. The droplets will shrink until their surface charge density reaches the Rayleigh limit where fission into smaller droplets occurs (Coulombic explosion). The Rayleigh limit is reached when the repulsive force between the charges is greater than the cohesion forces holding the droplets together. This limit is described by the Rayleigh

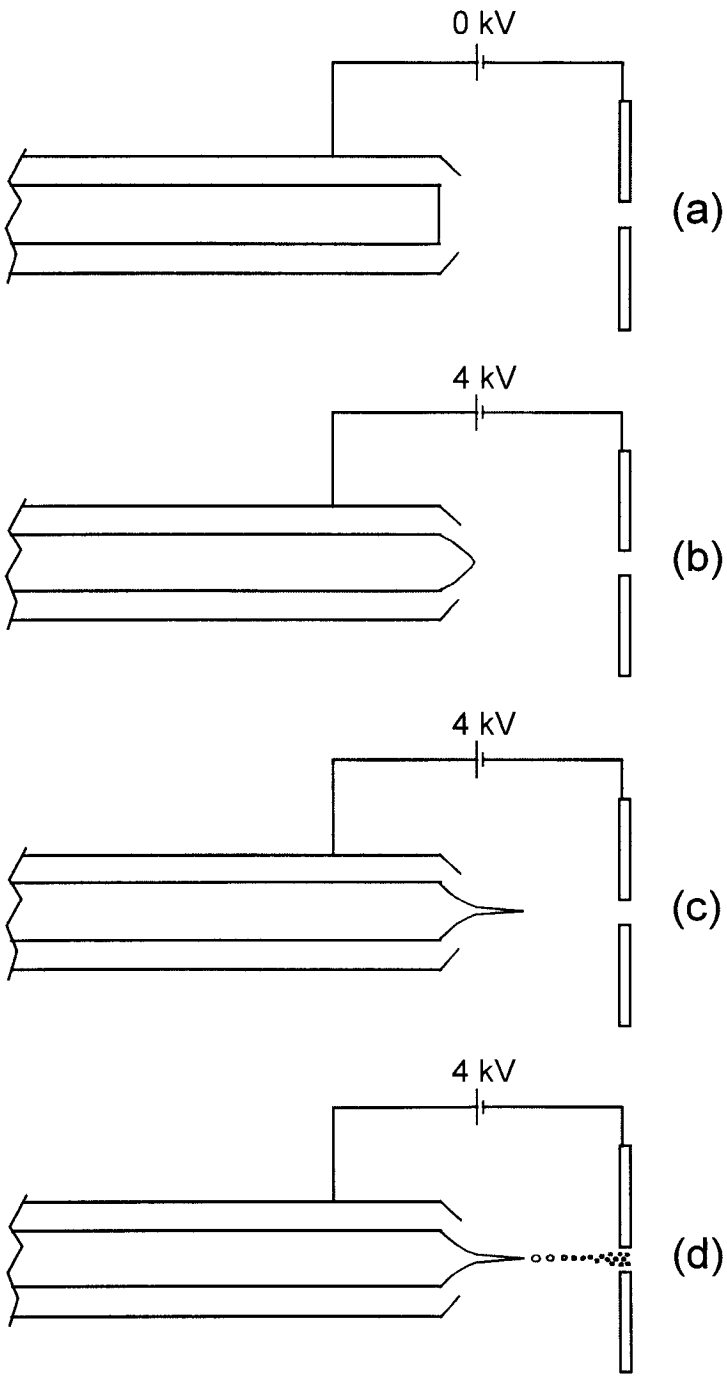

Figure 3.1: Electrospray ionization process: (a) capillary without potential difference, (b) accumulation of the positive charges at the surface under 4 kV, (c) destabilization of the surface leading to Taylor-cone formation, (d) generation and shrinkage of droplets.

equation[4] (3.1), where at a constant charge (q) the droplet radius (r) affects the surface tension of the drop (γ), and ε_0 represent the permittivity of a vacuum. In fact, fission occurs at a lower droplet size than predicted by the Rayleigh equation. Gomez and Tang[5] observed that the droplets are mechanically deformed reducing the repulsion between charges.

$$q = 8\pi\sqrt{(\varepsilon_0 \gamma r^3)} \qquad 3.1$$

The fission process is repeated until the electric field on the droplet surface becomes large enough to desorb ions. The ions can have a great number of charges if several ionizable sites are present on the molecule. The presence of multiple charge species (small m/z values) allows the analysis of compounds with a molecular weight greater than the mass limit of a mass analyzer. Ionization by electrospray does not require large amounts of electrolytes and polar solvents contain enough ions to observe a stable spray. In order to increase the sensitivity, salt or acid can be added; the maximum concentration of salt (tolerable by the technique) is about 10^{-3}M.

Fenn[6] demonstrated the extent of multiple charging and application to the ionization of biological macromolecules and polymers. ESI-MS can also be applied to the analysis of carbohydrates, nucleic acids, lipids, organometallic complexes and drug metabolites.[7]

3.2 Triple-quadrupole mass filter:

The principle of a quadrupole for ion focusing was described by Paul and Steinwegen.[8] Quadrupole mass analyzers are composed of four parallel rods with ideally a hyperbolic shape (more often they are cylindrical). The potential Φ_0, composed of a radio frequency (RF) potential and a direct current (DC) potential, is described in equation 3.2.

$$\Phi_0 = U - V \cos(\omega t) \qquad 3.2$$

V cos (ωt) represents the radio-frequency potential, U represents the direct current potential, ω is the angular frequency ($\omega = 2\pi\upsilon$) and υ is the radio frequency.

As shown in Figure 3.2, opposing rods in the assembly have the same charge. As the ions travel along the z-axis of the quadrupole, the charge on the rods is rapidly switched from positive to negative, trapping the ion motion in two dimensions.

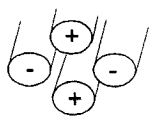

Figure 3.2: Quadrupole cylindrical rods (ideally they should be hyperbolic) and applied potential.

The ion motion is described by the Mathieu equation[9] (3.3):

$$\frac{\partial^2 u}{\partial \xi^2} + (a_u - 2q_u \cos 2\xi)u = 0 \qquad 3.3$$

where u represents either the x or y position of an ion,

$$\xi = \frac{\omega t}{2},$$

$$a_u = a_x = -a_y = \frac{8zeU}{m\omega^2 r_0^2},$$

$$b_u = b_x = -b_y = \frac{4zeV}{m\omega^2 r_0^2}.$$

The stable solutions for these equations represent conditions for stable trajectories of ions in the quadrupole mass analyzer. Stability diagrams can be drawn using a_u and q_u, or U and V (U is proportional to a_u and V is proportional to q_u). The stability diagram with different masses used for the operation of a quadrupole is shown in Figure 3.3. When certain U and V conditions are used, it is possible to successively detect different masses. An operating line can be drawn through the stability diagrams with ions above the line having a stable trajectory through the quadrupole. The resolution and the sensitivity of the mass filter is controled by adjusting the slope of the operating line. When the direct current potential equals zero (U = 0), the resolution is null and all the ions have a stable trajectory (RF-only mode).

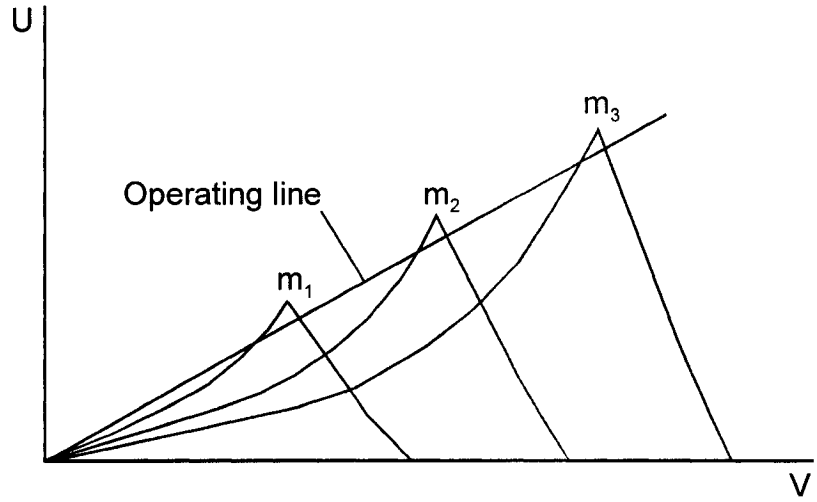

Figure 3.3: Stability diagram as a function of U and V.

Mass spectrometers can be equipped with several quadrupoles in order to perform a tandem mass spectrometry experiments (MS/MS) using collision-induced dissociation (CID). As shown in Figure 3.4, three mass filters can be aligned. The first quadrupole performs the mass selection of the precursor ion with a certain U and V. The second quadrupole in modern instruments is actually usually a hexapole. A target gas is introduced into the hexapole at a certain pressure so that the precursor ion can collide with the target and fragment. The hexapole is operated in RF-only mode to give a stable trajectory to all the product ions. The dissociation of the precursor ion can be increased by increasing the target gas pressure and the kinetic energy of the precursor ion (laboratory frame collision energy, E_{lab}). The third quadrupole then analyzes the product ions.

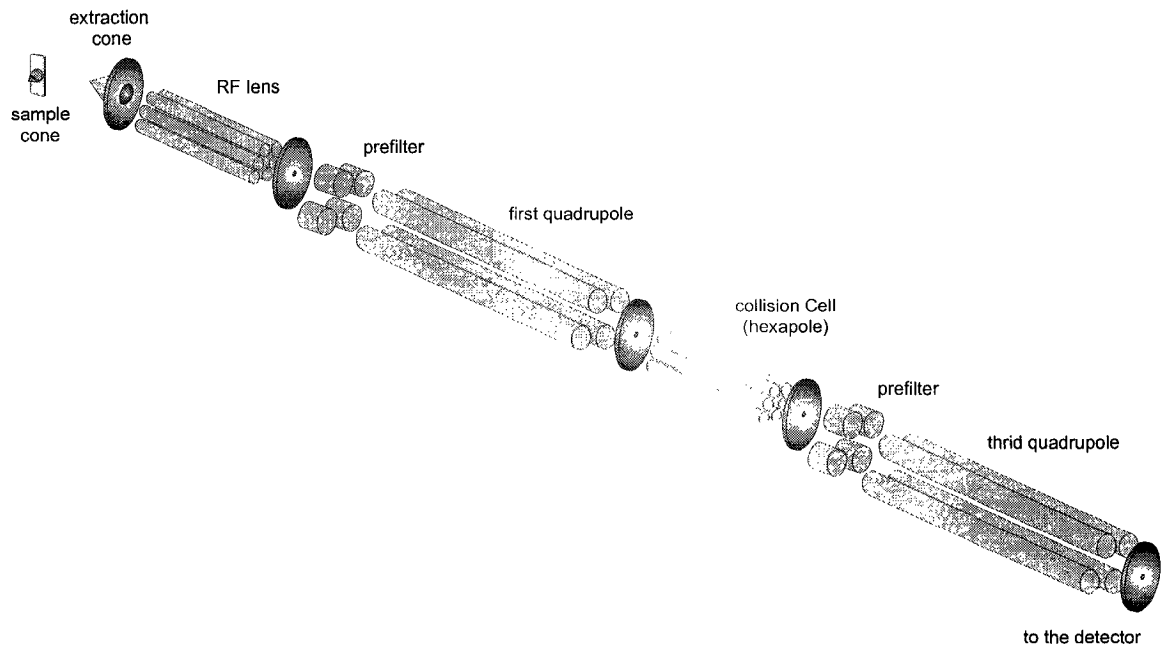

Figure 3.4: Triple quadrupole mass spectrometer with Z-spray source.

3.3 Experimental procedures

The ESI-MS and ESI-MS/MS experiments were performed using a Micromass Quattro LC triple quadrupole mass spectrometer equipped with a Z-spray source. Solutions of 1 mg/mL of polymer sample and 0.25 mg/mL of NaCl or LiCl in 9:1 acetone:water mixture were analyzed. NaCl and LiCl were used to ionize the polymer mixture. A volume of 20 μL was introduced into the mobile phase using a Rheodyne injector. The ESI was operated in positive mode with a capillary voltage of 4.3 kV and a sample cone voltage of 180 V. Collision-induced dissociation (CID) of the polymer ions utilized collision energies from 10 to 100 eV and argon was used as collision gas with pressures from $3x10^{-4}$ to $1.2x10^{-3}$ mBar. A flow rate of 60 μL/min of 9:1 acetone:water was used for MS and MS/MS analysis. The polymer samples were filtered with a 0.45

μm PFTE filter prior to the analysis in order to prevent clogging of the ESI probe. A 20% solution of formic acid was injected three times between the polymer injections to help avoid capillary blockage.

References

(1)Yamashita, M.; Fenn, J. B. *J. Phys. Chem.* **1984**, *88*, 4451.

(2)Kebarle, P.; Tang, L. *Anal. Chem.* **1993**, *65*, 972.

(3)Gaskell, S. J. *Int. J. Mass Spectrom.* **1997**, *32*, 677.

(4)Rayleigh, L. *Philos. Mag.* **1882**, *14*, 184.

(5)Gomez, A.; Tang, K. *Phys. Fluids* **1994**, *6*, 404.

(6)Fenn, J. B.; Mann, M.; Meng, C. K.; Wong, S. F. *Mass Spec. Rev.* **1990**, *9*, 37.

(7)Cole, R. B. *Electrospray ionization mass spectrometry: fundamentals instrumentation & applications*; John Wiley & sons inc: New York, 1997.

(8)Paul, W.; Steinwedel, H. S. *Z. Naturforsch* **1953**, *8a*, 448.

(9)Mathieu, E. *J. Math. Pure Appl.* **1868**, *13*, 137.

Chapter four

COMPUTATIONAL CHEMISTRY

Molecular mechanics/molecular dynamics, Hartree-Fock, semi-empirical and Density Functional Theories were used in the present study. They will be explained briefly in the following sections. Detailed derivations of the different theories will not be presented but their concepts, advantages and weaknesses will be described.

4.1 Molecular mechanics/molecular dynamics[1]

In molecular dynamic (MD) simulations, configurations of a system are produced by integrating Newton's Laws of motion. An initial conformation is required and can be based on experimental data (X-Ray structure, NMR spectra) if available. Velocities for all the particles are assigned randomly by a Maxwell-Boltzmann distribution. MD simulations have a deterministic approach; a particle of the system is moved and the new forces acting on the particles are calculated. From the forces of the new conformation, the velocities and the coordinates can be calculated. The size of the time steps in MD must be appropriate; short time steps will lead to conformations close to each other while long time steps will result in instabilities (energetic collisions). An appropriate time step is the size of a vibrational frequency allowing for the description of interactions between particles (1 fs).

Prior to a molecular dynamic simulation, the system must be equilibrated to the desired temperature since the randomly assigned initial velocities of the system will bias the results. Typical equilibration times are one hundred picoseconds (in steps of 1 fs)

Conformational analysis can be done by MD in order to find candidate structures for the global minimum energy conformation. This is achieved by simulated annealing. The temperature of the system is varied systematically between two extremes; say 300 K and 800 K. The high temperatures allow the structure to overcome rotational barriers and thus access lower energy conformations. A large number of annealing cycles must be run in order to generate low energy conformations. If one conformation is generated many times and if it is the lowest energy conformation, it can be the global minimum conformation energy.

Molecular mechanics (MM), also known as a force field method, is a computationally inexpensive alternative to quantum mechanics. MM does not define electrons and nuclei; it defines atoms with partial charges, and classical force constants for bond, stretching, bending and torsions motions. In MM the energy is expressed as a function of atomic coordinates based on the Born-Oppenheimer[2] approximation. The MM energy is expressed as a combination of the energy contribution of the internal coordinates of the system (bond stretches, bends, torsions, electrostatic and Van der Waals interactions). The force field basis components are described in equation 4.1.

$$V = \sum_{\text{bonds}} \frac{k_l}{2}(l - l_0)^2 + \sum_{\text{angles}} \frac{k_\theta}{2}(\theta - \theta_0)^2 + \sum_{\text{torsions}} \frac{V_n}{2}[1 - \cos(n\omega - \gamma)] + \sum_{i=1}^{N} \sum_{j=i+1}^{N} \left(4\varepsilon_{ij} \left[\left(\frac{\sigma_{ij}}{r_{ij}} \right)^{12} - \left(\frac{\sigma_{ij}}{r_{ij}} \right)^{6} \right] \right) + \frac{q_i q_j}{4\pi\varepsilon_0 r_{ij}}$$

4.1

The force fields can be more sophisticated but must contain these four contributions. The two first terms of equation 4.1 describe the contribution of the deviation of the bonds and angles from their reference equilibrium value (l_0 and θ_0). They should be described by the Morse potential but because it is too computationally demanding, the harmonic potential equation is usually used in MM. In order to describe the Morse potential more accurately, a quadratic or a cubic term can be added. The Hooke's law formula is used where the energy is proportional to the square of the displacement from the equilibrium value. ks stand for the force constants, l and θ are the bond length and the bond angle respectively.

The third term of the force field equation describes the effect of bond rotations (torsions) on the energy. V_n represents the barrier height for bond rotations, n is the multiplicity (the number of maxima or minima), ω is the torsion angle and γ the phase factor which help to situate the maxima and minima.

The fourth term describes the contributions to the energy from non-bonded atoms. They are calculated between pairs of atoms, i and j, which are separated by four or more

atoms. The left side of the fourth term describes the van der Waals interactions using the Lennard-Jones 12-6 function. The function has an attractive part "$\left(\frac{\sigma_{ij}}{r_{ij}}\right)^{6}$" and a repulsive part "$\left(\frac{\sigma_{ij}}{r_{ij}}\right)^{12}$" where ε represents the depth of the well described by the Lennard-Jones potential and σ is the collision diameter (the distance between the atoms to have an energy of zero). The right side of the fourth term describes the electrostatic interactions calculated between pairs of point charges using Coulomb's law. The charges of the atoms are represented by q, ε_0 is the permittivity of free space and r is the distance between i and j.

The major characteristic of the MM approach is the transferability of the functional groups. Parameterized models can be applied to large systems; for example, results obtains for peptides can be transferred to proteins and enzymes.

4.2 Hartree-Fock theory[3]

Hartree-Fock (HF) theory is a variational method in quantum mechanics. It is an iterative procedure and it does not required experimental input. This theory is based on the HF approximation used to simplify the Schrödinger equation (4.2).

$$\hat{H}\Psi = E\Psi \qquad 4.2$$

where $\hat{H}$ is the Hamiltonian operator representing the total energy, Ψ is the wave function and E is the energy of the state describe by Ψ. $\hat{H}$ and Ψ_i are represented by:

$$\hat{H} = -\frac{1}{2}\sum_{i=1}^{N}\nabla_i^2 - \frac{1}{2}\sum_{A=1}^{M}\frac{1}{M_A}\nabla_A^2 - \sum_{i=1}^{N}\sum_{A=1}^{M}\frac{Z_A}{r_{iA}} + \sum_{i=1}^{N}\sum_{j>1}^{N}\frac{1}{r_{ij}} + \sum_{A=1}^{M}\sum_{B>A}^{M}\frac{Z_A Z_B}{R_{AB}} \qquad 4.3$$

$$\Psi_i = \sum_{\mu=i}^{N} c_{\mu i}\phi_\mu \qquad 4.4$$

The Hamiltonian operator is shown in equation 4.3 for a system of M nuclei and N electrons without electric or magnetic fields. A and B represent the nuclei, i and j represent the electrons. The two first terms of the Hamiltonian use ∇_x^2, the Laplacien operator, to define the kinetic effect of the electrons and nuclei. M_A is the mass of the nucleus A. The three last terms are the potential part where the attractive electrostatic interaction between nuclei and electrons are represented as well as repulsive interactions between two electrons and two nuclei. R_{AB} and r_{ij} represent the distances between the particles A and B or i and j respectively.

The molecular orbital is the summation of a finite set of one-electron functions called basis function (φ_1, φ_2, φ_3,... φ_N) and $c_{\mu i}$ is the molecular orbital expansion coefficient.

According to the HF approximation, it is assumed that an electron in a spin orbital sees a mean field generated by the other electrons of the system. The electron motions are not correlated. The difference between the real energy of a system and the HF energy

is the correlation energy. The quality of the answer also depends on the basis set used. The HF equation for closed-shell systems has been solved by Roothaan[4] and Hall.[5] A closed-shell system has the same number of spin up and spin down electrons (even number of electrons) and they occupy the same orbitals. The Roothaan-Hall equations are:

$$\sum_{\nu=1}^{N}(F_{\mu\nu} - \varepsilon_i S_{\mu\nu})\, c_{\mu i} = 0 \qquad \mu = 1,2,...N \qquad 4.5$$

where $F_{\mu\nu}$ is the Fock operator (an N x N matrix), ε_i is the one-electron energy of the molecular orbital Ψ_i, and $S_{\mu\nu}$ is the overlap integral (an N x N matrix). An initial guess of $c_{\mu i}$ is taken to construct the Fock operator and the equation is solved to get a new $c_{\mu i}$. This is the self-consistent field method (SCF). The SCF approach is summarized in Figure 4.1. An initial guess is taken, the Schrödinger equation is solved and the cycle continue until the answer converges and Ψ and E stay constant.

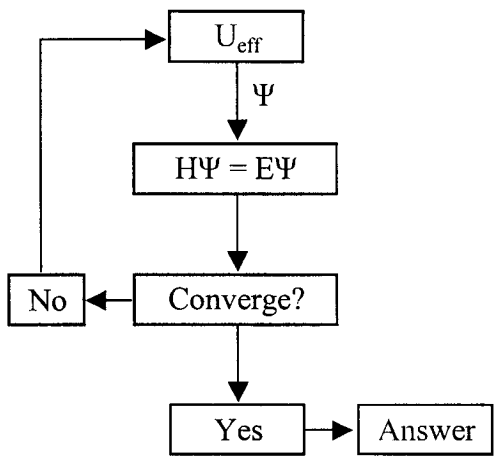

Figure 4.1: Self consistent field method.

4.3 Density Functional Theory[6]

Density Functional Theory (DFT) deals with electron density (ρ) rather than a wavefunction (Ψ) (as in HF theory). The wavefunction for an N electron system is defined in equation 4.4 and the electron density can be expressed by:

$$\rho(\vec{r}) = N\int\ldots\int|\Psi(\vec{x}_1,\vec{x}_2,\ldots\vec{x}_N)|^2 ds_1 d\vec{x}_2\ldots d\vec{x}_N \qquad 4.6$$

In order to get ρ, Ψ must be obtained from the Schrödinger equation. The Hohenberg-Kohn theorem (1964)[7] mentions that the energy of a ground state is determined by the electronic density only. The total electronic energy of a system can be written as a function of the electronic density:

$$E(\rho) = E_{ZE}(\rho) + E_C(\rho) + E_H(\rho) + E_{XC}(\rho) \qquad 4.7$$

where ZE represents the kinetic energy, C the electron-nuclear interaction, H the Coulombic exchange and XC the contribution from exchange and correlation. But the Hohenberg-Kohn theorem does not provide the equation for the unknown density functional, F[ρ].

Kohn and Sham in 1965,[8] optimized the energy using the Kohn-Sham (KS) orbitals, the KS orbitals and the density are related by equation 4.8:

$$\varphi(\vec{r}) = \sqrt{\frac{\rho(\vec{r})}{2}} \qquad 4.8$$

The one-electron equations (4.9) used by DFT allow it to be faster than HF. DFT is not an approximation of the HF theory but a new approach. As mentioned before, HF has no correlation but it perfectly describes the exchange while DFT describes approximately correlation and exchange (V_{XC}).

$$\begin{aligned}&\left(-\frac{\nabla^2}{2}+\left[\int\frac{\rho(\vec{r})}{r_{12}}d\vec{r}_2 + V_{XC}(\vec{r}_1) - \sum_A^M \frac{Z_A}{r_{1A}}\right]\right)\varphi_i \\ &=\left(-\frac{\nabla^2}{2}+V_{eff}(\vec{r}_1)\right)\varphi_i = \varepsilon_i\varphi_i\end{aligned} \qquad 4.9$$

Becke improved DFT calculations by applying the perfect concept of exchange from HF theory to DFT resulting in the B3-LYP functional where B3-LYP stands for Becke-style three parameter density functional theory using the Lee, Yang and Parr correlation function. With this hybrid method, DFT is no longer faster than HF but it provides more accurate answers.

4.4 Semi-empirical methods

Semi-empirical methods sit between molecular mechanical force fields (purely empirical) and quantum mechanical methods. They solve the Schrödinger equation (like HF) and generate wave-functions. Because semi-empirical methods require experimental empirical input to simplify the calculations, they are not *ab initio* methods. Semi-

empirical methods are closely related to HF theory, with most of the integrals set to zero according to the neglect of the differential diatomic overlap (NDDO) approximation. The results are calibrated against experimental data. Semi-empirical methods only consider the valence electrons in the calculation. Core electrons are frozen because it is assumed that only the electrons from the valence shell are involved in bonding.

Austin Model 1, AM1, a semi-empirical method developed by Dewar, Zoebisch, Healy and Stewart in 1985, was used in the present study. It is an improvement of the MNDO approach (Dewar and Thiel, 1977), which overestimates the repulsion between atoms, fails to describe hydrogen bonded sterically hindered systems.

4.5 Basis sets[3]

In ab initio packages, the first basis set used was labeled as Slater Type Orbitals (STO) due to their relationship with hydrogen-like atomic orbitals. In the 50's Boys developed an alternative, the Gaussian Type Orbitals (GTO), which are easier to calculate but do not perfectly represent the shape of orbitals. Contracted Gaussians can approximate the STO function by summing a number of GTO functions. The basis sets STO-NG are called minimal basis sets, the basis functions are contracted Gaussians where N primitive Gaussians are combined to approximate the STO function.

Using the above approach results in orbitals that are the same for every type of electron environment. For example, a lone-pair will be described by the same *p*-orbital as

a π-bond. In order to give the orbital description flexibility to expand and contract, a correction can be applied to the basis set. The contracted Gaussians of the minimal basis set are replaced by tight and diffuse contracted Gaussians, resulting in a double-zeta (or split-valence) basis set. Because the core electrons are less affected by their environment, the double-zeta can be calculated only for the valence orbitals. Split-valence basis sets are represented by **n-ijG** where **n** represents the number of primitive Gaussians in the contracted Gaussian assigned to the core orbitals, **i** is the number of primitive Gaussians in the tight contracted Gaussian assigned to the valence orbitals and **j** is the number of primitive Gaussians in the diffuse contracted Gaussian assigned to the valence orbitals. For systems with more diffuse density, diffuse functions can be added to the basis set. A basis set named **n-ij+G** indicates the addition of diffuse functions to all the elements except H and He, while «++» means the addition of diffuse functions to all the elements.

Polarization function can be added to the basis set in order to allow atoms to displace their electron density. For example, *p* functions can be added to hydrogen and helium, *d* functions to the elements of the main group and *f* functions to the transition metals. A basis set named **n-ijG(d)** indicates the addition of polarization functions to all the elements except H and He, **(d,p)** implies the addition of polarization functions to all the elements. Multiple polarization function can be added to the basis set. The basis set named **n-ij++G(3df,2pd)** adds three polarization functions with *d* and *f* functions to heavy elements and two polarization functions with *p* and *d* functions to H and He.

4.6 Computational procedures

Molecular mechanics/molecular dynamics (MM/MD), semi-empirical, ab initio and Density Functional Theory calculations were performed to predict the structure and the relative energies of poly(vinyl acetate) ion in the gas phase and the various fragments observed by collision-induced dissociation mass spectrometry. The Cerius2 modeling environment[9] (a molecular mechanics/molecular dynamics program) was used to model structures of a 5mer of PVAc ionized with lithium and the experimentally observed fragments. To study the conformation of the polymer equilibration and annealing phases were performed. During the equilibration phase, an energy-minimized structure of the ionized polymer was run for 100 ps at constant NVT (constant number of moles, volume and temperature 300K) to determine the equilibrium structure. The lowest energy equilibrium structure was then evaluated at constant NVT using 100 to 200 annealing cycles from 300 to 800 K with temperature increments of 100 K. One thousand steps (1ps) were done at each temperature increment and the model was minimized to 0 K after each complete annealing cycle. Annealing cycles were continued until the energy of the structures reached a low energy plateau.

Standard *ab initio* molecular orbital calculations were done using the Gaussian 98 suite of programs.[10] The geometries of the lowest energy structures from the annealing runs for each structure were optimized using semi-empirical (AM1) and DFT (B3-LYP/3-21G). The optimized geometries from each level of theory were used to calculate the single-point energy by Hartree-Fock and DFT (using the HF/6-31+G(d) and B3-

LYP/6-31+G(d) levels of theory). Relative energies were corrected for zero-point vibrational energy (ZPVE) at each level of theory (scaled by the appropriate factors, 0.95 for the AM1, 0.98 for the DFT structures).[11] The ZPVE of the DFT structure were used in all cases. The ZPVE values from semi-empirical theory were close to the DFT values (less then 5 kJ/mol of difference) but we choose the higher level of theory.

References

(1)Leach, A. R. *Molecular Modelling: Principles and Applications*; Addison Wesley Longman: Singapore, 1996.

(2)Born, M.; Oppenheimer, J. R. *Ann. Phisik* **1927**, *79*, 361.

(3)Hehre, W. J.; Radom, L.; Schleyer, P. v. R.; Pople, J. A. *Ab initio Molecular Orbital Theory*; John Wiley & Sons: New York, 1986.

(4)Roothaan, C. C. J. *Rev. Mod. Phys.* **1951**, *23*, 69.

(5)Hall, G. G. *Proc. Roy. Soc.(London)* **1951**, *A205*, 541.

(6)Koch, W.; Holthausen, M. C. *A Chemist's Guide to Density functional Theory*; WILEY-VCH: Weinheim, 2000.

(7)Hohenberg, P.; Kohn, W. *Phys. Rev.* **1964**, *136*, B864.

(8)Kohn, W.; Sham, L. J. *Phys. Rev.* **1965**, *140*, A1133.

(9)Molecular Simulations Inc., *Cerius2 Modeling Environment*, Release 4.0; Molecular Simulations Inc.: San Diego, 1999.

(10)Frisch, M. J.; Trucks, G. W.; Schlegel, H. B.; Scuseria, G. E.; Robb, M. A.; Cheeseman, J. R.; Zakrzewski, V. G.; Montgomery, J., J.A. ; Stratmann, R. E.; Burant, J. C.; Dapprich, S.; Millam, J. M.; Daniels, A. D.; Kudin, K. N.; Strain, M. C.; Farkas, O.; Tomasi, J.; Barone, V.; Cossi, M.; Cammi, R.; Mennucci, B.; Pomelli, C.; Adamo, C.; Clifford, S.; Ochterski, J.; Petersson, G. A.; Ayala, P. Y.; Cui, Q.; Morokuma, K.; Malick, D. K.; Rabuck, A. D.; Raghavachari, K.; Foresman, J. B.; Cioslowski, J.; Ortiz, J. V.; Baboul, A. G.; Stefanov, B. B.; Liu, G.; Liashenko, A.; Piskorz, P.; Komaromi, I.; Gomperts, R.; Martin, R. L.; Fox, D. J.; Keith, T.; Al-Laham, M. A.; Peng, C. Y.; Nanayakkara, A.; Gonzalez, C.; Challacombe, M.; Gill, P. M. W.; Johnson, B.; Chen, W.; Wong, M. W.; Andres, J. L.; Gonzalez, C.; Head-Gordon, M.; Replogle, E. S.; Pople, J. A. *GAUSSIAN 98 RevA.7. Gaussian Inc.* **1998.**

(11)Scott, A. P.; Radom, L. *J. Phys. Chem.* **1996**, *100*, 16502.

Chapter five

RESULTS AND DISCUSSION: HOMOPOLYMERIZATION

Three different homopolymers were produced by free radical polymerization and their fragmentation studied by ESI-MS/MS.

5.1 Analysis of Poly(methyl methacrylate)

The ESI mass spectrum of PMMA ionized with lithium chloride (Figure 5.1) shows the presence of two singly charged distributions of oligomers with molecular weights from m/z 400 to 1800. The end groups of the polymer are either one hydrogen atoms and dodecanethiol (labelled A on Figure 5.1) or one hydrogen atom and isobutyronitrile from the initiator of the reaction (labelled B on Figure 5.1). The presence of the CTA as an end group was confirmed by observing the expected shift of 112 Da when butanethiol is substituted in the synthesis for dodecanethiol. Free radical polymerization initiated by AIBN should yield isobutyronitrile as at least one of the end groups, but the presence of CTA has been observed previously by Busfield et al.[1]

CID experiments were performed on the two oligomer distributions. The tandem mass spectrum of the polymer ion $[PMMA_4+Li]^+$ from distribution B (with isobutyronitrile and hydrogen as end group) is shown in Figure 5.2. Fragmentation by homolytic cleavage was observed along the backbone to produce a progression of

distonic ions: $[100n+68+M]^+$ (x75) from the isobutyronitrile-terminal end and $[100n+87+M]^+$ (x94) from the hydrogen-terminal end. Hydrogen rearrangement also

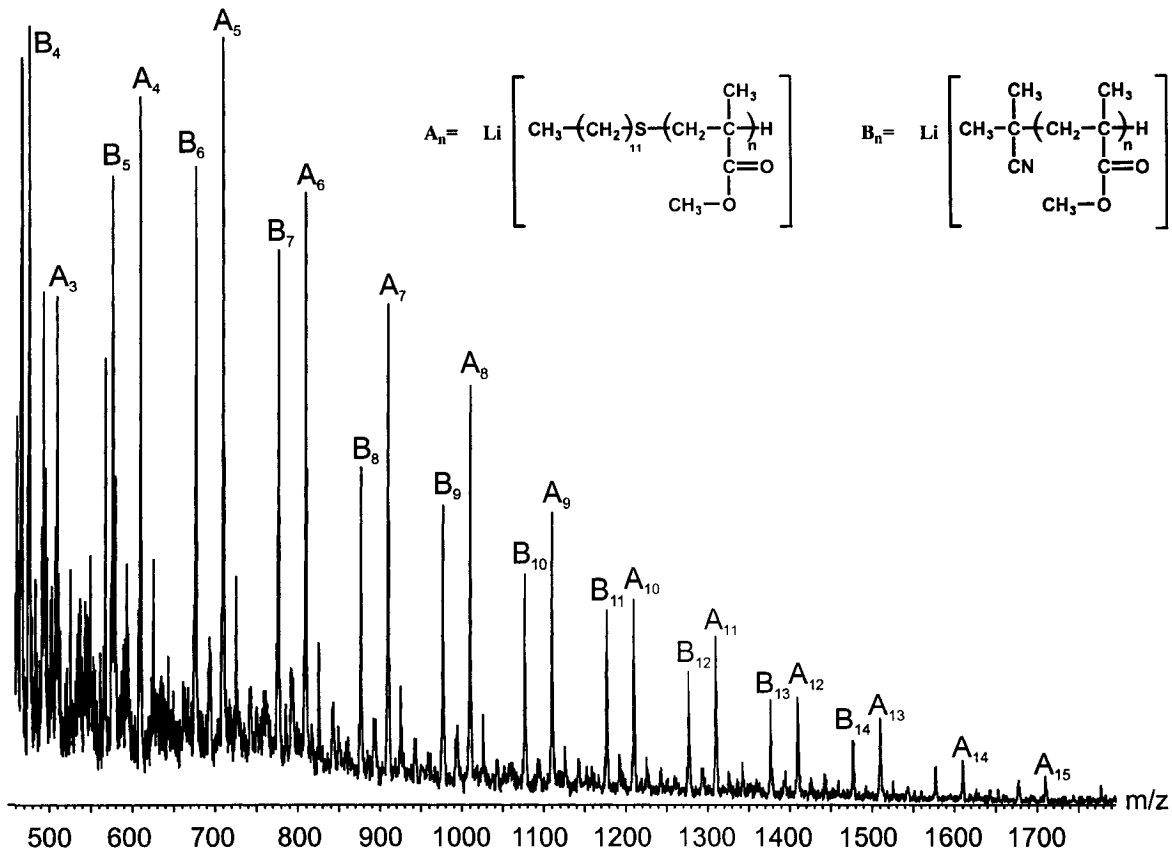

Figure 5.1: ESI mass spectrum of PMMA mixture ionized with lithium.

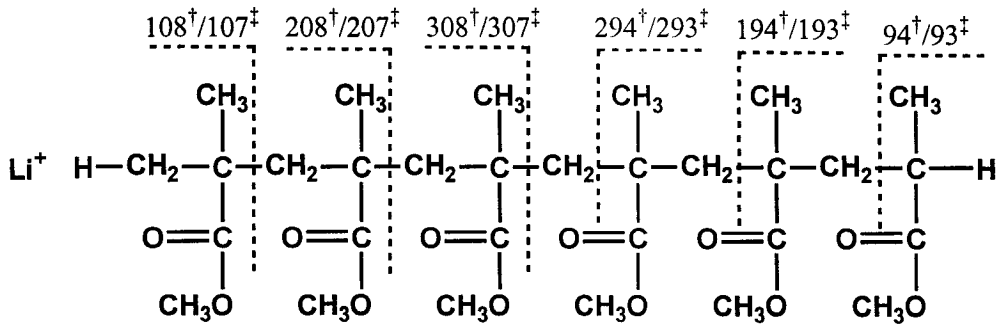

Scheme 5.1: CID fragmentation pattern of poly(methyl methacrylate) Li^+. "†" is formed by direct cleavage, "‡" is formed by hydrogen rearrangement.

occurs to form $[100n+100+M]^+$ (x07). In the notation $[100n+68+M]^+$, for instance, the "100" refers to the polymer repeat unit, "68" refers to the end groups and "M" to the alkali metal ion. The notation (x75) refers to the peaks with m/z 75, 175, 275... found in the tandem mass spectrum. The results are consistent with the results presented by Scrivens and Jackson,[2-4] in which they showed that PMMA ions fragment along the backbone by homolytic bond cleavage and by 1,5-hydrogen shifts (Scheme 5.1).

The fragmentation by hydrogen rearrangement proposed by Scrivens and Jackson does not necessary happen only from the hydrogen terminal end. When PMMA was synthesized without the chain transfer agent, one product was polymer with two isobutyronitrile end groups. When CID is performed on a distribution with isobutyronitrile at both ends, the progression $[100n+100+M]^+$ (x07) is still observed, as shown in Figure 5.3, indicating that the end group has been lost prior to the formation of m/z 107 and 207.

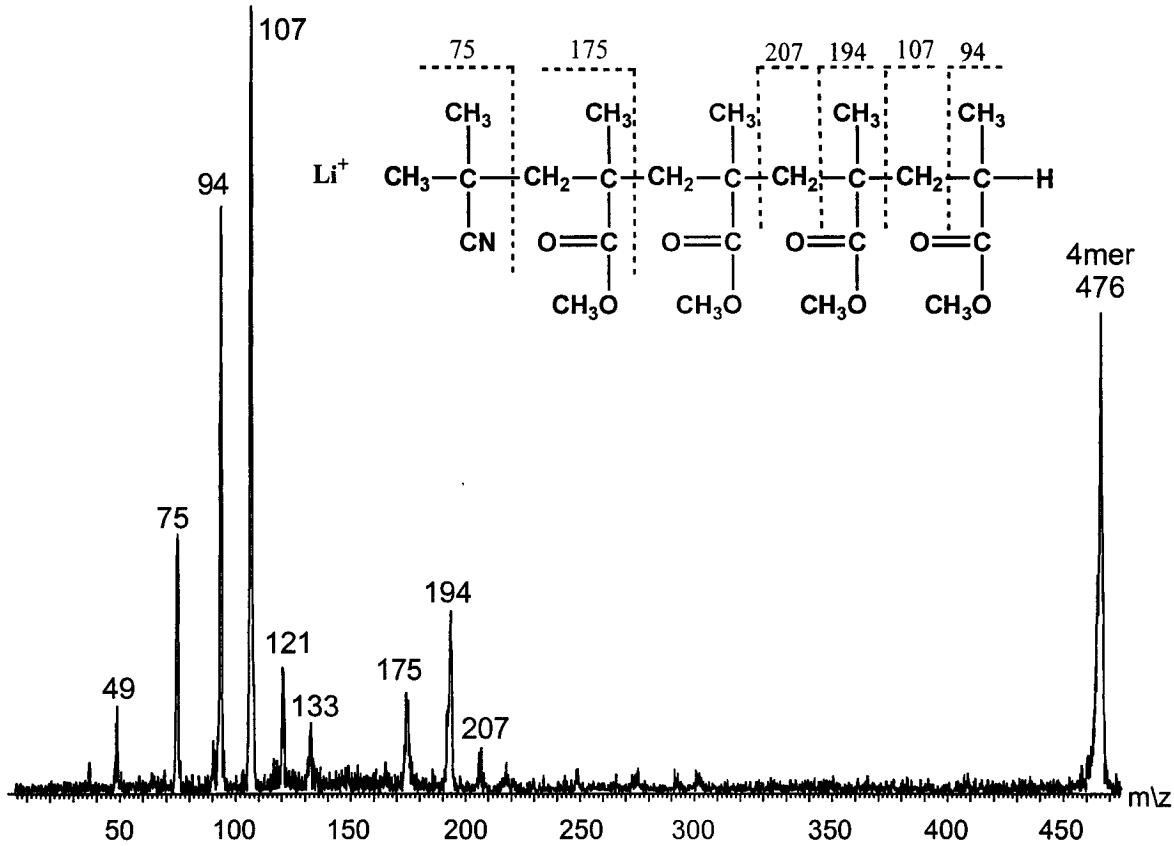

Figure 5.2: Tandem mass spectrum of $[PMMA_4+Li]^+$ from distribution B (E_{Lab} = 70eV, collision gas pressure = $4.4x10^{-4}$mBar).

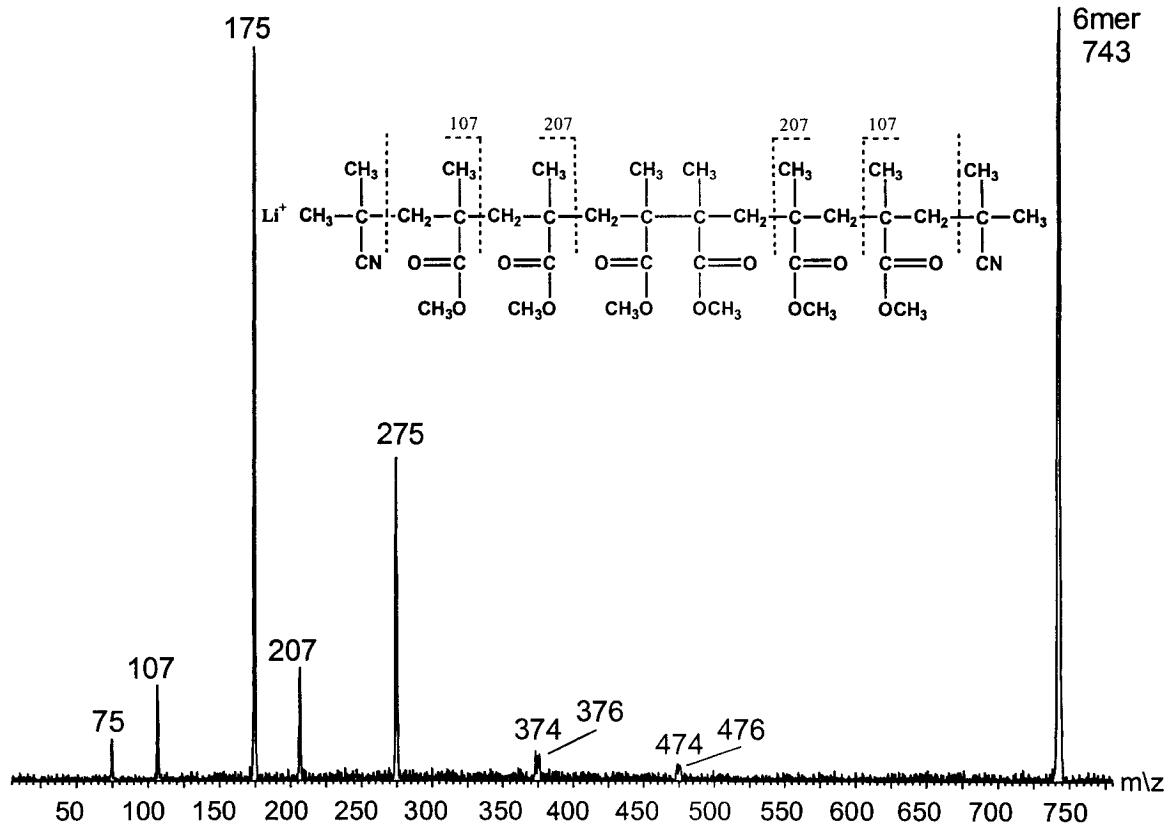

Figure 5.3: Tandem mass spectrum of a $[PMMA_6+Li]^+$ with two isobutyronitrile molecule end groups produced by polymerization without CTA (E_{Lab} = 50eV, collision gas pressure $3.5x10^{-4}$mBar).

5.2 Analysis of Poly(butyl acrylate)

The ESI mass spectrum of PBA ionized with sodium chloride shows the presence of three singly and one doubly charged distributions with molecular weights from m/z 700 to 3200 (Figure 5.4). The major distribution, labelled A on the figure, has hydrogen and the chain transfer agent, dodecanethiol, as end groups. Singly and doubly charged ions of this distribution were observed (A and A^{2+}). The initiator is not a spectator in the polymerization since when the synthesis is done without AIBN, the same products are observed but the reaction is slower. The distribution labelled B in Figure 5.4 has hydrogen and butyl acrylate as end groups while distribution C has CTA and butylether.

CID was performed on the distribution A of PBA and the CID mass spectrum of $[PBA_8+Na]^+$ is shown in Figure 5.5. PBA ions also fragment along the backbone starting at the CTA terminal to produce a progression represented by $[128n+128+M]^+$. The losses of two butene molecules from the side chain were also observed.

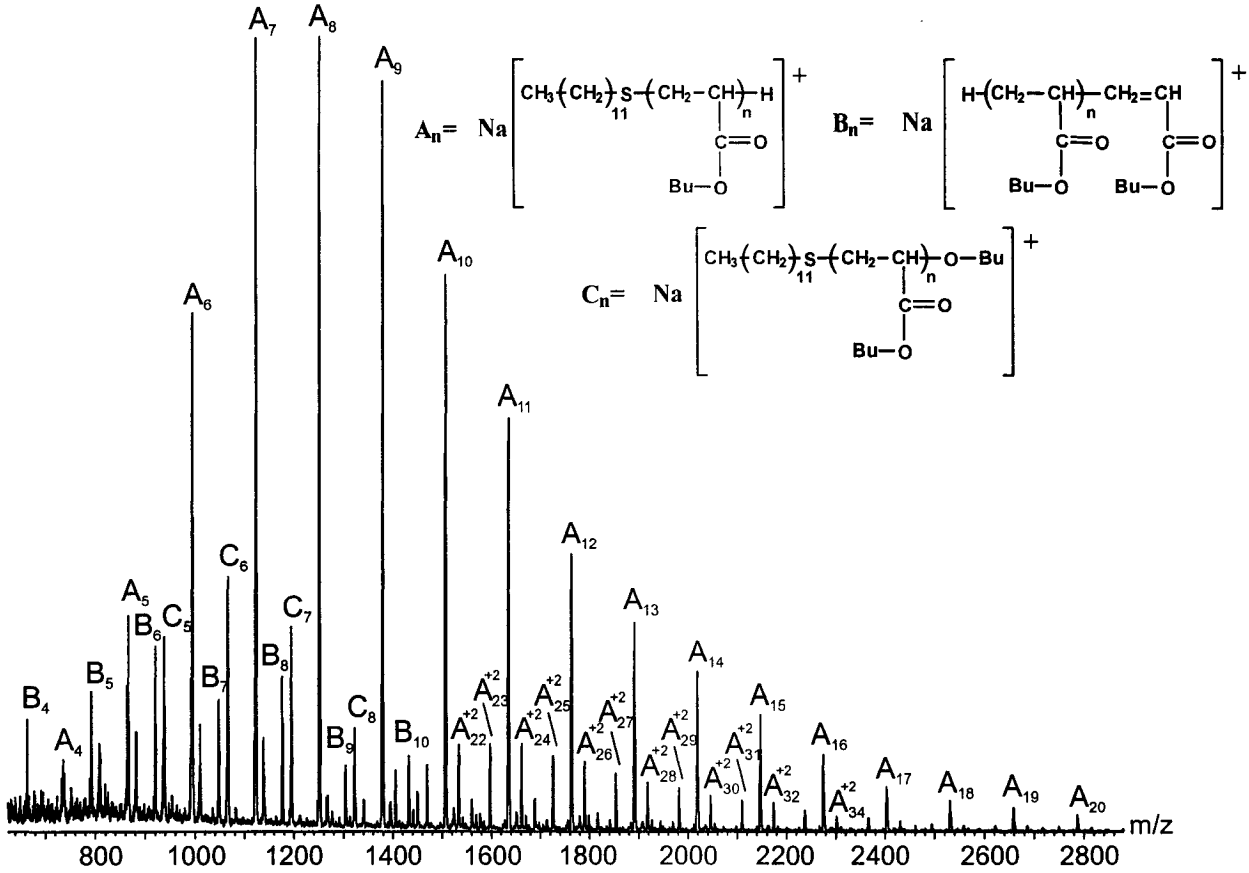

Figure 5.4: ESI mass spectrum of the PBA mixture ionized with sodium.

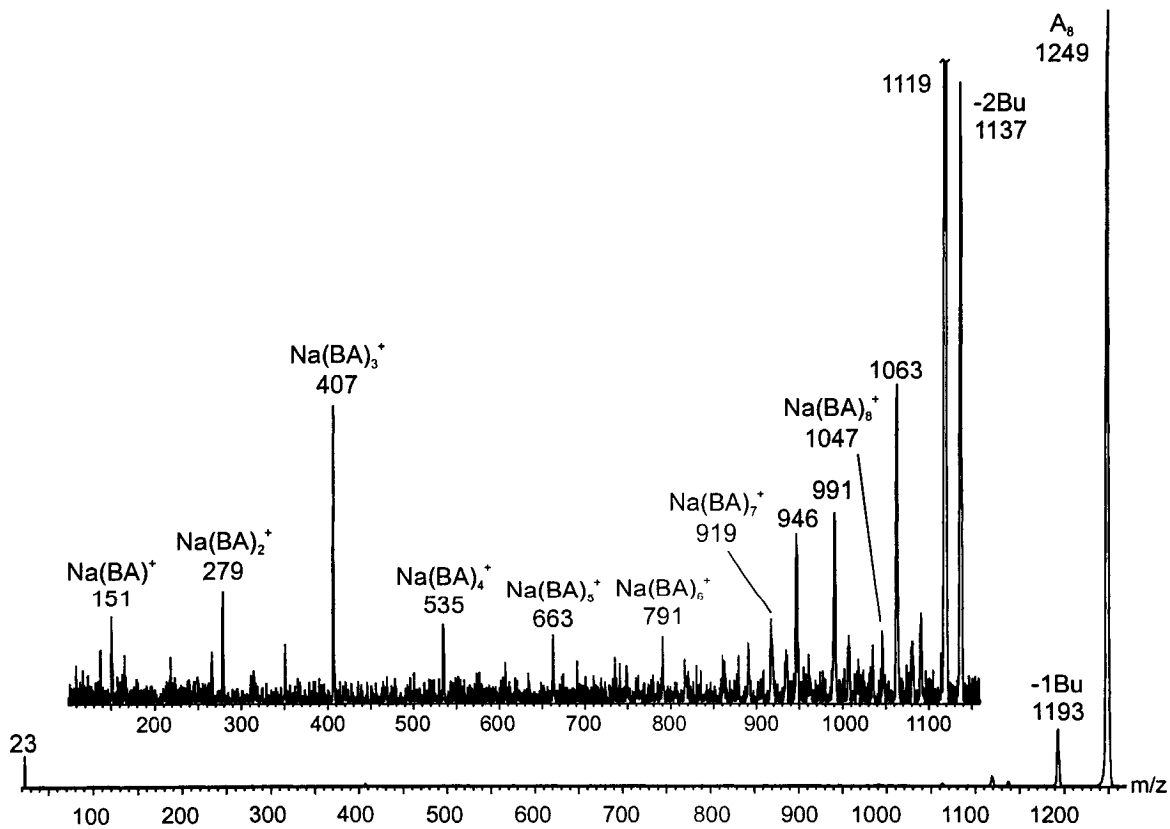

Figure 5.5: Tandem mass spectrum of $[PBA_8+Na]^+$ from distribution A (E_{Lab} = 90eV, collision gas pressure = $3.4x10^{-4}$mBar).

5.3 Analysis of Poly(vinyl acetate)

5.3.1 Mass spectrometry of Poly(vinyl acetate)

Figure 5.6 shows the ESI mass spectrum of the PVAc mixture ionized with lithium ions when the polymerization was stopped at 85% of completion. One polymer distribution is observed $[86n+69+Li]^+$ indicating that the end groups are hydrogen and isobutyronitrile (from the initiator of the polymerization). The peaks are separated by 86 mass units confirming that the repeat unit is vinyl acetate.

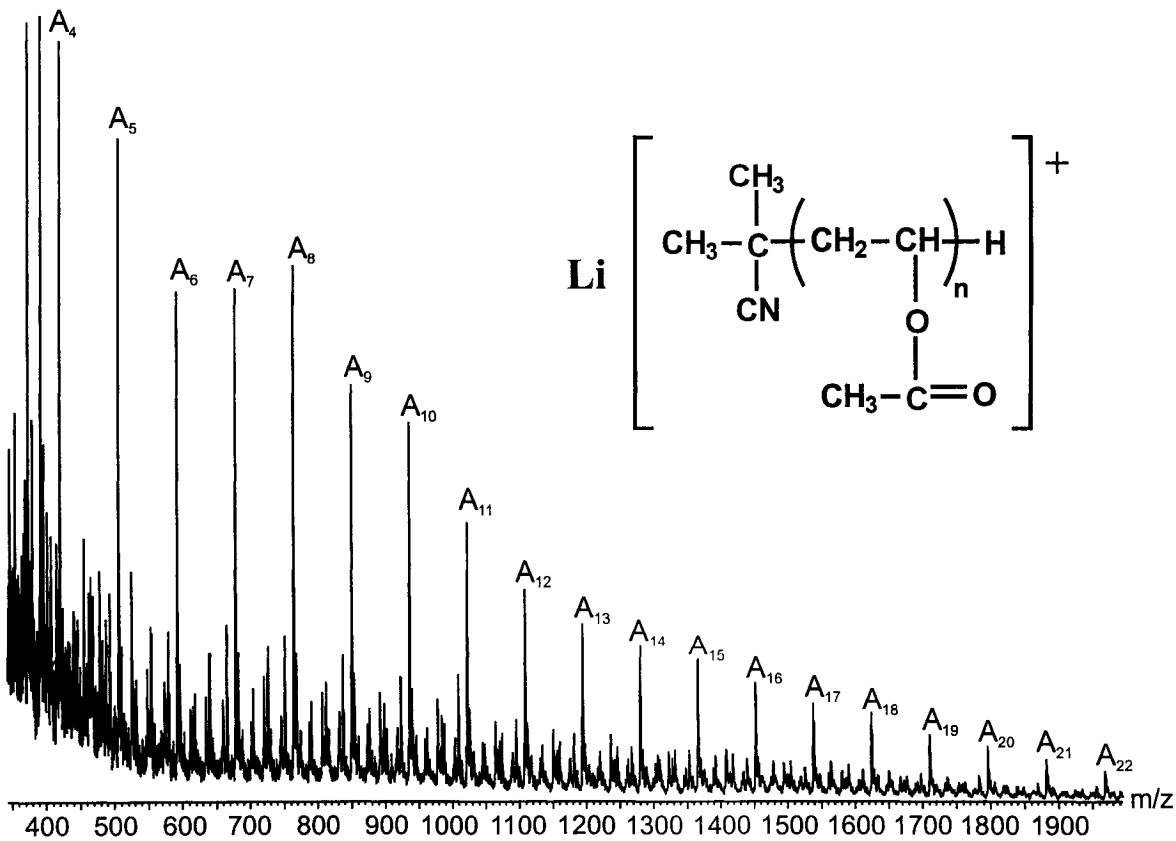

Figure 5.6: ESI mass spectrum of the PVAc mixture ionized with lithium.

CID mass spectrometry was carried out on the 4-mer to the 12-mer using either sodium or lithium ions to ionize the polymer. The CID mass spectrum of $[PVAc_5+Li]^+$ is shown in Figure 5.7. The mass spectrum shows acetic acid (AcH) loss from the polymer side chain. For the 5mer, five repetitive losses are observed as well as two losses of lithium acetate (AcLi) (m/z 260 and 200). The peak at m/z 200 corresponds to a polyene chain with hydrogen and isobutyronitrile as end groups. The oligomer can then lose the initiator terminus resulting in a fragment ion appearing at m/z 131. The fragment ions at m/z 260, 200, 131 do not contain a metal cation since when the ionization salt is changed from LiCl to NaCl, the mass of these ions do not shift (Figure 5.8) while the other peaks are shifted in m/z by the difference in mass between ^7Li and ^{23}Na. Therefore m/z 260, 200 and 131 have a positive charge on the polymer backbone. The fragmentation of $[PVAc_5+Li]^+$ is summarized in Figure 5.9. In the case of larger oligomers, most of the side chains are lost as acetic acids. The $[PVAc_9+Li]^+$ shown in Figure 5.10 loses eight acetic acids and three peaks due to the loss of lithium acetate. The polyene chains with and without the initiator end groups are at m/z 304 and 235 respectively.

The unlabelled peaks in the low mass range of each spectrum in Figures 5.7, 5.8 and 5.10 are independent of the salt used, meaning that they come from the fragmentation of the polyene chains. Pseudo MS^3 experiments on m/z 131 (resulting from skimmer-cone dissociation) showed peaks separated by 26 mass units consistent with the fragmentation of a carbocation chain with alternating single and double bonds.

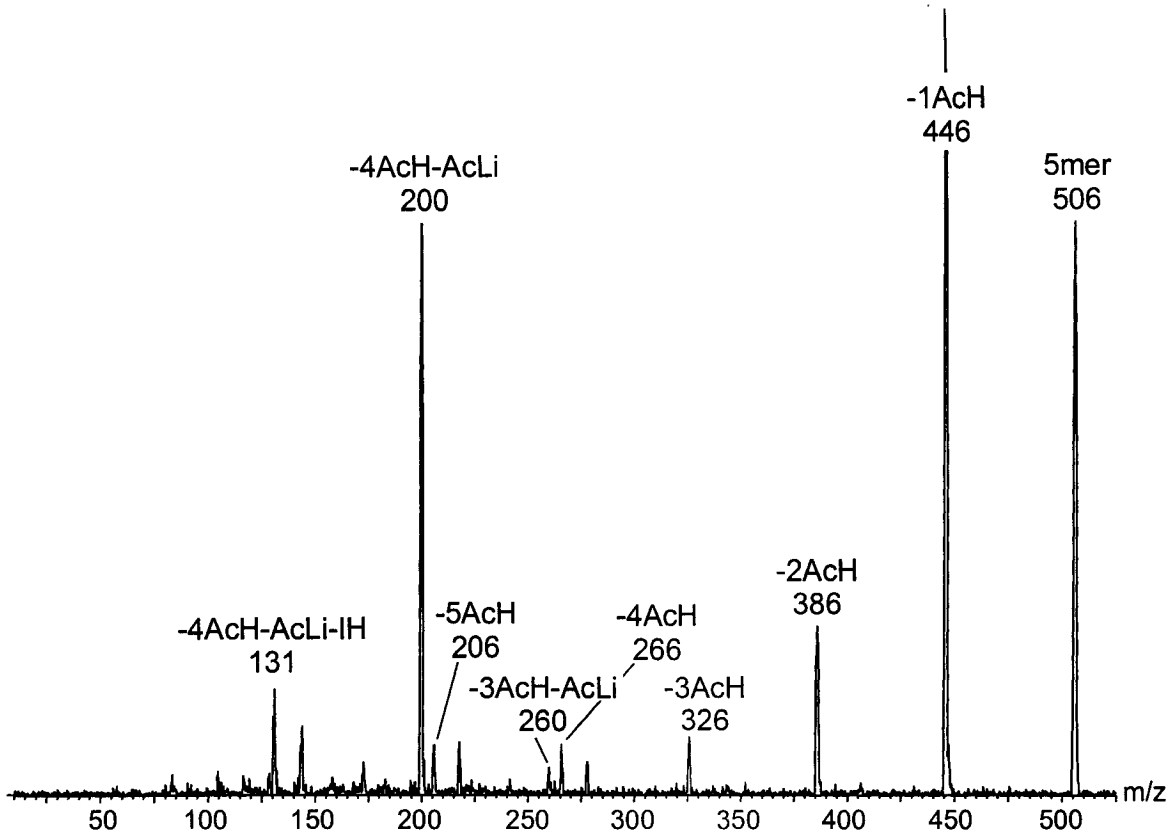

Figure 5.7: Tandem mass spectrum of $[PVAc_5+Li]^+$ (E_{Lab} = 26eV, collision gas pressure = $8x10^{-4}$mBar).

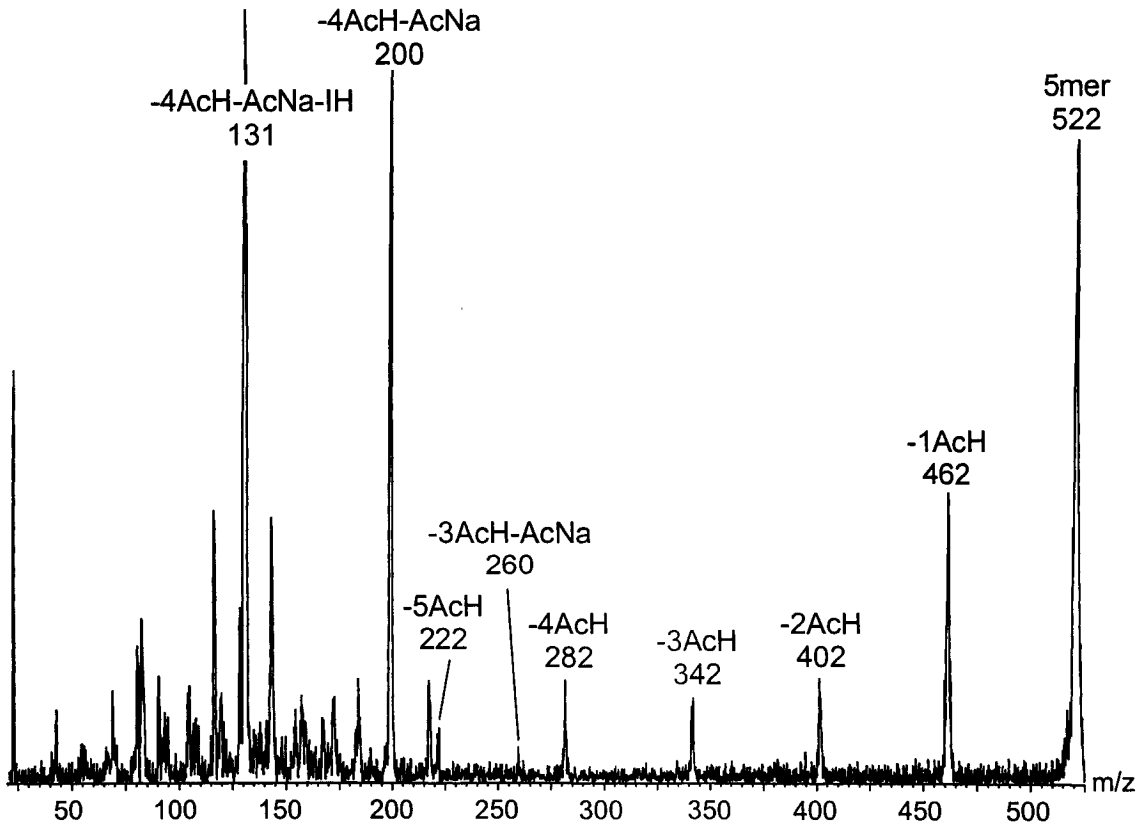

Figure 5.8: Tandem mass spectrum of $[PVAc_5+Na]^+$ (E_{Lab} = 60eV, collision gas pressure = $3.8x10^{-4}$mBar).

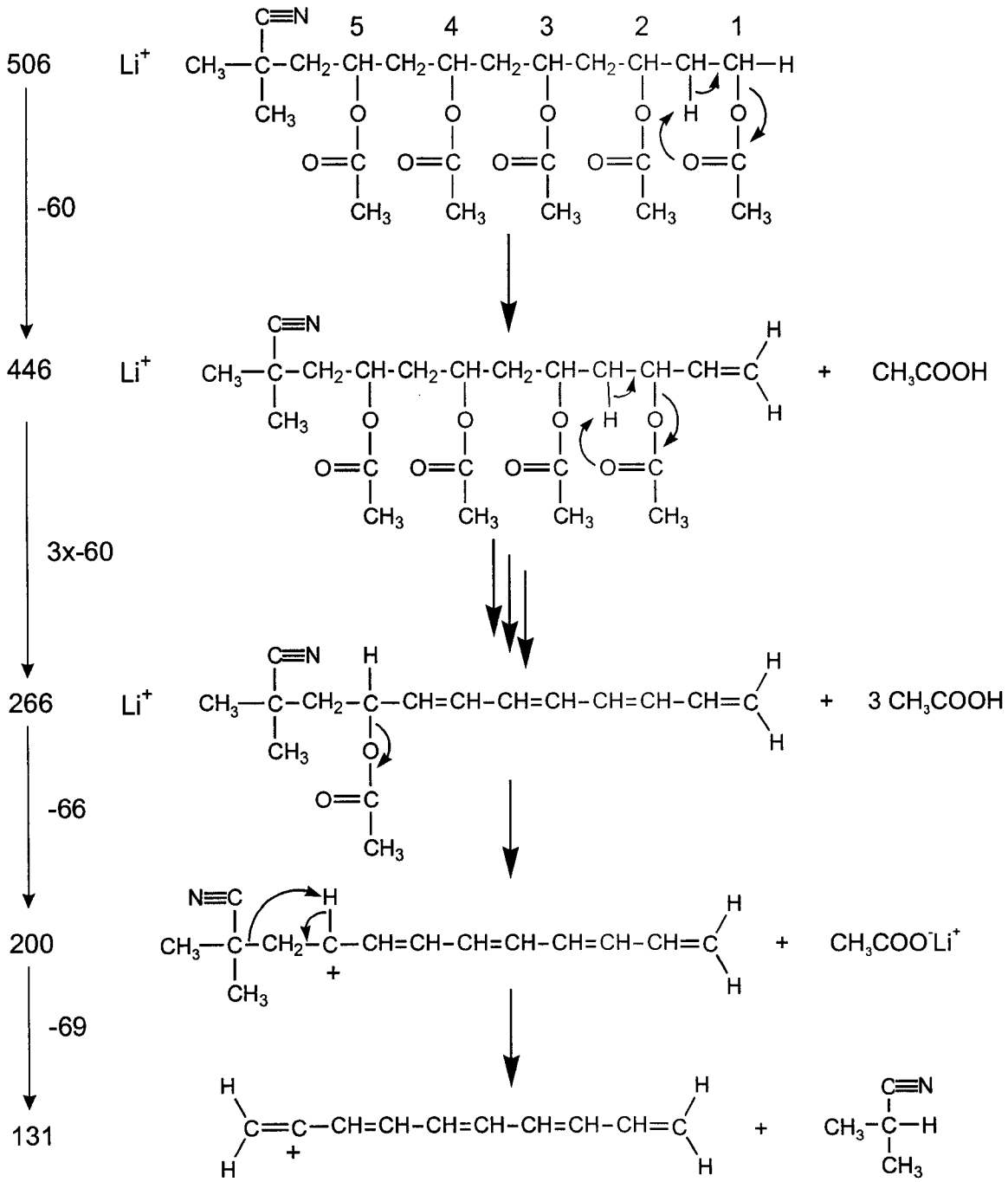

Figure 5.9: Proposed fragmentation pathway for $[VAc_5+Li]^+$

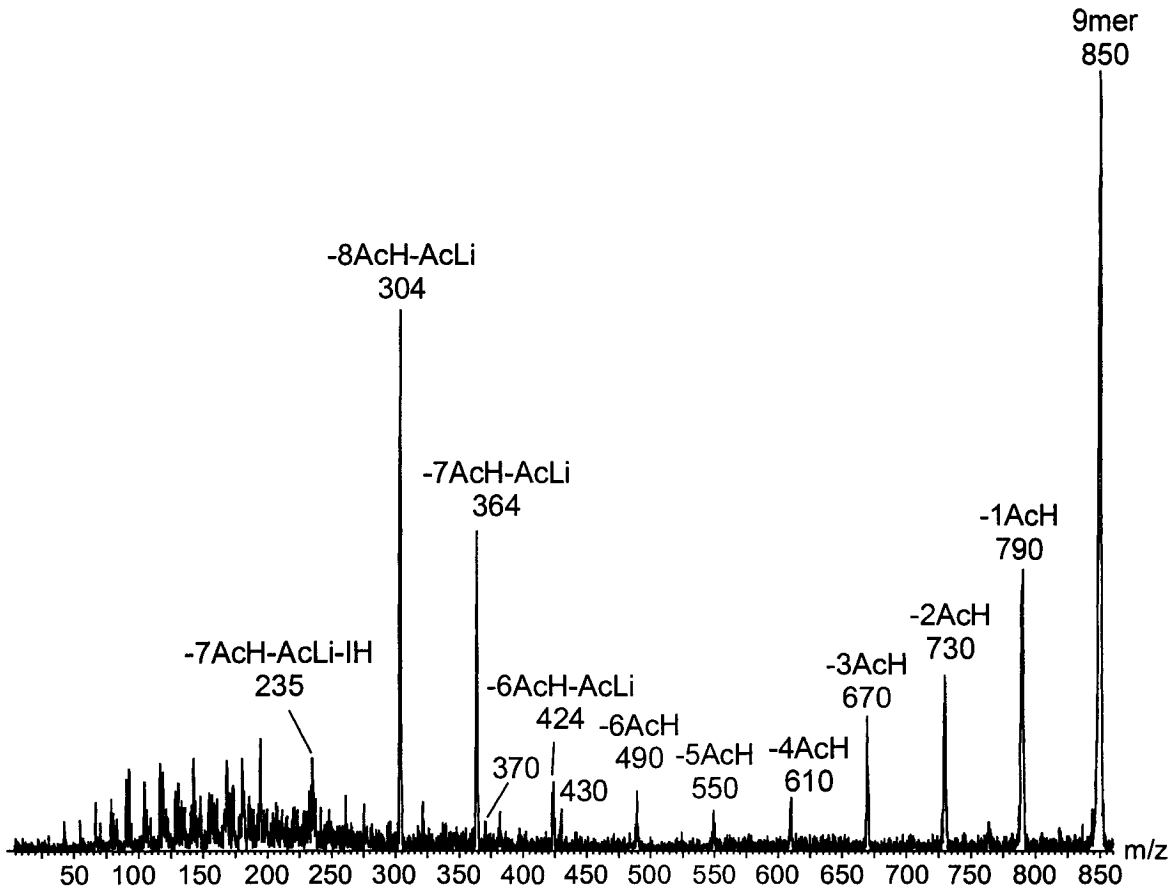

Figure 5.10: Tandem mass spectrum of $[PVAc_9+Li]^+$ (E_{Lab} = 70eV, collision gas pressure = $3.6x10^{-4}$mBar).

The loss of an ionizing metal ion prior to dissociation has been previously observed for poly(ethylene terephthalate).[5] According to Jackson et al. the loss of the metal in this case can be caused by the rigidity of the polymer resulting in weaker interactions between the heteroatoms of the polymer and the metal cation. In addition, fragments of low mass-to-charge ratio in the CID mass spectrum of poly(styrene) do not contain metal ion adducts.[4, 6, 7] These peaks were more intense when a larger metal such as ^{107}Ag or ^{63}Cu was used to ionize the polymer. It was proposed that fragment ions with lower m/z ratio are less stable because of the weaker binding affinity with the metal ion. These hypotheses cannot be extended to PVAc where, as shown in Figure 5.10, the 9mer

produced large oligomeric fragments without metal ion adducts (m/z 235, 304, 364 and 424).

A study of the relative abundance of the fragment ions versus collision energy was made at different collision gas pressures (4, 8 and $12x10^{-4}$ mBar) and is shown in Figure 5.11 for the $[PVAc_5+Li]^+$ ion at $8x10^{-4}$ mBar. The highest abundance process (up to 2.2 eV) is the loss of one acetic acid to produce the peak with m/z 446. The second major fragment at m/z 200 corresponds to the loss of four acetic acid molecules and a metal acetate. This signal becomes dominant at a center-of-mass collision energy of 2.2 eV when the collision gas pressure is $8x10^{-4}$ mBar. This fragment appears before the emergence of peaks from multiple losses of acetic acid. The next dominant peak is the polyene chain without the initiator terminus (m/z 131). When lower collision gas pressures are used, the overall pattern stays the same but the maximum intensity of the distributions are shifted to higher center-of-mass collision energy.

5.3.2 Molecular modeling of Poly(vinyl acetate)

The optimized structures of $[PVAc_5+Li]^+$ and its fragmentation product ions are shown in Figure 5.12 and the relative energies can be found in Table 5.1. The energy needed for the loss of acetic acid was investigated from the five different positions on the 5-mer, starting at the hydrogen end with position 1 and finishing at the isobutyronitrile end with position 5 as shown in Figure 5.9. The resulting structures were optimized using AM1 and their energies were calculated using HF/6-31+G(d). As shown in Table

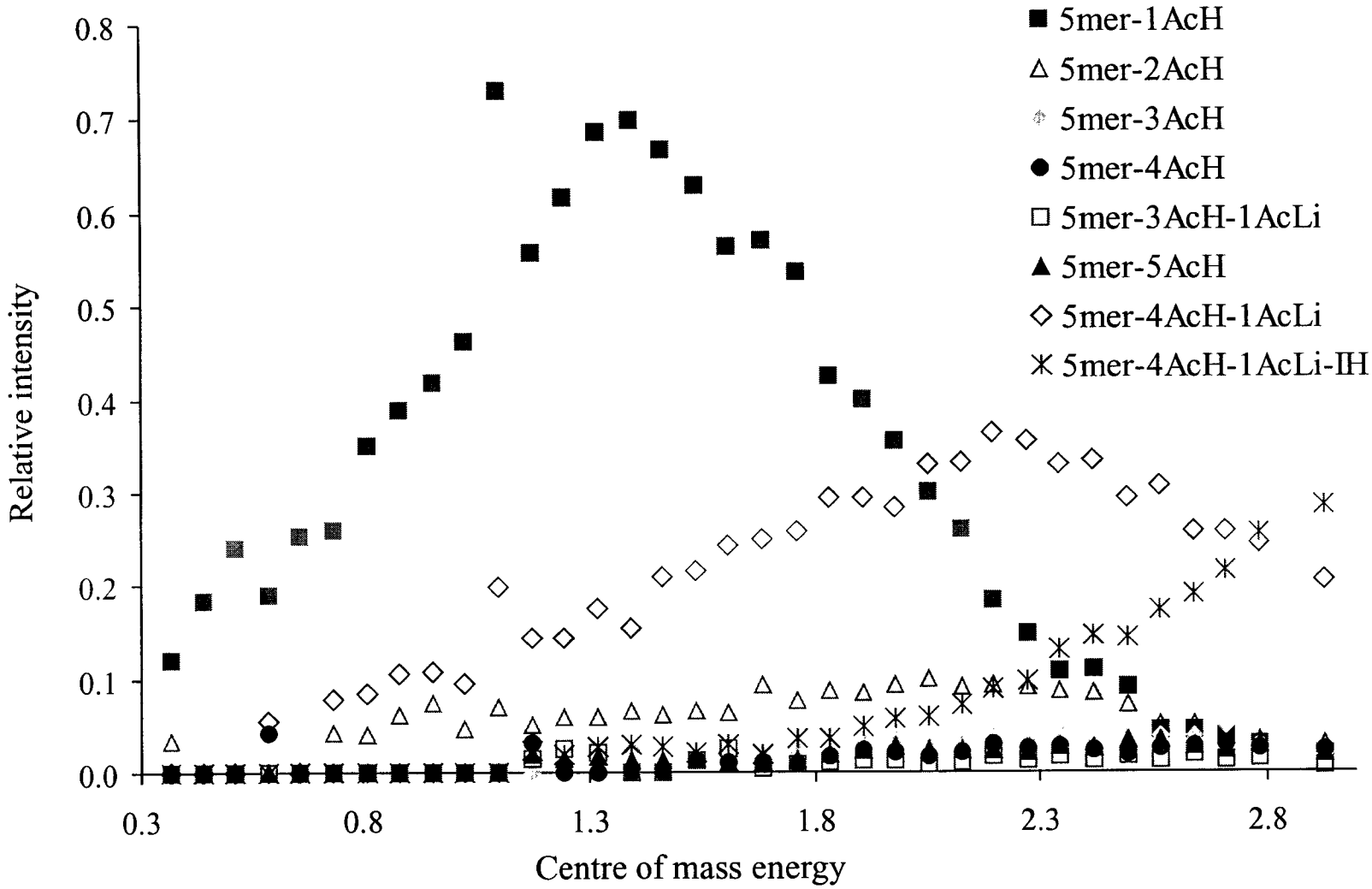

Figure 5.11: CID of $[PVAc_5+Li]^+$ at a collision gas pressure of $8x10^{-4}$ mBar as a function of collision energy.

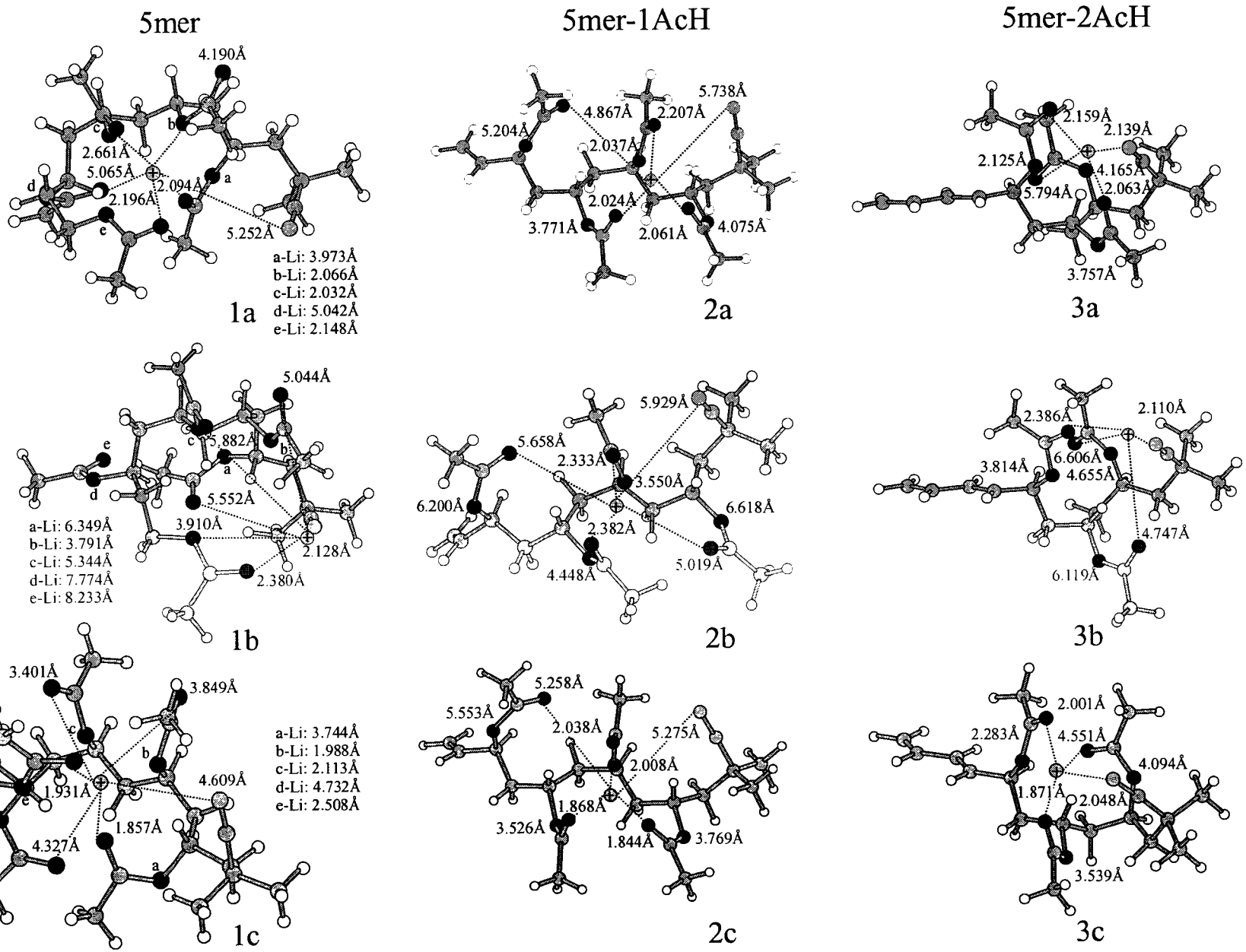

Figure 5.12: The optimized structure of $[PVAc_5+Li]^+$ and its fragments from (a) MM/MD, (b) AM1 and (c) B3-LYP/3-21G optimization. Lithium atoms are labeled with a "+" on the atom and carbon atoms with a positive charge have a "+" beside them.

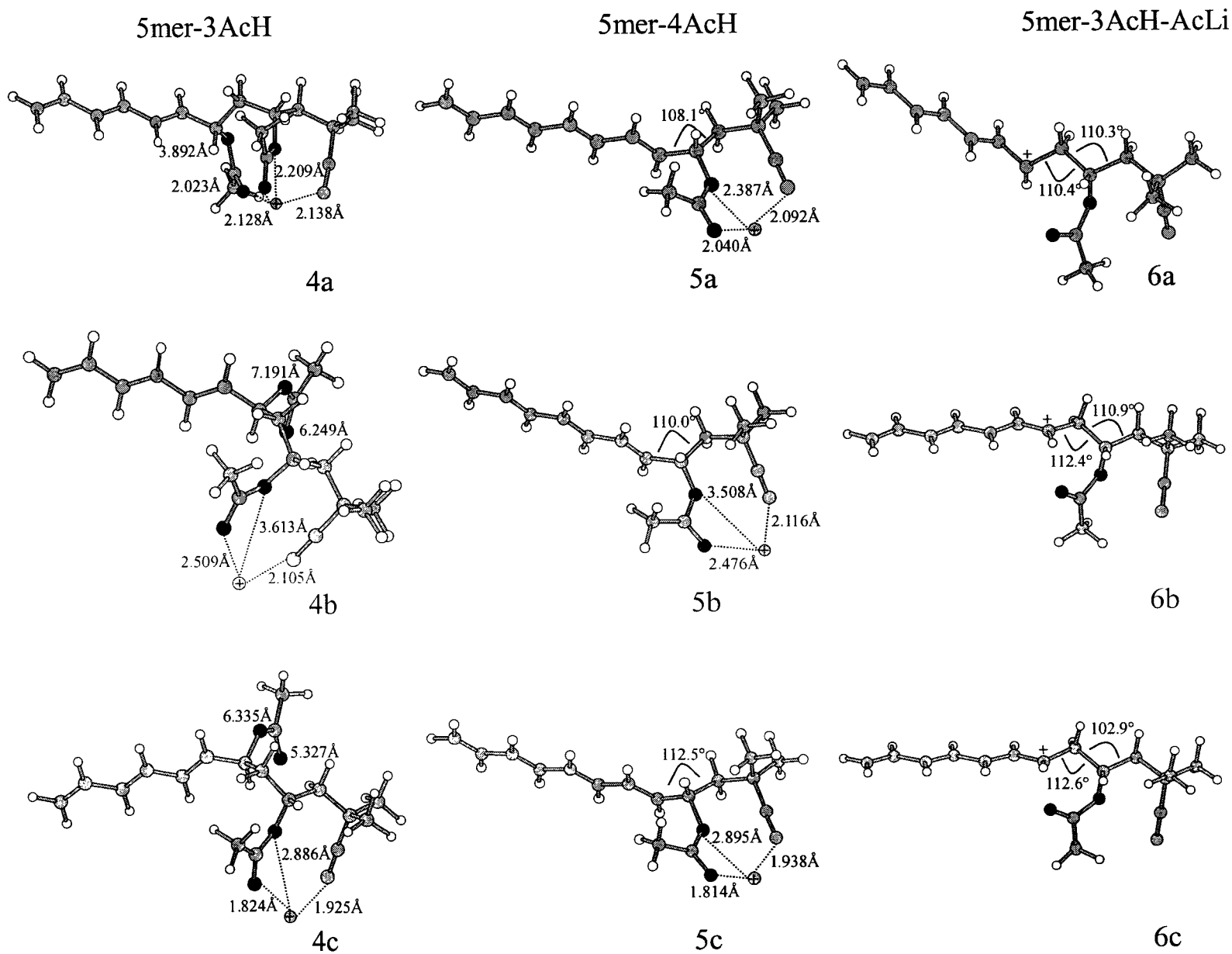

Figure 5.12 cont'd: The optimized structure of $[PVAc_5+Li]^+$ and its fragments from (a) MM/MD, (b) AM1 and (c) B3-LYP/3-21G optimization. Lithium atoms are labeled with a "+" on the atom and carbon atoms with a positive charge have a "+" beside them.

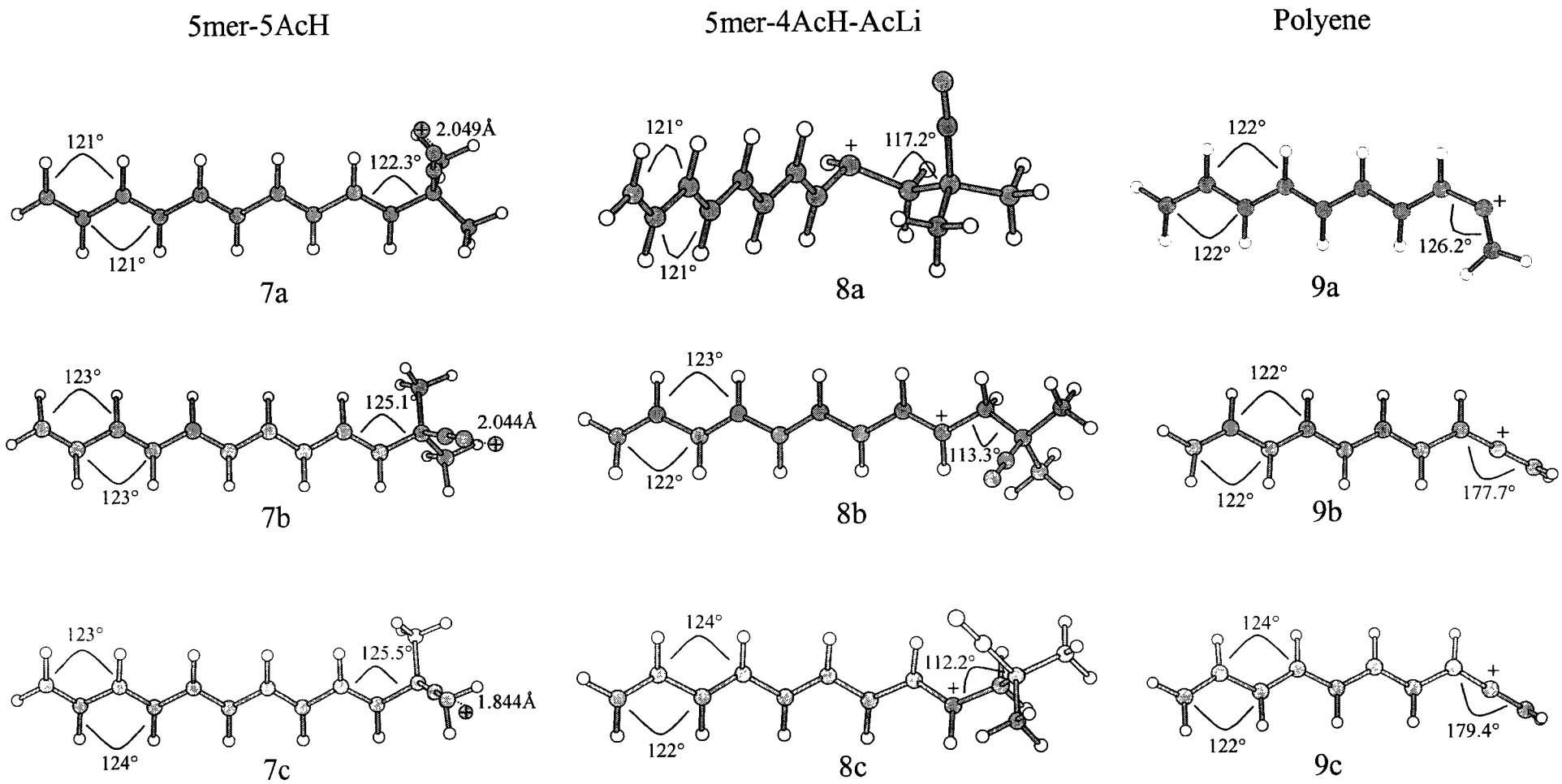

Figure 5.12 cont'd: The optimized structure of $[PVAc_5+Li]^+$ and its fragments from (a) MM/MD, (b) AM1 and (c) B3-LYP/3-21G optimization. Lithium atoms are labeled with a "+" on the atom and carbon atoms with a positive charge have a "+" beside them.

Table 5.1: Calculated relative energies for MM/MD, AM1 and B3-LYP structures of the decomposition products of poly(vinyl acetate) ionized with lithium.

Structure	Mass (Da)	Relative energies (kJ/mol)							
		MM/MD structures			AM1 structures			B3-LYP/3-21G structures	
		MM/MD	HF/ 6-31+G(d)	B3LYP/ 6-31+G(d)	AM1	HF/ 6-31+G(d)	B3LYP/ 6-31+G(d)	B3LYP/ 3-21G	B3LYP/ 6-31+G(d)
5mer	506	0	0	0	0	0	0	0	0
[5mer-1AcH] + 1AcH	446	57	49	52	189	18	39	155	22
[5mer-2AcH] + 2AcH	386	162	150	132	95	86	90	304	106
[5mer-3AcH] + 3AcH	326	274	217	194	123	146	143	546	188
[5mer-4AcH] + 4AcH	266	391	324	288	141	179	165	636	205
[5mer-3AcH-1AcLi] + 3AcH + 1AcLi	260	-148	747	661	345	286	261	726	290
[5mer-5AcH] + 5AH	206	463	474	428	162	258	240	877	332
[5mer-4AcH-1AcLi] + 4AcH+1AcLi	200	-231	857	708	329	248	237	828	301
[Polyene] + 4AcH + 1AcLi + InH	131	-70	980	794	459	389	358	955	405

5.2 the lowest energy product corresponds to the loss of acetic acid closest to the hydrogen end (1). It is believed that the sequential loss of acetic acid occurs from neighbouring positions since the product ion will benefit from a conjugated double bond structure. For all the fragments discussed in Table 5.1, the losses were assumed to start at position 1.

Table 5.2: Calculated relative energies for the fragment 5mer-1AcH after AM1 optimization

Structure	Position of AcH	Relative energies (kJ/mol)† HF/6-31+G(d) // AM1
[5mer-1AcH] + 1AcH	1	21.9
[5mer-1AcH] + 1AcH	2	55.4
[5mer-1AcH] + 1AcH	3	29.9
[5mer-1AcH] + 1AcH	4	25.1
[5mer-1AcH] + 1AcH	5	47.0

† The energies are relative to the 5mer

It is clear from Table 1 that the relative energies of the fragments obtained from MM/MD are unreliable as might be expected from the molecular mechanics treatment of gas-phase ions. In addition, MM/MD alone does not seem to provide reliable geometries for further single-point energy calculations. The relative energies for the reactions involving a loss of lithium acetate are particularly poorly represented at this level of theory of geometry optimization. The relative energies using AM1 geometries with HF/6-31+G(d) and B3-LYP/6-31+G(d) single-point energy calculations are slightly lower than the AM1 energies. The relative energies using DFT geometries with B3-LYP/3-21G were higher then the AM1 energies but the B3-LYP/6-31+G(d) single-point

energy calculations give energies approximately equal to the AM1 results. The B3-LYP/6-31+G(d)//B3-LYP/3-21G structures are believed to be more reliable results but the AM1 results still present an interest because of the lower calculation time required.

The gas phase conformation of ionized poly(vinyl acetate) is similar to that of PMMA with the side chains of the polymer coordinating to the metal ion. When the 5mer ion was optimized by MM/MD, all ten oxygen atoms and the nitrogen atom of the initiator end group coordinate the Li^+ ion. The distance between the oxygen atoms and the Li^+ range from 2.03 to 5.07 Å. When the structure is optimized by AM1, the Li^+ moves above the molecule, and only four oxygen atoms are at less then 5.07 Å from Li^+. The nitrogen atom on the initiator-terminal is now closer to the metal ion (2.12 compared to 5.25 Å at MM/MD). The B3-LYP structure shows the shortest distances between the lithium cation and the oxygen atoms (1.86 to 4.73 Å). The Li^+ is surrounded by the side chains of the polymer.

The structure for 5mer-AcH, m/z 446, exhibits the Li^+ moving away from the double bond, but also further from the nitrogen atom of the initiator end group. For the AM1 structure, the oxygen atoms are generally further from the Li^+ ion compared to the MM and DFT structures. Unlike structures 2a and 2c from Figure 5.12, the oxygen atoms on the side chain adjacent to the isobutyronitrile end group in 2b are far from the metal ion. The structures and trends are similar for the fragment at m/z 386, corresponding to the loss of two terminal acetic acid molecules.

For the fragment at m/z 326 (loss of three terminal acetic acid molecules), there is more rigidity, limiting the coordination of the salt for the DFT and AM1 structures compared to the MM/MD structure. Only one side chain and the nitrogen atom stabilize the cation since the oxygen atoms of the other side chain are more then 5.3 Å from the cation. The structures for the fragment at m/z 266, corresponding to the loss of four acetic acid molecules are similar to those of m/z 326. In the fragment ion at m/z 206, corresponding to the loss of five acetic acid molecules, only the nitrogen of the isobutyronitrile remains to complex the Li^+ ion. The structures from the three levels of theory are almost identical except for the orientation of the isobutyronitrile terminal in structure 7a and the slightly smaller distance between the nitrogen and the Li^+ in the DFT structure 7c.

The fragments at m/z 260 and 200 (loss of three or four acetic acid molecules and one lithium acetate) are less planar in the MM/MD optimization compare to the AM1 and DFT optimizations. According to the bond angle, the carbocation of the polyene fragment (m/z 131) has a sp^2 character when optimized by MM/MD and sp character when AM1 or B3-LYP is used.

The potential energy surface (PES) in Figure 5.13 shows the relative energies obtained at the B3-LYP/6-31+G(d)//B3-LYP/3-21G level of theory. The PES shows regular steps of around 100 kJ/mol for the losses of acetic acid molecules except for the loss of the first (m/z 446) and fourth acetic acid (m/z 266) which are only around 20 kJ/mol higher than the 5mer and the reaction leading to $[5mer\text{-}3AcH]^+$ (m/z 326).

According to the relative energy diagram, the reaction leading to the loss of a fourth acetic acid molecule was significantly lower in energy than the reaction leading to the loss of lithium acetate. This is consistent with the CID mass spectra in which m/z 266 always predominates over m/z 260. However, once only a single acetic acid remains on the polymer, it is preferentially lost as a metal acetate (Figures 5.7 and 13). The polyene ion (m/z 131) is the highest energy channel on the surface. The early appearance of m/z 200 and m/z 131 in the CID mass spectra can be explained if there is a high activation energy required for the 1,5-hydrogen rearrangement resulting in the loss of acetic acid. The 1,5-hydrogen rearrangement is known to require up to 175 to 200 kJ/mol in pyrolysis experiments.[8, 9] In the present system, the loss of acetic acid does not appear to be assisted by the metal cation and so, similar barriers can be expected. It is also known that the stability of the resulting ene product affects the barrier height in these reactions. As the polymer loses acetic acid, a conjugated polyene structure is obtained that may successively lower the transition state to acetic acid loss.

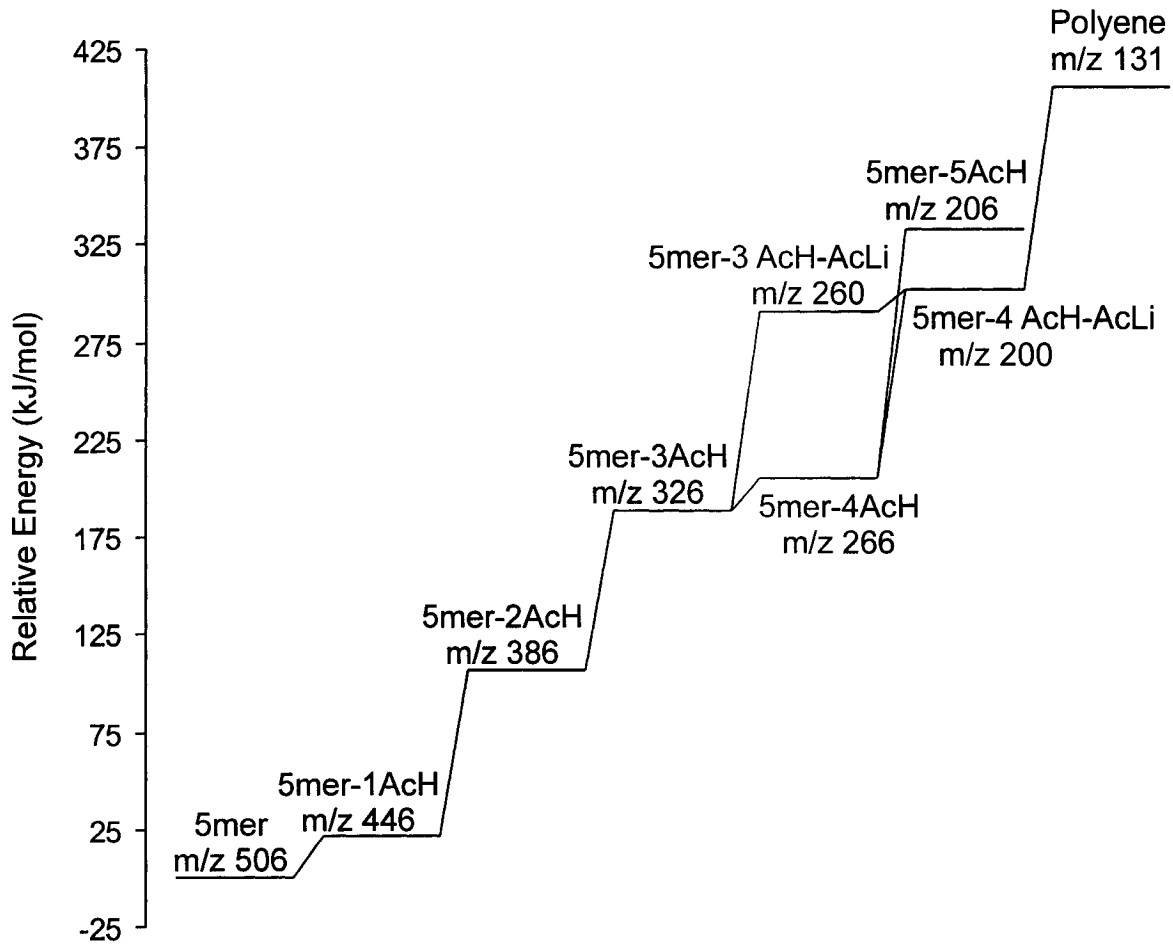

Figure 5.13: Potential energy surface for the decomposition of poly(vinyl acetate) ionized with lithium using the B3-LYP/6-31+G(d)//B3-LYP/3-21G fragment geometries.

Another explanation may be in the "sudden death" approximation in chemical kinetics. Futrell and co-workers[10] have observed and modeled the shattering of peptide ions in collision-induced dissociation experiments involving surfaces. This approximation assumes that the energy deposited into the projectile ion is not statistically randomized among the internal modes (rotations and vibrations) of the ion, but rather localized leading to dissociation channels that would otherwise be inaccessible.

The loss of a dimer of acetic acid was also considered but the resulting relative energies do not correspond to the mass spectrometry results (Table 5.3). If acetic acid is lost as a dimer, it might be expected that the CID mass spectra would exhibit stronger peaks due to these processes, but this is not observed. Indeed, the reaction for loss of one acetic acid molecule is higher in energy than for the loss of a dimer, but the mass spectra in Figures 5.7, 8 and 10 show a larger abundance for VAc-1AcH. The same pattern is observed for VAc-$(AcH)_2$ -1AcH and VAc-2$(AcH)_2$.

Table 5.3: Calculated relative energies B3-LYP/6-31+G(d)//B3-LYP/3-21G structures of the decomposition products of poly(vinyl acetate) ionized with lithium considering dimer losses.

Structure	Mass (Da)	Relative energies (kJ/mol) B3-LYP/6-31+G(d)// B3-LYP/3-21G
5mer	506	0
[5mer-AcH] + AcH	446	22
[5mer-AcH_2] + AcH_2	386	3
[5mer-AcH-AcH_2] + AcH+AcH_2	326	86
[5mer-2AcH_2] + 2AcH_2	266	-1
[5mer-AcH-AcH_2-AcLi] + AcH+AcH_2+AcLi	260	187
[5mer-AcH-2AcH_2] + AcH+2AcH_2	206	127
[5mer-2AcH_2-1AcLi] + 2AcH_2+AcLi	200	199
[Polyene] + 2AcH_2+AcLi+InH	131	200

5.4 Conclusion

Electrospray ionization tandem mass spectrometry of PMMA ions shows them to fragment along the polymer backbone by either homolytic cleavage or 1,5-hydrogen rearrangement. When PBA ions fragment by cleavage after the CTA terminal group and PVAc ions fragment by the sequential loss of acetic acid from the polymer backbone. The mechanism of dissociation of PVAc ions was subject of a computational study, the mass spectra can be understood in terms of the relative product energies and transition for 1,5-sigmatropic rearrangements.

References

(1)Busfield, W. K.; Jenkins, I. D.; Nakamura, T.; Monteiro, M. J.; Rizzardo, E.; Sayama, S.; Tang, S. H.; Van Le, P.; Zayas-Holdsworth, C. I. *Polym. Adv. Technol.* **1998**, *9*, 94.

(2)Gidden, J.; Jackson, A. T.; Scrivens, J. H.; Bowers, M. T. *Int. J. Mass Spectrom.* **1999**, *188*, 121.

(3)Jackson, A. T.; Yates, H. T.; Scrivens, J. H.; Green, M. R.; Bateman, R. H. *J. Am. Soc. Mass Spectrom.* **1997**, *8*, 1206.

(4)Scrivens, J. H.; Jackson, A. T.; Yates, H. T.; Green, M. R.; Critchley, G.; Brown, J.; Bateman, R. H.; Bowers, M. T.; Gidden, J. *Int. J. Mass Spectrom.* **1997**, *165/166*, 363.

(5)Jackson, A. T.; Yates, H. T.; Scrivens, J. H.; Critchley, G.; Brown, J.; Green, M. R.; Bateman, R. H. *Rapid Commun. Mass Spectrom.* **1996**, *10*, 1668.

(6)Jackson, A. T.; Yates, H. T.; Scrivens, J. H.; Green, M. R.; Bateman, R. H. *J. Am. Soc. Mass Spectrom.* **1998**, *9*, 269.

(7)Jackson, A. T.; Bunn, A.; Hutchings, L. R.; Kiff, F. T.; Richards, R. W.; Williams, J.; Green, M. R.; Bateman, R. H. *Polymer* **2000**, *41*, 7437.

(8)Lin, M. C.; Laidler, K. J. *Trans. Faraday Soc.* **1968**, *64*, 927.

(9)Wieder, G. M.; Marcus, R. A. *J. Chem. Phys.* **1962**, *37*, 1835.

(10) Laskin, J.; Bailey, T. H.; Futrell, J. H. *J. Am. Chem. Soc.* **2003**, *125*, 1625.

Chapter six

RESULTS AND DISCUSSION: COPOLYMERIZATION

The dissociation of the synthetic homopolymers poly(butyl acrylate), poly(methyl methacrylate) and poly(vinyl acetate) was investigated by electrospray-ionization tandem mass spectrometry. Based on these results it was possible to use tandem mass spectrometry to sequence three copolymers produced by free radical polymerization (PBA/PVAc, PBA/PMMA and PMMA/PVAc).

6.1 Analysis of Poly(butyl acrylate/vinyl acetate) (PBA/PVAc)

The copolymer was produced with both 7% w/w BA, 17% w/w of VAc and with 11% of each monomer. Similar distributions of products were observed by mass spectrometry with both reaction conditions. The mass spectrum of the copolymer from the 7/17% mixture at 29 % of completion is shown in Figure 6.1. The composition does change over the course of the reaction because of the large difference between the reactivity ratios (r) of BA and VAc (Table 6.1).

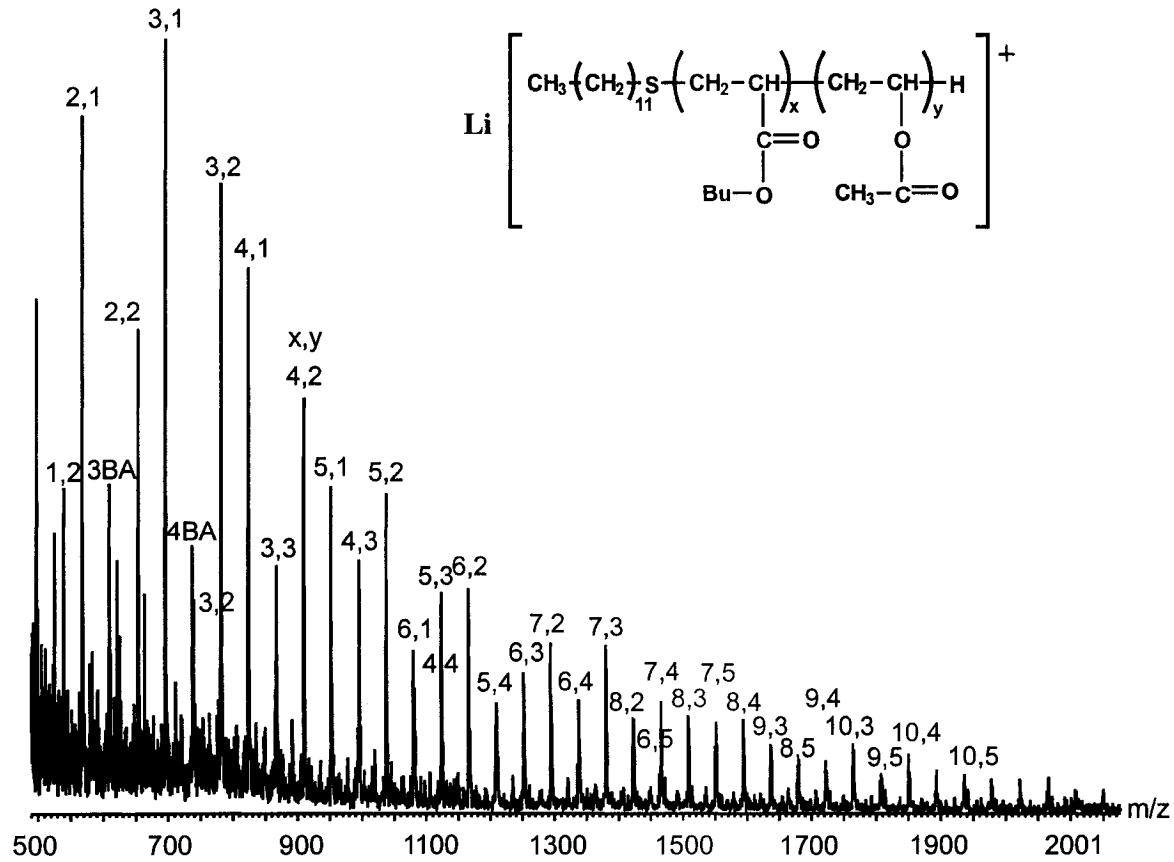

Figure 6.1: ESI mass spectrum copolymers of PBA/PVAc ionized with lithium.

Table 6.1: Reactivity ratios of monomers.

Copolymer composition (r_1- r_2)	Reactivity ratio			Expected copolymer
	r_1	r_2	r_1r_2	
BA-VAc[1]	5.938	0.026	0.154	Homopolymer of BA
BA-MMA[2]	0.297	1.789	0.531	Random
MMA-Vac[2]	24.0254	0.02611	0.6272	Homopolymer of MMA

(1) Jovanovic, R.; Dubé, M. A. *J Appl Polym Sci* **2001**, *82*, 2958.
(2) Dubé, M. A.; Penlidis, A. *Polymer* **1995**, *36*, 587.

Initially, BA reacts with a small portion of VAc to produce homopolymers of BA (A_n) and copolymers of PBA/PVAc. The mass spectrum of PBA/PVAc after 29% of completion shows six different distributions: homopolymers of BA (A_n) and five copolymer distributions having various numbers of BA and from one to five units of VAc

(x,y in Figure 6.1). The BA is consumed early in the reaction and when the reaction reaches completion, the polymer mixture is dominated by homopolymers of VAc. The end groups of the copolymers are a hydrogen atom and CTA (according to the mass shift when dodecanethiol is exchange for butanethiol). CID experiments were performed on all the copolymer distributions in order to determine their sequence. Figures 6.2 and 6.3 show the CID mass spectra of $[PBA_4/PVAc_1+Li]^+$ and $[PBA_4/PVAc_2+Li]^+$.

The amount of VAc in the copolymer can be determined by considering the losses of acetic acid molecules; the presence of BA is confirmed by butene losses. Partial information about the sequence is obtained because fragment ions resulting from backbone cleavage between monomers of BA are also observed. Fragments without CTA and metal cation were observed in the low mass region (they were identify by the exchange of CTA and salts). Some of these fragments form progressions with 28 Da between peaks corresponding to the fragmentation of an alkene chain. In the mass spectrum of $[PBA_4/PVAc_1+Li]^+$ (Figure 6.2) the fragments m/z 361 and 489 have a difference of 128 Da. The same peaks are observed in $[PBA_4/PVAc_2+Li]^+$ (Figure 6.3) at m/z 447 and 575, their mass is 86 Da larger (corresponding to the mass of one VAc). These fragments contain lithium but their mass remains constant when butanethiol is used as CTA. The fragment m/z 575 from $[PBA_4/PVAc_2+Li]^+$ and m/z 489 from $[PBA_4/PVAc_1+Li]^+$ represent the loss of the dodecanethiol end group, and the loss of AcH and butene from the copolymer side chain.

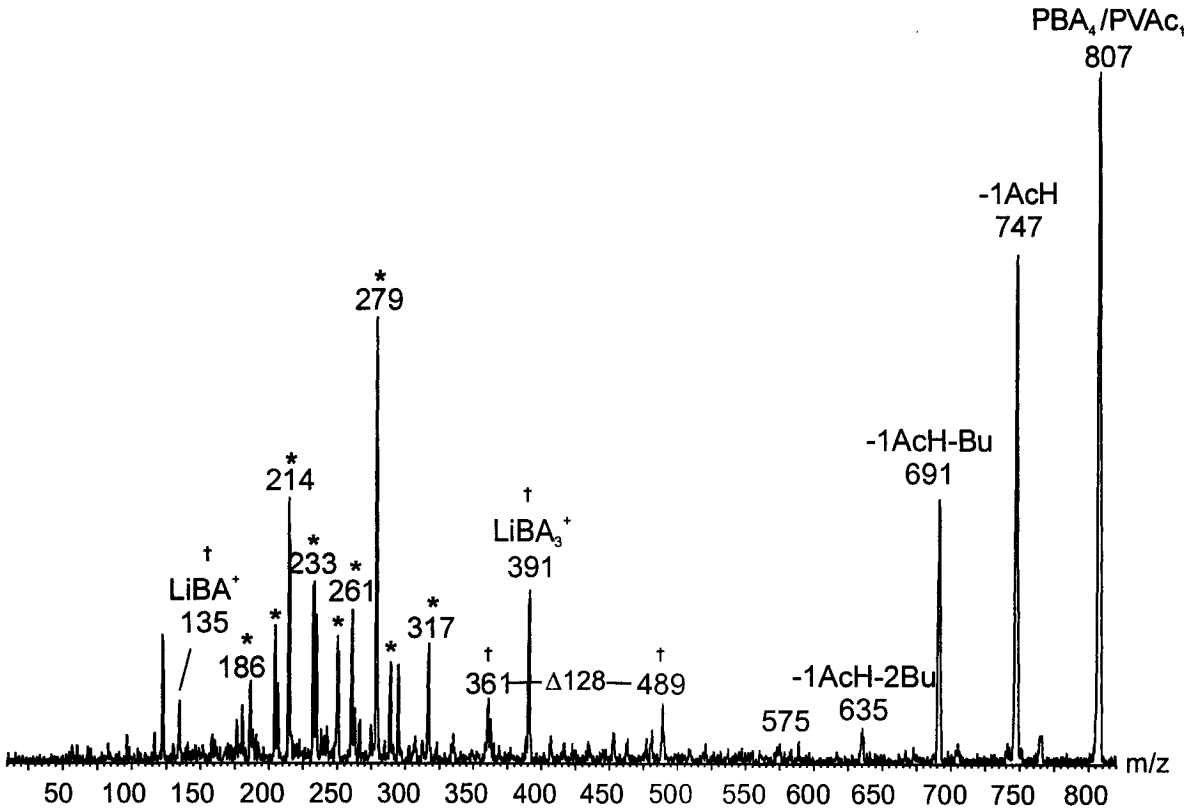

Figure 6.2: Tandem mass spectrum of $[PBA_4/PVAc_1+Li]^+$ (E_{Lab} = 55eV, collision gas pressure = $4.8x10^{-4}$mBar). The peaks without CTA are labelled with (†) and the peaks without the metal cation and CTA are labelled with (*).

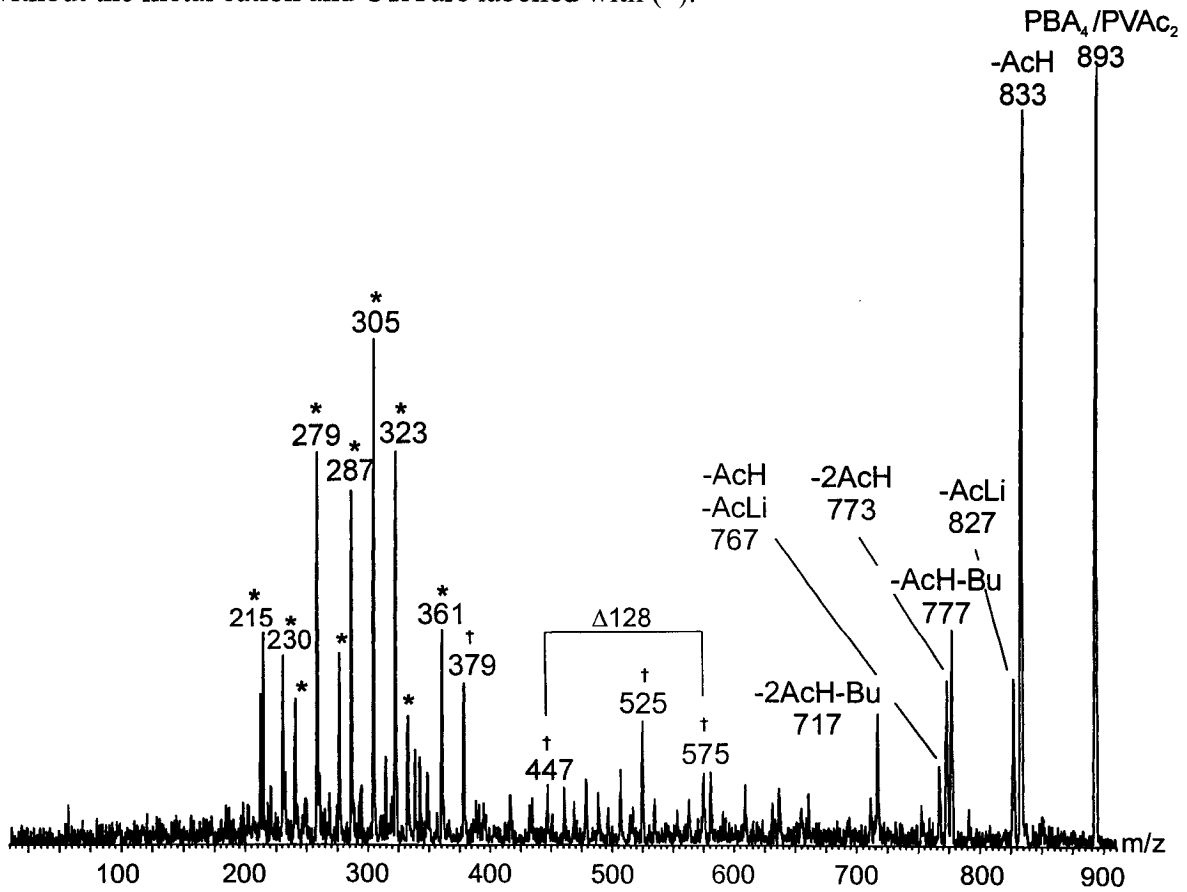

Figure 6.3: Tandem mass spectrum of $[PBA_4/PVAc_2+Li]^+$ (E_{Lab} = 40eV, collision gas pressure = $5.7x10^{-4}$mBar). The peaks without CTA are labelled with (†) and the peaks without the metal cation and CTA are labelled with (*).

6.2 Poly(butyl acrylate/methyl methacrylate) (PBA/PMMA).

This copolymer was produced with 5% w/w of BA and 5% w/w MMA. Similar distributions of products were observed by mass spectrometry over the course of the reaction. The mass spectrum of the copolymer mixture after 10% completion is shown in Figure 6.4. Four different distributions are observed with one to four units of BA and various numbers of MMA (x,y in Figure 6.4). As for PBA/PMMA, the end groups of the copolymers are a hydrogen atom and the CTA.

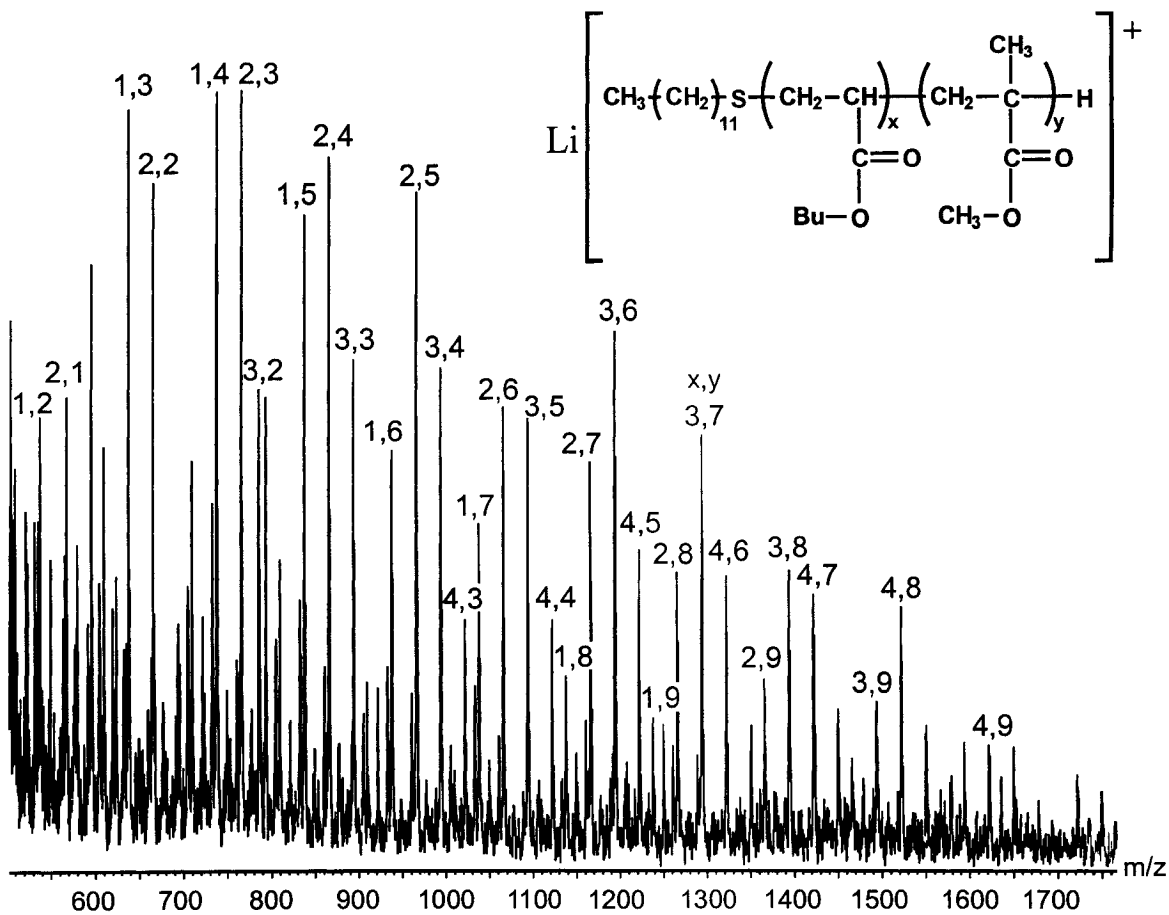

Figure 6.4: ESI mass spectrum copolymers of PBA/PMMA ionized with lithium.

CID experiments were performed on all the distributions in order to characterize the polymer mixture. It is possible to obtain the complete sequence of each copolymer because of the presence of peaks from the fragmentation of the polymer ions along the carbon backbone. Figure 6.5 shows the tandem mass spectrum of $[PBA_1/PMMA_4+Li]^+$. The polymer has one BA close to the CTA end and four MMA in a row. Two progressions of fragments from MMA were observed: $[100n+87+M]^+$ (x94) resulting from cleavage of MMA near the hydrogen terminal and $[100n+100+M]^+$ (x07) from hydrogen rearrangement. A third progression is observed, $[128+100n+M]^+$ (x35) showing the fragmentation of the copolymer along the backbone after the CTA terminal end has been cleaved.

Figure 6.6 shows the tandem mass spectrum of $[PBA_3/PMMA_3+Li]^+$. The polymer has multiple sequences according to the fragmentation of the copolymer along the backbone. It can be random, alternating or block. Again the progressions $[100n+87+M]^+$ (x94) and $[100n+100+M]^+$ (x07) are observed, showing that from one to three MMA can be in a row at the hydrogen terminal end of the chain. The ions at m/z 463 and 491 due to fragmentation along the backbone are missing but the sequences can still be proposed. When the numbers of BA in the copolymer increase, the possible sequences for this polymer also increase. With more than four BA units in the copolymer, CID gives only partial information about the sequence.

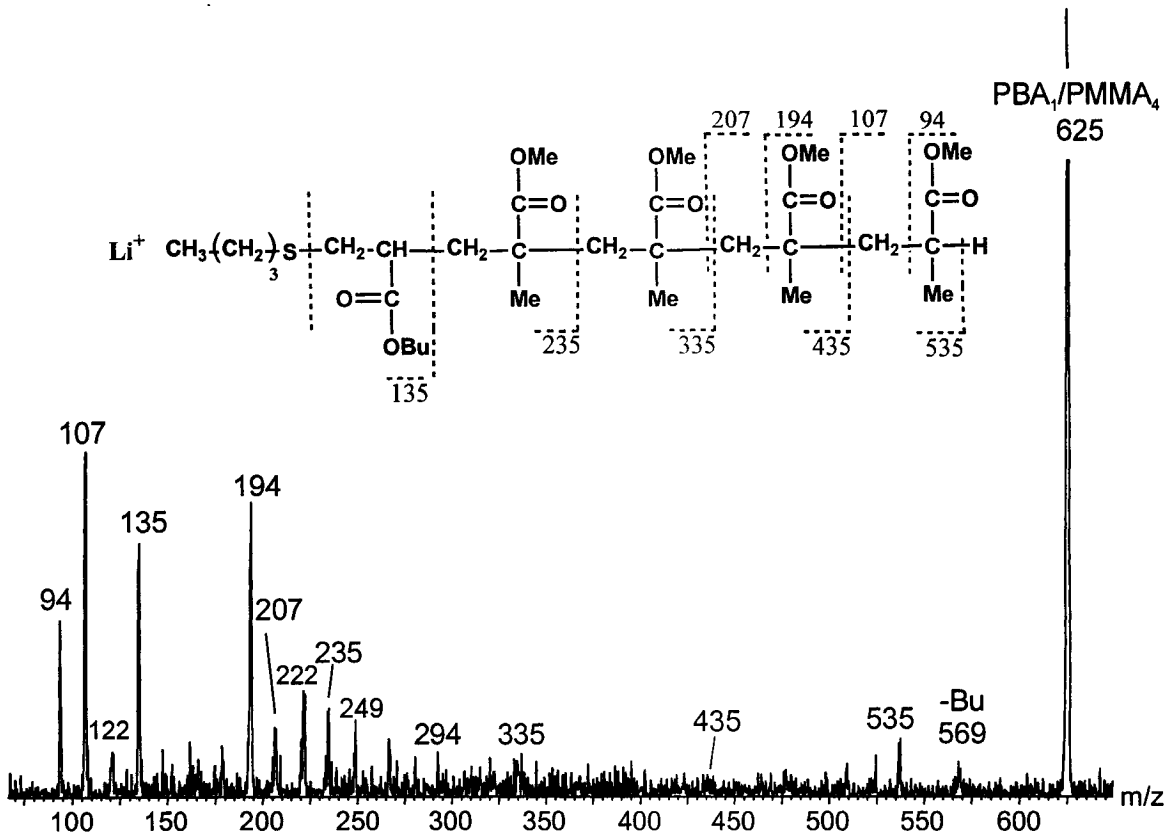

Figure 6.5: Tandem mass spectrum of $[PBA_1/PMMA_4+Li]^+$ (E_{Lab} = 47eV, collision gas pressure = $6.1x10^{-4}$mBar).

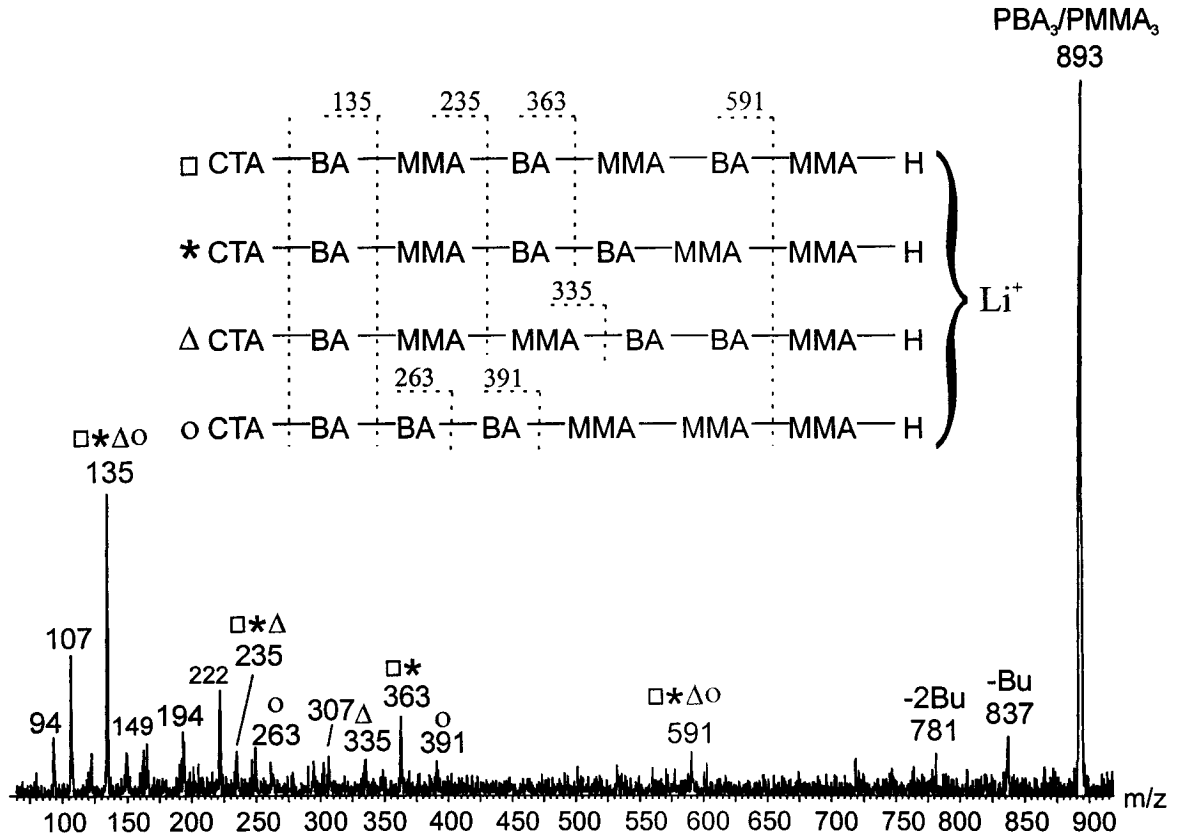

Figure 6.6: Tandem mass spectrum of $[PBA_3/PMMA_3+Li]^+$ (E_{Lab} = 60eV, collision gas pressure = $6.2x10^{-4}$mBar).

6.3 Poly(methyl methacrylate/vinyl acetate) (PMMA/PVAc).

The copolymer was produced with 7% w/w of MMA and 7% w/w VAc. The composition of the polymer mixture during the course of the reaction is nearly constant. The mass spectrum of the copolymer mixture at 26% of completion is shown in Figure 6.7. Three distributions containing homopolymers of MMA (labeled A, B and C on Figure 6.7) were observed; they are the most important products. Three small distributions of copolymer (labeled D, E and F on Figure 6.7) were also observed; they all contain one VAc and various amounts of MMA. Distributions A and D have two hydrogen atoms as end groups, distributions B and E have butene and hydrogen as end groups and distributions C and F have hydrogen and isobutyronitrile as end groups. For the copolymers D and F, the complete sequence of the polymer cannot be assigned, but the presence of VAc was confirmed by tandem mass spectrometry. At higher polymer conversions, PVAc homopolymer is observed.

As shown on Figure 6.8, for $[PMMA_6/PVAc_1+Li]^+$ (E_7) the complete sequence of the polymer was found with VAc bound to the butene terminal and the six MMA units sequentially following it. Four different progressions due to cleavage along the backbone are observed. The typical fragmentation of PMMA is observed with progression $[100n+87+M]^+$ (x94) resulting from cleavage of MMA near the hydrogen terminal and progression $[100n+100+M]^+$ (x07) from hydrogen rearrangement. Cleavage at the butene end is also observed with the two progressions (m/z 133, 233, 333, 433 and 533) and (m/z 147, 247, 347) resulting from hydrogen rearrangement. The mass spectrum in

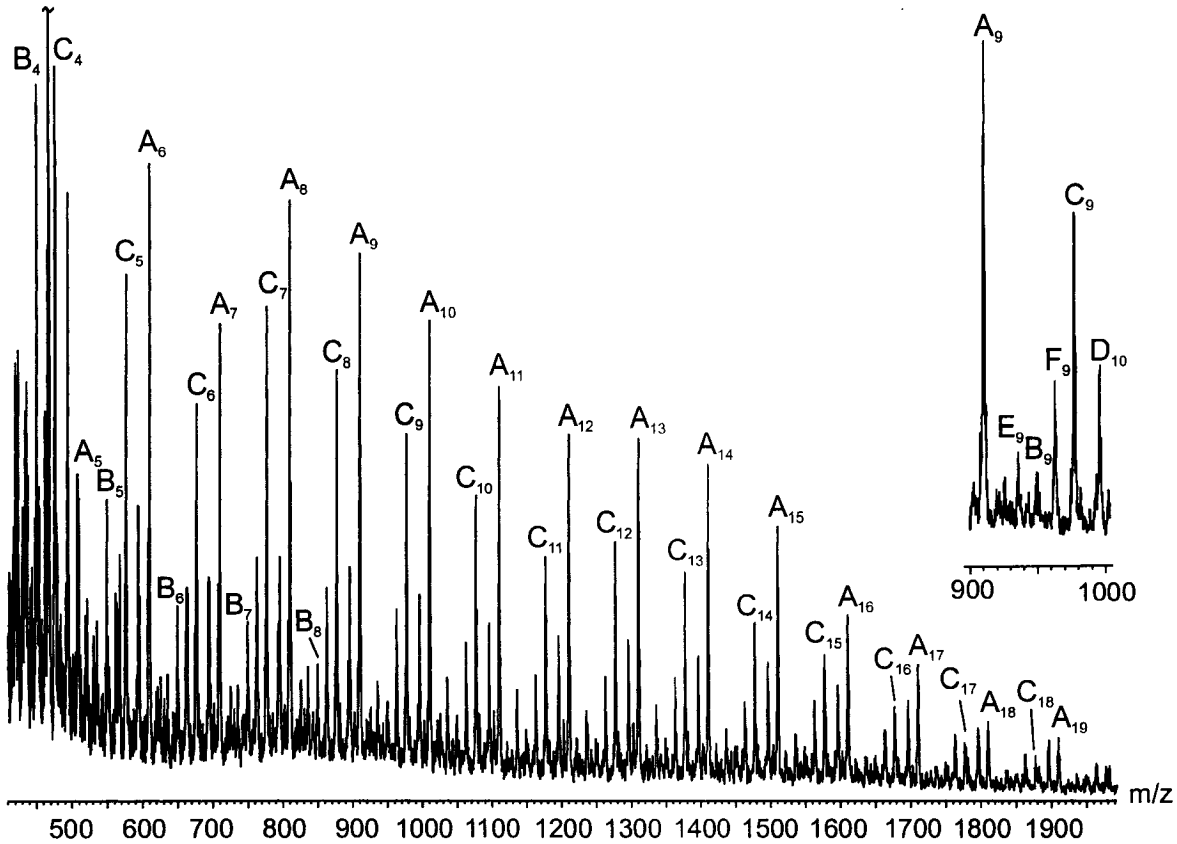

Figure 6.7: ESI mass spectrum copolymers of PMMA/PVac ionized with lithium.

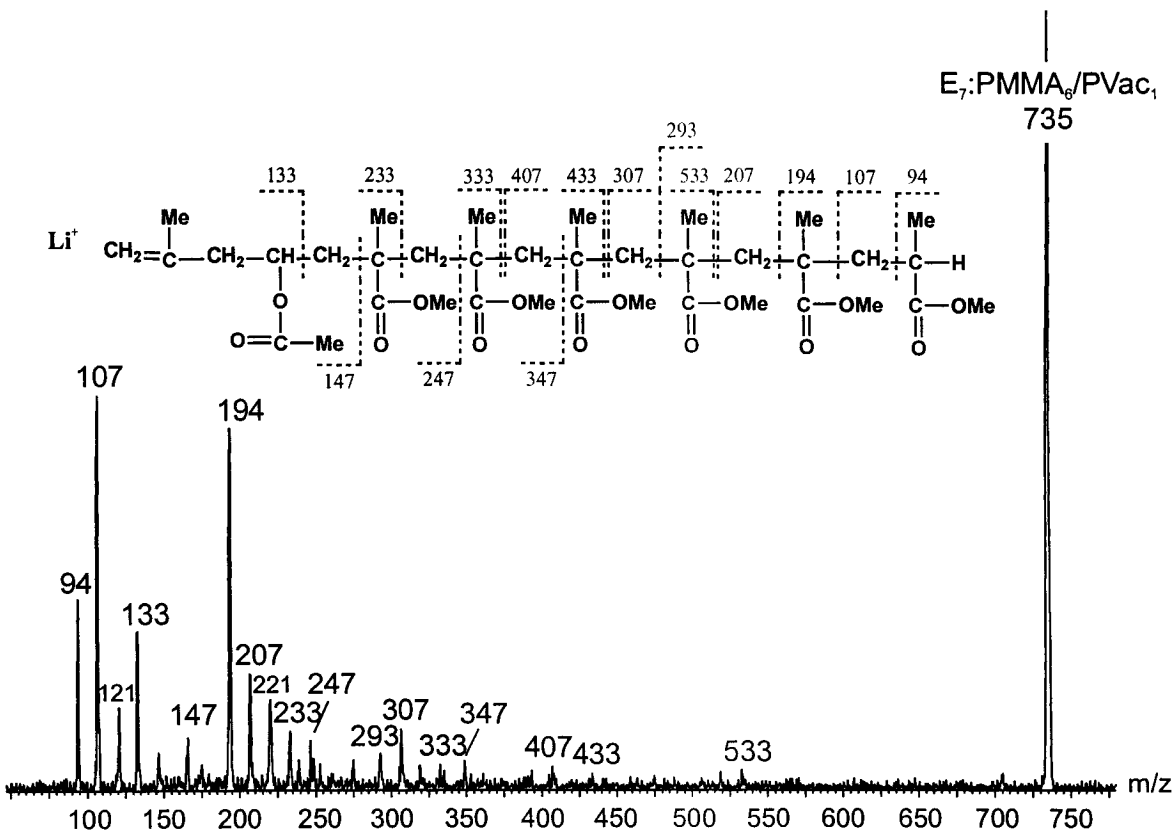

Figure 6.8: Tandem mass spectrum of $[PMMA_6/PVAc_1+Li]^+$ (E_{Lab} = 55eV, collision gas pressure = $4.8x10^{-4}$mBar).

Figure 6.8 does not show the loss of acetic acid from the side chain of VAc but it is observed from the lower molecular weight homologues $[PMMA_5/PVAc_1+Li]^+$ and $[PMMA_4/PVAc_1+Li]^+$.

6.4 Comparison between *Impress* output and experimental results

As mentioned in Chapter 2, *Impress* has been used to predict the results of free radical polymerization. As output it gives the ratio of monomer that can be expected along the reaction, the average molecular weight of the mixture and the conversion over the course of the reaction (a complete list is described in Chapter 2).

The cumulative copolymer composition can easily be obtained by proton NMR. NMR experiments were performed using a 500 MHz instrument, 15 mg of polymer mixture were dissolved in deuterated chloroform. A signal caused by one characteristic group of each repeat unit was considered. For the three monomers, the group alpha to the oxygen atom of the ester group was taken into account. The integration of the peak obtained by NMR was scaled according to the number of hydrogen atoms in the group of interest as shown in Table 6.2. Examples of copolymer NMR spectra are shown in Figure 6.9 to 6.11, the integrations of the peaks of interest are on the spectrum.

Table 6.2: Displacements observed by ^{1}H NMR for BA, MMA and VAc.

Monomer	Structure	Chemical shift[1, 3] (ppm)	Scaling factor
BA	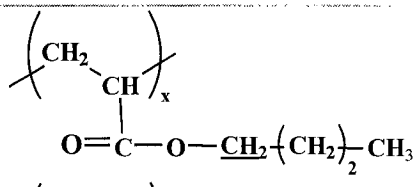	4.0	1/2
MMA	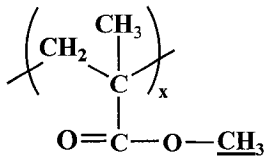	3.5-3.6	1/3
VAc	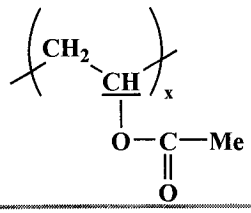	4.9	1

The composition of the polymer from *Impress*, from the ESI-MS and NMR results are compared in Tables 6.3 to 6.6 for the different copolymers produced using AIBN and dodecanethiol (initiator and CTA) for the polymerization process. The ESI-MS compositions were calculated using the peak intensity of each polymer; the abundance of each monomer is equal to the product of the intensity multiplied by the number of each monomer as shown. The *Impress* compositions were based on the conversion obtained by gravimetry (in order to compare the NMR and ESI-MS composition).

Impress hardly reproduced the composition of the polymer from diluted systems at low conversion (especially for a copolymer of MMA/VAc, Table 6.3) but at larger polymer conversion, the composition output is accurate (especially for a copolymer of BA/MMA Table 6.6).

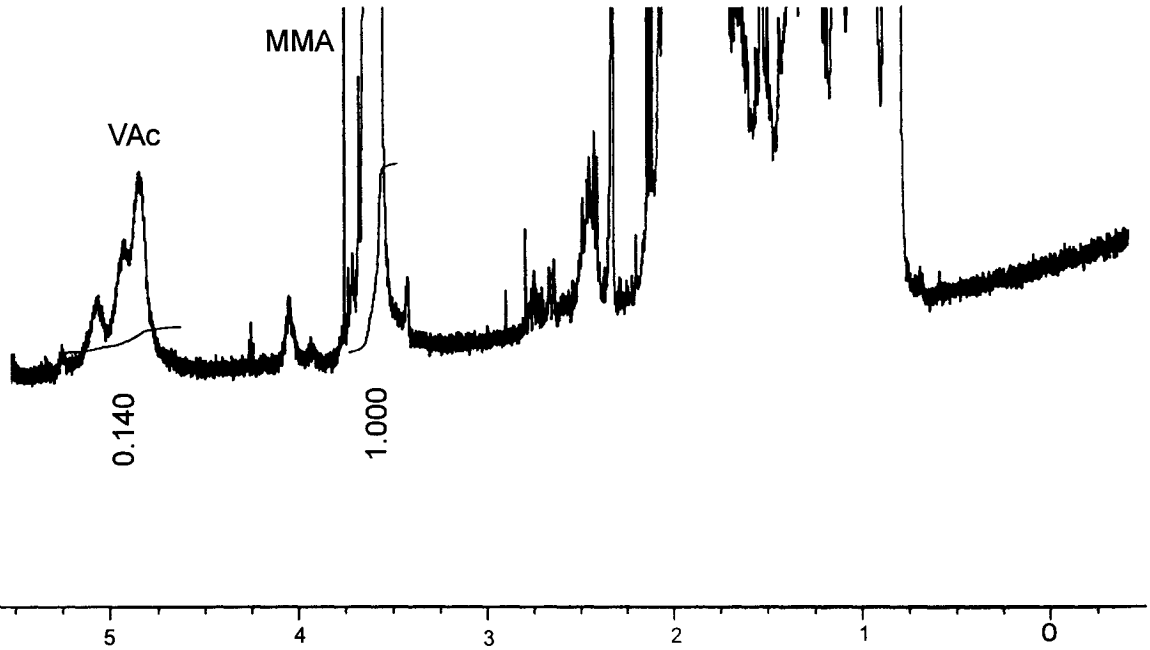

Figure 6.9: NMR spectrum of PMMA/PVAc after 85 % conversion.

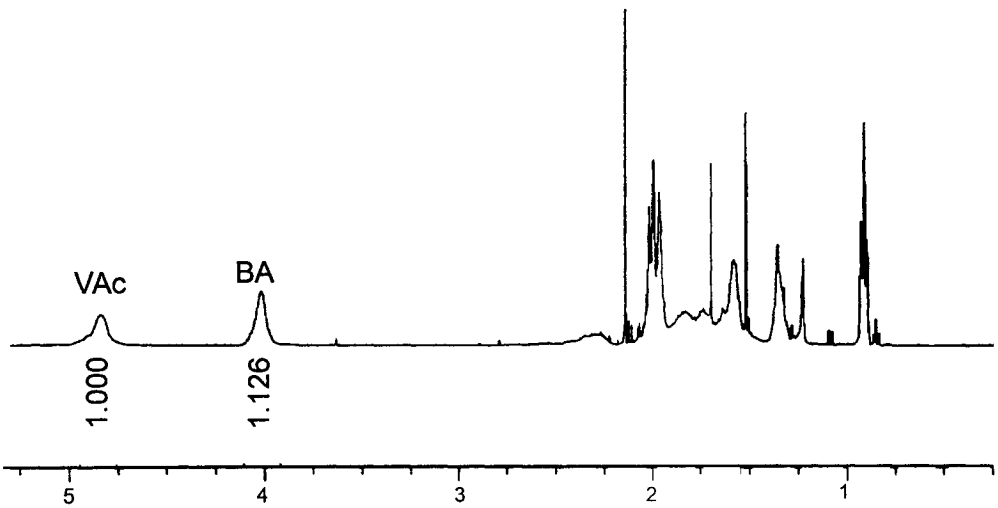

Figure 6.10: NMR spectrum of PBA/PVAc after 91 % conversion.

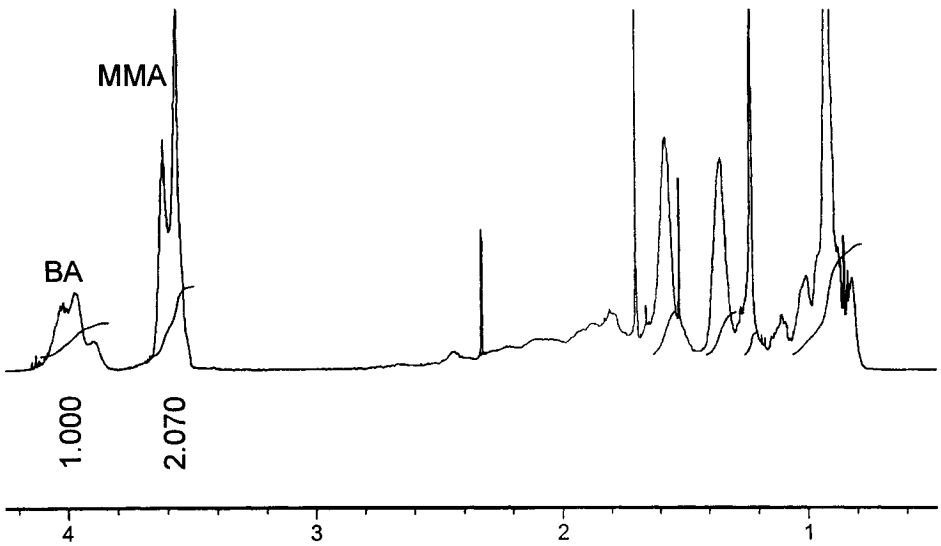

Figure 6.11: NMR spectrum of PBA/PMMA after 98 % conversion.

The monomer reactivity ratios (r_1 and r_2) are the ratios of the rate constant for a monomer radical reacting with its monomer to the rate constant for a monomer radical reacting with the other monomer (equations 6.1). When the ratio is large it implies that the monomer radical ($M_1\bullet$) preferentially reacts with itself (M_1) and when the ratio is small the monomer radical ($M_1\bullet$) reacts with the other monomer (M_2).

Equations :	Rates :	Reactivity ratios :
$M_1^{\bullet} + M_1 \rightarrow M_1^{\bullet}$	$k_{11}\left[M_1^{\bullet}\right][M_1]$	$r_1 = k_{11}/k_{12}$
$M_1^{\bullet} + M_2 \rightarrow M_2^{\bullet}$	$k_{12}\left[M_1^{\bullet}\right][M_2]$	6.1
$M_2^{\bullet} + M_1 \rightarrow M_1^{\bullet}$	$k_{21}\left[M_2^{\bullet}\right][M_1]$	$r_2 = k_{22}/k_{21}$
$M_2^{\bullet} + M_2 \rightarrow M_2^{\bullet}$	$k_{22}\left[M_2^{\bullet}\right][M_2]$	

The monomer reactivity ratios of interest are listed in Table 6.1. According to those reactivity ratios, the copolymerization of MMA and VAc should lead to homopolymerization of MMA during the early stages of the polymerization.[4] Both monomer radicals prefer to react with MMA and thus MMA is consumed much faster from the reaction mixture than VAc. This is in agreement with the ESI-MS and NMR results. Table 6.3 shows that the polymer mixture contains more MMA (almost only MMA) at the beginning of the reaction. A large composition drift is observed by NMR but it is not that obvious by mass spectrometry, the same six products are observed over the course of the reaction (A to F) with about the same abundance, but small peaks from

homopolymers of VAc are observed at large conversion and they contribute to the increase in the ratio VAc/MMA.

Table 6.3: Ratio of MMA and VAc obtained by ESI-MS and ^{1}H NMR on MMA 7%, Vac 7%.

Reaction time	Conversion (%)		Ratio of VAc / MMA		
(minutes)	*Impress*	Gravimetry	*Impress*†	NMR	ESI-MS
20	4	10	1 / 18.6	1 / 128.2	N/A
120	21	25	1 / 15.2	1 / 10.1	N/A
200	30	36	1 / 12.5	N/A	1 / 41.4
404	44	50	1 / 8.1	1 / 8.9	1 / 30.2
1891	70	75	1 / 1.7	1 / 4.7	1 / 7.7
4144	86	85	1 / 1.2	1 / 2.4	1 / 4.9

† *Impress* compositions are related to the gravimetric conversion

A smaller composition drift is observed for PBA/PVAc reflecting the fact that their reactivity ratios are closer than for PMMA/PVAc. From *Impress* PBA homopolymerization was expected at the beginning of the reaction, and was confirmed by the ESI-MS and NMR results (Tables 6.4 and 6.5).

Table 6.4: Ratio of BA and Vac obtained by ESI-MS and ^{1}H NMR on BA 7%, VAc 17%.

Reaction time	Conversion (%)		Ratio of BA / VAc		
(minutes)	*Impress*	Gravimetry	*Impress*†	NMR	ESI-MS
80	39	43	1.3 / 1	1.9 / 1	1.8 / 1
252	51	54	0.8 / 1	1.5 / 1	N/A
505	60	63	0.6 / 1	0.9 / 1	1.9 / 1
1500	81	78	0.4 / 1	0.6 / 1	1.2 / 1
3007	92	91	0.2 / 1	0.6 / 1	0.3 / 1

† *Impress* compositions are related to the gravimetric conversion

Table 6.5: Ratio of BA and VAc obtained by ESI-MS and ^{1}H NMR on BA 11%, VAc 11%.

Reaction time	Conversion (%)		Ratio of BA / VAc		
(minutes)	*Impress*	Gravimetry	*Impress*†	NMR	ESI-MS
10	14	23	4.1 / 1	5.7 / 1	2.1 / 1
46	44	43	3.3 / 1	4.1 / 1	N/A
80	57	51	3.0 / 1	3.8 / 1	2.0 / 1
1500	89	90	0.8 / 1	1.4 / 1	0.51 / 1
3037	95	100	0.7 / 1	1.2 / 1	0.48 / 1

† *Impress* compositions are related to the gravimetric conversion

In the case of PBA/PMMA copolymer, the monomer reactivity ratios are close, compare to the other copolymers, and the ratio for one monomer is close to the inverse of the ratio for the other monomer. According to Billmeyer,[5] a random copolymer should be expected when r_1 is equal to $1/r_2$ as both of the monomer radicals have the same preference for one monomer over the other. The composition of the polymer depends on the composition of the reaction mixture and on the reactivity of the two monomers. In the present case MMA tends to react first according to the ESI-MS and NMR values and the *Impress* output (Table 6.6). ESI-MS results and *Impress* output are in very good agreement in this case, they differ by less then 0.3 (except for after 48% conversion).

Table 6.6: Ratio of BA and MMA obtained by ESI-MS and ^{1}H NMR on BA 5%, MMA 5%.

Reaction time	Conversion		Ratio of BA / MMA		
(minutes)	*Impress*	Gravimetry	*Impress*†	NMR	ESI-MS
20	7	10	1 / 2.5	1 / 3.1	1 / 2.3
120	37	32	1 / 2.3	1 / 2.4	1 / 2.0
199	53	48	1 / 2.1	1 / 2.2	1 / 1.2
900	96	98	1 / 1.3	1 / 1.4	N/A
2425	99	100	1 / 1.3	1 / 1.3	1 / 1.4

† *Impress* compositions are related to the gravimetric conversion

Figure 6.12 shows plots of the *Impress* mole fraction of BA against the polymer conversion for the copolymers BA 5%, MMA 5% and BA 7%, VAc17% (dotted and full lines, respectively). The experimental results from ^{1}H NMR and ESI-MS are also plotted on the graph. The large composition drift of the BA/VAc reaction mixture can be confirmed by the decrease in mole fraction of BA over the course of the reaction.

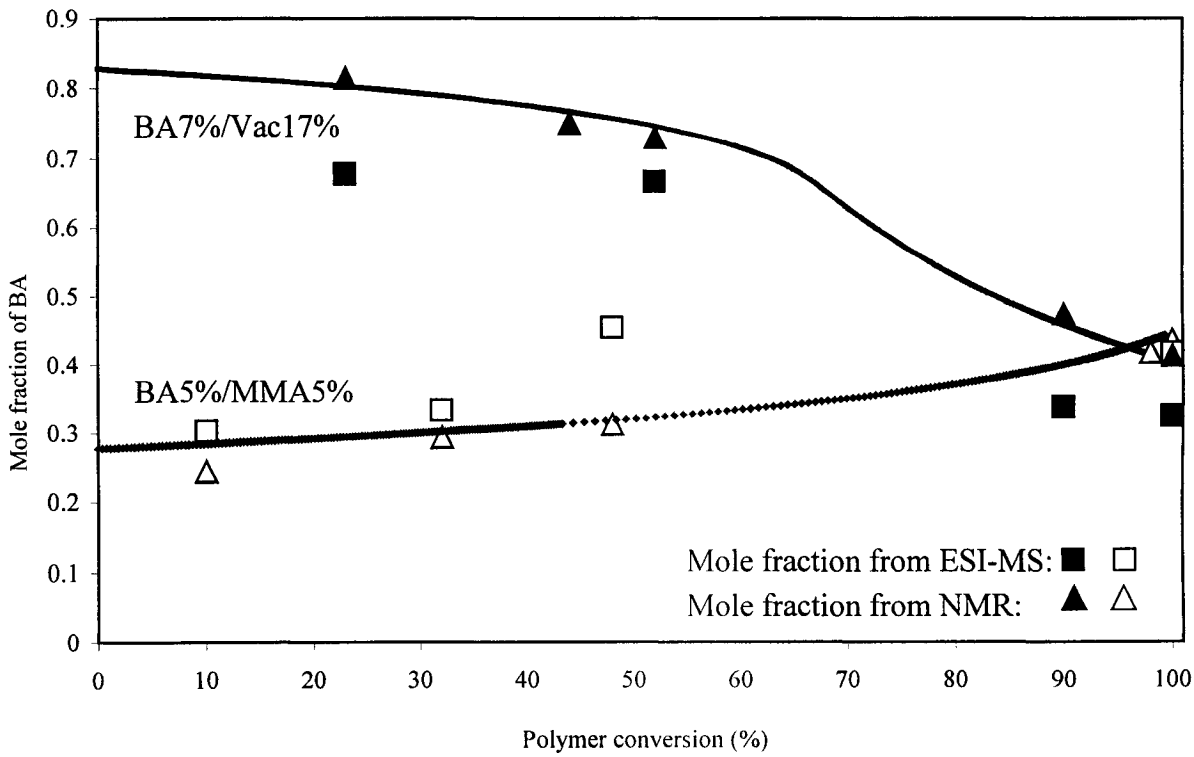

Figure 6.12: Mole fraction of BA obtained by *Impress* and by ESI-MS and ^{1}H NMR as a function of the reaction conversion

The experimental conversions of the polymer were calculated by gravimetry using equation 2.2 (the conversion from equation 2.1 was not used, the mass of the empty ampoule not being accurate because of the loss of glass pieces). In all cases, *Impress* reproduces the experimental conversion. According to the proton NMR experiments, the

polymers at high conversion were not perfectly dry; the presence of toluene was observed at 3.6 and 7.1 ppm. It is possible that *Impress* overestimated the polymer conversion close to the completion (the solvent might be harder to evaporate because of the high viscosity of the sample). For the homopolymerizations, the model did not perfectly reproduce the experimental results at large conversion.

The NMR results reflect what was observed by mass spectrometry in the case of PBA/PVAc and PBA/PMMA, as shown in Figure 6.12. There is more divergence in the case of PMMA/PVAc. ESI-MS can be less accurate because of the large number of low intensity distributions observed in the mass spectra. The NMR results are also questionable, a small signal at 4.9 ppm was considered and the amount of VAc in the copolymer can be overestimated if impurities are present in the same region of the spectrum (as shown in Figure 6.9).

6.5 Conclusion

The fragmentation of PBA PMMA and PVAc by CID has been used to assist in the determination of the sequence of synthetic copolymers analysed by electrospray ionization mass spectrometry. Fragmentation along the copolymer backbone results in complete sequence coverage of PBA/PMMA and PMMA/PVAc. The number of VAc present in the copolymer can be determined by considering the losses of acetic acid molecules. Because vinyl acetate does not fragment along the backbone but rather by acetic acid loss, the sequence of copolymer containing VAc can be difficult to determine.

References

(1)Jovanovic, R.; Dubé, M. A. *J. Appl. Polym. Sci.* **2001**, *82*, 2958.

(2)Dubé, M. A.; Penlidis, A. *Polymer* **1995**, *36*, 587.

(3)Montaudo, M. S.; Montaudo, G. *Macromolecules* **1999**, *32*, 7015.

(4)Gao, J.; Penlidis, A. *J.M.S.-Rev. Macromol. Chem. Phys.* **1998**, *C38*, 651.

(5)Billmeyer, F. W. *Textbook of Polymer Science*, 3rd ed.; John Wiley & Sons: New York, 1984.

Chapter seven

CONCLUSION

Electrospray ionization tandem mass spectrometry of PMMA ions shows them to fragment along the polymer backbone by either homolytic cleavage or 1,5-hydrogen rearrangement. When PBA ions fragment by cleavage after the CTA terminal group and PVAc ions fragment by the sequential loss of acetic acid from the polymer backbone. The mechanism of dissociation of PVAc ions was subject of a computational study, the mass spectra can be understood in terms of the relative product energies and transition for 1,5-hydrogen rearrangements.

The fragmentation of PBA PMMA and PVAc by CID has been used to assist in the determination of the sequence of synthetic copolymers analysed by electrospray ionization mass spectrometry. Fragmentation along the copolymer backbone results in complete sequence coverage of PBA/PMMA and PMMA/PVAc. The number of VAc present in the copolymer can be determined by considering the losses of acetic acid molecules. Because vinyl acetate does not fragment along the backbone but rather by acetic acid loss, the sequence of copolymer containing VAc can be difficult to determine.

SUPPORTING INFORMATION

Appendix A Gaussian archive entries for optimized geometries

5mer:

Single point energy B3-LYP/6-31+G(d) on the MM/MD structure

N-N= 4.459869448641D+03 E-N=-1.297377650470D+04 KE= 1.734318829965D+03
1\1\GINC-MS5\SP\RB3LYP\6-31+G(d)\C24H37Li1N1O10(1+)\MARIE\13-May-2003\
0\\# B3LYP/6-31+G(D)\\5mer after MMMD opt. energy from DFT\\1,1\C,0,2.
342,-6.679,6.157\N,0,2.844,-5.641,6.228\C,0,0.695,-8.05,4.882\C,0,0.91
8,-8.323,7.354\C,0,1.708,-8.029,6.054\H,0,0.18,-9.035,4.81\H,0,-0.091,
-7.27,5.005\H,0,1.188,-7.873,3.903\H,0,0.443,-9.331,7.324\H,0,1.576,-8
.292,8.254\H,0,0.103,-7.58,7.521\C,0,2.79,-9.146,5.849\C,0,4.025,-8.77
4,4.983\H,0,2.308,-10.05,5.414\H,0,3.181,-9.462,6.844\H,0,4.596,-8.007
,5.555\O,0,3.581,-8.296,3.708\C,0,4.104,-7.072,3.259\C,0,3.366,-6.319,
2.222\O,0,5.204,-6.677,3.624\H,0,3.204,-6.984,1.352\H,0,2.388,-6.,2.63
4\H,0,3.939,-5.424,1.908\C,0,4.91,-10.029,4.785\C,0,6.344,-9.759,4.259
\H,0,4.383,-10.744,4.117\H,0,5.014,-10.547,5.763\H,0,6.988,-10.632,4.5
31\O,0,6.884,-8.554,4.834\C,0,7.238,-8.624,6.199\C,0,7.7,-7.393,6.879\
O,0,7.156,-9.666,6.826\H,0,7.919,-7.613,7.945\H,0,8.625,-7.025,6.394\H
,0,6.907,-6.622,6.823\C,0,6.369,-9.684,2.716\C,0,7.778,-9.468,2.127\H,
0,5.691,-8.893,2.367\H,0,5.963,-10.636,2.309\H,0,8.364,-10.389,2.347\O
,0,8.337,-8.287,2.704\C,0,9.589,-8.336,3.342\C,0,10.58,-9.434,3.158\O,
0,9.873,-7.396,4.057\H,0,10.227,-10.348,3.672\H,0,10.739,-9.621,2.077\
H,0,11.552,-9.141,3.609\C,0,7.718,-9.299,0.592\C,0,7.267,-7.886,0.13\H
,0,7.035,-10.068,0.173\H,0,8.713,-9.527,0.153\H,0,6.517,-7.477,0.845\O
,0,6.684,-7.967,-1.172\C,0,5.366,-8.452,-1.251\C,0,4.744,-8.632,-2.581
\O,0,4.724,-8.717,-0.246\H,0,5.469,-8.344,-3.369\H,0,4.461,-9.696,-2.7
14\H,0,3.842,-7.993,-2.655\C,0,8.462,-6.906,0.045\C,0,8.123,-5.525,0.6
08\H,0,8.785,-6.799,-1.015\H,0,9.344,-7.289,0.598\H,0,9.018,-4.873,0.4
79\O,0,7.801,-5.676,1.998\C,0,7.607,-4.517,2.763\C,0,7.67,-3.133,2.211
\O,0,7.361,-4.684,3.942\H,0,7.455,-2.403,3.019\H,0,8.686,-2.927,1.818\
H,0,6.911,-3.01,1.414\H,0,7.268,-5.086,0.037\Li,0,7.288,-6.867,3.711\\
Version=x86-Linux-G98RevA.7\HF=-1751.3355081\RMSD=1.459e-05\Dipole=1.1
5496,-0.5440468,-2.8241305\PG=C01 [X(C24H37Li1N1O10)]\\@

Single point energy B3-LYP/6-31+G(d) on the AM1 structure

N-N= 4.389757118574D+03 E-N=-1.283690401041D+04 KE= 1.734165611677D+03
1\1\GINC-MS5\SP\RB3LYP\6-31+G(d)\C24H37Li1N1O10(1+)\MARIE\14-Nov-2002\
0\\# B3LYP/6-31+G(D) SCF=(QC,MAXCYCLE=1024) DIRECT\\5mer, after AM1 op
timization, calcul of the B3LYP energy\\1,1\C,0,-3.930178,-0.334343,0.
94796\N,0,-3.471962,-1.175266,1.607579\C,0,-4.23114,2.075852,0.775378\

C,0,-6.033961,0.507804,0.060249\C,0,-4.522397,0.726273,0.126003\H,0,-4
.731491,2.8811,0.184101\H,0,-4.623279,2.104049,1.819817\H,0,-3.130214,
2.272425,0.789292\H,0,-6.490235,1.299162,-0.583098\H,0,-6.27301,-0.490
346,-0.378147\H,0,-6.483476,0.574971,1.07979\C,0,-3.951311,0.670746,-1
.298179\C,0,-2.425269,0.7111,-1.368242\H,0,-4.368315,1.544942,-1.86808
5\H,0,-4.326031,-0.265021,-1.790246\H,0,-1.975497,0.429074,-0.37451\O,
0,-2.053339,2.061111,-1.712911\C,0,-1.183053,2.746396,-0.905903\C,0,-0
.814947,4.078345,-1.456001\O,0,-0.810668,2.215465,0.14508\H,0,0.293553
,4.0932,-1.628994\H,0,-1.346848,4.280637,-2.416556\H,0,-1.077522,4.866
255,-0.708248\C,0,-1.866876,-0.197169,-2.467244\C,0,-0.702574,-1.05979
7,-1.983651\H,0,-1.507102,0.430949,-3.325302\H,0,-2.669848,-0.875356,-
2.855525\H,0,-0.335788,-1.708488,-2.826542\O,0,-1.230647,-1.88341,-0.9
20791\C,0,-0.874729,-3.204137,-0.863141\C,0,-1.198504,-3.810917,0.4678
51\O,0,-0.371747,-3.739496,-1.847943\H,0,-0.932011,-4.899505,0.43221\H
,0,-0.559306,-3.305491,1.25422\H,0,-2.30418,-3.708523,0.672343\C,0,0.4
23003,-0.21713,-1.395038\C,0,1.810819,-0.82104,-1.575819\H,0,0.22178,-
0.075115,-0.296392\H,0,0.418892,0.797276,-1.876486\H,0,1.957548,-1.128
656,-2.649823\O,0,1.857902,-1.977886,-0.730216\C,0,2.760351,-2.985468,
-1.002432\C,0,3.470393,-3.075363,-2.304219\O,0,2.834562,-3.769675,-0.0
54643\H,0,2.728077,-3.235094,-3.126136\H,0,4.051452,-2.143106,-2.50637
3\H,0,4.173938,-3.945188,-2.282059\C,0,2.909603,0.166372,-1.189349\C,0
,2.695756,0.878439,0.143868\H,0,2.965661,0.94913,-1.993742\H,0,3.89291
2,-0.372158,-1.159688\H,0,1.656893,1.311539,0.20447\O,0,3.648052,1.962
024,0.243112\C,0,3.38491,3.119854,-0.435091\C,0,4.435278,4.156905,-0.2
42763\O,0,2.351754,3.186854,-1.107423\H,0,5.246456,3.788932,0.430898\H
,0,4.870184,4.419339,-1.239105\H,0,3.966544,5.069704,0.20102\C,0,3.001
257,-0.019773,1.338306\C,0,2.26607,0.403724,2.595947\H,0,4.104452,0.00
483,1.544554\H,0,2.716693,-1.077732,1.079558\H,0,2.901688,0.235509,3.5
04406\O,0,1.094706,-0.439494,2.679734\C,0,0.388299,-0.428663,3.839333\
C,0,0.771368,0.41626,5.001873\O,0,-0.584352,-1.207051,3.814734\H,0,-0.
025845,0.373192,5.785357\H,0,1.729587,0.039498,5.441355\H,0,0.911833,1
.477193,4.676932\H,0,1.927643,1.471537,2.553024\Li,0,-2.218279,-2.5169
86,2.683538\\Version=x86-Linux-G98RevA.7\HF=-1751.3067734\RMSD=0.000e+
00\Dipole=-2.0223244,0.6645091,2.0882467\PG=C01 [X(C24H37Li1N1O10)]\\@

Single point energy B3-LYP/6-31+G(d) on the DFT structure

N-N= 4.519609005871D+03 E-N=-1.309388228976D+04 KE= 1.734570151994D+03
1\1\GINC-SFNODE1\SP\RB3LYP\6-31+G(d)\C24H37Li1N1O10(1+)\HPC1392\01-
May
-2003\0\\#N B3LYP/6-31+G(D)\\5mer\\1,1\C,0,-4.6520545237,-0.8419449044
,0.8577691947\N,0,-4.2522814759,-1.9097819449,1.0944209811\C,0,-4.7068
811292,1.4727209547,1.6932443809\C,0,-6.6088362879,0.5537212625,0.2828
527731\C,0,-5.0758026365,0.5252784945,0.5204647159\H,0,-4.9581261984,2
.5006491842,1.413884906\H,0,-5.2758362702,1.1985125688,2.5861249834\H,

0,-3.6421041029,1.4194618525,1.9293239823\H,0,-6.909246035,1.571792043
4,0.0139116227\H,0,-6.8904174647,-0.1256109998,-0.527451618\H,0,-7.140
4376497,0.259486847,1.1922215762\C,0,-4.3435225723,0.9213087666,-0.804
6468259\C,0,-2.8155025522,0.7407919326,-0.7467550988\H,0,-4.5716173872
,1.9666487387,-1.0342171619\H,0,-4.7495039211,0.2954242343,-1.60605109
61\H,0,-2.5484125078,-0.0313067708,-0.0283941439\O,0,-2.2932457779,2.0
542396598,-0.2272518124\C,0,-1.2235958261,2.0751033736,0.6072722146\C,
0,-0.9237179108,3.4577620305,1.106609362\O,0,-0.5579370697,1.056029239
3,0.877629825\H,0,-0.0855684677,3.8361503428,0.5080740898\H,0,-1.79057
19347,4.1054645831,0.9876619035\H,0,-0.6073762068,3.4096548346,2.15160
58252\C,0,-2.1829685504,0.3861258785,-2.1095082694\C,0,-0.8842615869,-
0.4657536716,-2.0314061365\H,0,-1.9983208834,1.3022007603,-2.680048944
8\H,0,-2.9226360356,-0.2042282502,-2.6601578981\H,0,-0.8485360471,-1.1
614509282,-2.8731197901\O,0,-1.0122401957,-1.3364345815,-0.8109623674\
C,0,-0.9910186131,-2.7521365837,-1.0260787215\C,0,-1.3929295049,-3.465
9314822,0.2272750592\O,0,-0.6635494875,-3.205741599,-2.112087791\H,0,-
1.3791075181,-4.5413694676,0.0488396231\H,0,-0.7078248038,-3.211920423
7,1.0446983058\H,0,-2.3955681888,-3.140975162,0.5339724734\C,0,0.41541
29031,0.3604303122,-2.0105915595\C,0,1.7123126329,-0.4635968533,-1.935
8516204\H,0,0.4099504226,1.1169583963,-1.2285388981\H,0,0.4492544718,0
.9046774138,-2.9640492835\H,0,1.7880318564,-1.1135035375,-2.8097429722
\O,0,1.6338394217,-1.3232045862,-0.7079267906\C,0,2.3348238012,-2.5534
868264,-0.6343338764\C,0,2.5505672821,-3.2995773047,-1.926949128\O,0,2
.6692970726,-2.9271451135,0.480614346\H,0,1.5895793328,-3.4347176213,-
2.4328933411\H,0,3.2389553338,-2.7676886985,-2.5924116957\H,0,2.981941
0908,-4.2711594822,-1.6853298017\C,0,2.967819731,0.4247074869,-1.78105
53747\C,0,3.0759408805,0.9885742225,-0.3407546682\H,0,2.8941951779,1.2
53737564,-2.4908526993\H,0,3.8708804024,-0.1454195462,-2.0281788821\H,
0,2.0845292794,1.0851453286,0.0952584209\O,0,3.6687059397,2.359114685,
-0.3781753159\C,0,2.7806847161,3.3994683268,-0.5652668763\C,0,3.508436
1985,4.7184332526,-0.5480014807\O,0,1.5700920851,3.2150735718,-0.71719
55852\H,0,4.2757522346,4.7234591067,-1.3282699705\H,0,2.8010100996,5.5
304738243,-0.7114035794\H,0,4.0164970178,4.8468700676,0.4128919895\C,0
,3.9963699035,0.1927614395,0.6015607853\C,0,3.539146318,0.3194763045,2
.0598523479\H,0,5.0139750006,0.5832240009,0.5020468933\H,0,3.998166802
6,-0.8643688804,0.3394423789\H,0,4.1556426767,-0.2790206984,2.73263567
85\O,0,2.116708178,-0.1243835042,2.1145452387\C,0,1.6839699867,-1.3285
973509,2.6108681059\C,0,2.5475754664,-2.1095984244,3.5556440252\O,0,0.
5537854493,-1.6754934106,2.2219176427\H,0,1.9330616067,-2.8712397314,4
.0359064257\H,0,3.3278100953,-2.6143155679,2.974262048\H,0,3.007994229 3,-
1.4697546339,4.3124431769\H,0,3.528219258,1.3611958605,2.382683499\
Li,0,0.1554272948,-0.6424474156,0.6400453394\\Version=Sun64-SVR4-Unix-
G98RevA.9\HF=-1751.3681915\RMSD=6.502e-05\Dipole=1.5054662,1.8104712,-
0.3337032\PG=C01 [X(C24H37Li1N1O10)]\\@

5mer – one acetic acid

Single point energy B3-LYP/6-31+G(d) on the MM/MD structure

N-N= 3.503999894471D+03 E-N=-1.052824579487D+04 KE= 1.507336117743D+03
1\1\GINC-MS5\SP\RB3LYP\6-31+G(d)\C22H33Li1N1O8(1+)\MARIE\14-Sep-2002\0
\\# B3LYP/6-31+G(D) SCF=(QC,MAXCYCLE=1024)\\5mer - 1 CH3COOH charge =1
.45 after MD\\1,1\C,0,3.197,-8.86,7.485\N,0,4.17,-9.312,7.913\C,0,1.68
8,-6.873,7.496\C,0,0.749,-9.176,7.226\C,0,1.959,-8.271,6.892\H,0,0.83,
-6.375,6.989\H,0,1.451,-6.933,8.584\H,0,2.568,-6.2,7.394\H,0,0.868,-10
.202,6.809\H,0,0.611,-9.284,8.328\H,0,-0.197,-8.755,6.814\C,0,2.103,-8
.185,5.341\C,0,3.259,-7.286,4.831\H,0,1.154,-7.808,4.895\H,0,2.245,-9.
217,4.945\H,0,4.134,-7.429,5.507\O,0,2.833,-5.92,4.887\C,0,3.829,-4.93
2,4.801\C,0,3.419,-3.511,4.789\O,0,5.019,-5.222,4.732\H,0,2.859,-3.295
,5.72\H,0,4.304,-2.845,4.728\H,0,2.759,-3.333,3.917\C,0,3.632,-7.655,3
.372\C,0,4.882,-8.548,3.303\H,0,3.818,-6.729,2.798\H,0,2.777,-8.145,2.
859\H,0,4.65,-9.465,3.891\O,0,5.987,-7.805,3.832\C,0,6.851,-8.381,4.77
7\C,0,6.78,-9.792,5.247\O,0,7.701,-7.638,5.23\H,0,5.856,-9.947,5.835\H
,0,6.816,-10.483,4.383\H,0,7.646,-10.012,5.905\C,0,5.203,-8.992,1.858\
C,0,6.03,-7.979,1.033\H,0,4.266,-9.234,1.312\H,0,5.778,-9.935,1.938\H,
0,6.97,-7.739,1.579\O,0,5.228,-6.82,0.777\C,0,5.716,-5.578,1.213\C,0,5
.173,-4.343,0.61\O,0,6.512,-5.493,2.14\H,0,4.455,-4.613,-0.19\H,0,4.65
6,-3.745,1.386\H,0,6.003,-3.754,0.17\C,0,6.432,-8.553,-0.336\C,0,7.533
,-9.624,-0.271\H,0,6.808,-7.711,-0.957\H,0,5.535,-8.96,-0.851\H,0,7.14
6,-10.523,0.262\O,0,8.698,-9.062,0.341\C,0,9.123,-9.621,1.555\C,0,10.5
13,-9.394,2.005\O,0,8.35,-10.225,2.282\H,0,11.058,-8.82,1.229\H,0,10.5
09,-8.829,2.957\H,0,11.014,-10.373,2.148\C,0,7.912,-10.026,-1.671\C,0,
7.808,-11.284,-2.118\H,0,8.323,-9.266,-2.333\H,0,8.114,-11.524,-3.132\
H,0,7.441,-12.092,-1.492\Li,0,6.828,-5.967,4.083\\Version=x86-Linux-G9
8RevA.7\HF=-1522.2345193\RMSD=0.000e+00\Dipole=-1.2101209,1.7675022,-1
.22927\PG=C01 [X(C22H33Li1N1O8)]\\@

Single point energy B3-LYP/6-31+G(d) on the AM1 structure

N-N= 3.488164217815D+03 E-N=-1.049990464334D+04 KE= 1.507174752956D+03
1\1\GINC-MS3\SP\RB3LYP\6-31+G(d)\C22H33Li1N1O8(1+)\MARIE\05-Nov-2002\0
\\#B3LYP/6-31+G(D) SCF=(QC,MAXCYCLE=1024) DIRECT\\5mer-CH3COOH after
am1 opti.\\1,1\C,0,-3.680446,-2.428809,0.395423\N,0,-3.19419,-2.903401,
1.338678\C,0,-5.523577,-1.040915,-0.395839\C,0,-4.696547,-2.959688,-1.
749919\C,0,-4.286936,-1.83885,-0.794783\H,0,-6.014048,-0.633038,-1.312
433\H,0,-6.250735,-1.69351,0.143652\H,0,-5.23922,-0.186685,0.264591\H,
0,-3.810112,-3.569029,-2.046558\H,0,-5.445358,-3.628035,-1.261094\H,0,
-5.154871,-2.519232,-2.667818\C,0,-3.265191,-0.940394,-1.502263\C,0,-2
.722272,0.193465,-0.634418\H,0,-3.76088,-0.498786,-2.409053\H,0,-2.409
254,-1.572001,-1.855791\H,0,-2.785474,-0.044069,0.463413\O,0,-3.58669,
1.313853,-0.924761\C,0,-3.631702,2.360159,-0.04876\C,0,-4.635527,3.391

498,-0.430245\O,0,-2.870267,2.350995,0.923762\H,0,-5.471232,3.370515,0
.313146\H,0,-4.152388,4.399001,-0.407088\H,0,-5.045522,3.195669,-1.450
759\C,0,-1.2913,0.575361,-0.99933\C,0,-0.247941,-0.432042,-0.525216\H,
0,-1.060294,1.575807,-0.540775\H,0,-1.205342,0.674471,-2.113078\H,0,-0
.536343,-1.469218,-0.855179\O,0,-0.245804,-0.372202,0.916706\C,0,0.149
998,-1.459277,1.642019\C,0,0.403211,-2.799286,1.05478\O,0,0.249133,-1.
181022,2.85405\H,0,-0.501203,-3.162156,0.506528\H,0,1.275937,-2.744122
,0.351814\H,0,0.642411,-3.526938,1.87126\C,0,1.137552,-0.093603,-1.073
324\C,0,1.988823,0.832363,-0.210542\H,0,1.015159,0.357503,-2.092731\H,
0,1.717437,-1.052925,-1.180642\H,0,2.241559,0.325056,0.761389\O,0,1.23
8994,2.04866,0.028989\C,0,0.941439,2.433693,1.292728\C,0,0.139358,3.68
7841,1.356578\O,0,1.375263,1.760351,2.247376\H,0,-0.950838,3.420867,1.
317076\H,0,0.359037,4.225988,2.310972\H,0,0.378521,4.349082,0.487573\C
,0,3.259173,1.282758,-0.927602\C,0,4.207309,0.142724,-1.284294\H,0,3.7
99031,2.014709,-0.270192\H,0,2.977449,1.817029,-1.873355\H,0,3.64941,-
0.719853,-1.744352\O,0,4.895339,-0.300724,-0.092836\C,0,4.498411,-1.46
3605,0.499529\C,0,5.449511,-1.939662,1.540754\O,0,3.430849,-1.97565,0.
142311\H,0,6.063236,-1.094146,1.936188\H,0,4.881075,-2.421474,2.372481
\H,0,6.132451,-2.695876,1.077012\C,0,5.278732,0.642723,-2.20495\C,0,5.
322157,0.336555,-3.498232\H,0,6.03663,1.281161,-1.723106\H,0,6.109086,
0.72435,-4.160463\H,0,4.584515,-0.313928,-3.987876\Li,0,0.543187,0.695
168,4.209051\\Version=x86-Linux-G98RevA.7\HF=-1522.2022884\RMSD=0.000e
+00\Dipole=0.4009654,1.5240229,1.7666778\PG=C01 [X(C22H33Li1N1O8)]\\@

Single point energy B3-LYP/6-31+G(d) on the DFT structure

N-N= 3.525732922162D+03 E-N=-1.057187522267D+04 KE= 1.507613404266D+03
1\1\GINC-MS5\SP\RB3LYP\6-31+G(d)\C22H33Li1N1O8(1+)\MARIE\18-Mar-2003\0
\\# B3LYP/6-31+G(D) SCF=(QC,MAXCYCLE=1024)\\5mer - 1 CH3COOH after DFT
optimization\\1,1\C,0,-3.577217,-2.570099,-0.201677\N,0,-2.798637,-3.
242052,0.344685\C,0,-5.429595,-0.954387,0.082374\C,0,-5.302239,-2.4605
75,-1.962236\C,0,-4.479072,-1.659075,-0.919289\H,0,-6.069633,-0.258274
,-0.468816\H,0,-6.060578,-1.692387,0.585419\H,0,-4.87238,-0.396624,0.8
39753\H,0,-4.64341,-2.972738,-2.670264\H,0,-5.929739,-3.203224,-1.4617
31\H,0,-5.947653,-1.769076,-2.513426\C,0,-3.55781,-0.63699,-1.657167\C
,0,-2.640434,0.169536,-0.722294\H,0,-4.181766,0.066794,-2.217164\H,0,-
2.945672,-1.195287,-2.374733\H,0,-2.528354,-0.313709,0.249268\O,0,-3.3
77914,1.459067,-0.470159\C,0,-3.078853,2.17931,0.643844\C,0,-3.995364,
3.360688,0.806761\O,0,-2.170701,1.86162,1.432084\H,0,-4.885425,3.04495
8,1.36638\H,0,-3.492996,4.14259,1.378114\H,0,-4.318373,3.727595,-0.167
968\C,0,-1.236443,0.441227,-1.307866\C,0,-0.20016,-0.555738,-0.747028\
H,0,-0.901524,1.446465,-1.058852\H,0,-1.253445,0.359983,-2.399714\H,0,
-0.518315,-1.587841,-0.924093\O,0,-0.221619,-0.302313,0.720139\C,0,-0.
07803,-1.178572,1.80846\C,0,0.151153,-2.630221,1.580451\O,0,-0.178987,
-0.570092,2.884267\H,0,-0.701182,-3.062921,1.039546\H,0,1.083514,-2.78
1569,1.022445\H,0,0.227702,-3.118722,2.553204\C,0,1.231785,-0.334665,-

1.283643\C,0,2.039672,0.768154,-0.585805\H,0,1.178412,-0.132275,-2.358
646\H,0,1.801062,-1.253745,-1.118073\H,0,2.070727,0.61104,0.490709\O,0
,1.408158,2.124614,-0.819314\C,0,0.971641,2.863057,0.240247\C,0,0.7095
08,4.294627,-0.145344\O,0,0.796551,2.391975,1.379134\H,0,-0.274108,4.5
97132,0.225873\H,0,1.453838,4.935142,0.34314\H,0,0.776552,4.420255,-1.
224479\C,0,3.456268,0.943988,-1.158894\C,0,4.390139,-0.265925,-0.97877
\H,0,3.914993,1.804631,-0.660938\H,0,3.386626,1.168944,-2.227994\H,0,3
.992575,-1.162853,-1.456216\O,0,4.517303,-0.536888,0.495232\C,0,3.8595
96,-1.630957,1.006131\C,0,4.281696,-1.87581,2.431639\O,0,3.034442,-2.2
80874,0.352351\H,0,4.13014,-0.96795,3.023655\H,0,3.710283,-2.703327,2.
850162\H,0,5.350875,-2.109749,2.456294\C,0,5.782965,0.042099,-1.453671
\C,0,6.323003,-0.495604,-2.543956\H,0,6.322301,0.766946,-0.850632\H,0,
7.319416,-0.226392,-2.875942\H,0,5.795181,-1.228881,-3.147485\Li,0,-0.
530104,1.226049,1.985641\\Version=x86-Linux-G98RevA.7\HF=-1522.2670013
\RMSD=0.000e+00\Dipole=-1.0192609,1.8158725,-1.2876801\PG=C01 [X(C22H3
3Li1N1O8)]\\@

5mer – two acetic acids

Single point energy B3-LYP/6-31+G(d) on the MM/MD structure

N-N= 2.808281119777D+03 E-N=-8.602759897522D+03 KE= 1.280473289031D+03
1\1\GINC-MS5\SP\RB3LYP\6-31+G(d)\C20H29Li1N1O6(1+)\MARIE\23-Sep-2002\0
\\# B3LYP/6-31+G(D) SCF=(QC,MAXCYCLE=1024)\\5mer-2 CH3COOH, after mole
cular dynamic, charge = 1.4498\\1,1\C,0,4.131,-7.152,6.58\N,0,4.341,-6
.09,6.153\C,0,2.516,-8.508,7.891\C,0,4.959,-8.994,8.072\C,0,3.846,-8.5
28,7.099\H,0,1.66,-8.187,7.254\H,0,2.265,-9.519,8.288\H,0,2.564,-7.814
,8.763\H,0,4.755,-10.02,8.455\H,0,5.959,-9.023,7.589\H,0,5.04,-8.321,8
.956\C,0,3.696,-9.541,5.914\C,0,4.87,-9.652,4.883\H,0,2.749,-9.319,5.3
77\H,0,3.525,-10.558,6.337\H,0,5.261,-10.697,4.958\O,0,5.923,-8.725,5.
195\C,0,7.202,-9.004,4.683\C,0,8.341,-8.173,5.131\O,0,7.385,-9.89,3.86
8\H,0,9.271,-8.501,4.621\H,0,8.138,-7.111,4.895\H,0,8.465,-8.293,6.225
\C,0,4.382,-9.433,3.427\C,0,3.911,-7.989,3.157\H,0,3.559,-10.144,3.198
\H,0,5.211,-9.703,2.742\H,0,4.399,-7.345,3.91\O,0,2.491,-7.922,3.322\C
,0,1.939,-6.65,3.555\C,0,0.469,-6.494,3.566\O,0,2.651,-5.677,3.782\H,0
,-0.004,-7.472,3.343\H,0,0.138,-6.141,4.563\H,0,0.172,-5.761,2.79\C,0,
4.295,-7.498,1.742\C,0,5.628,-6.738,1.748\H,0,3.508,-6.813,1.36\H,0,4.
335,-8.349,1.027\H,0,6.421,-7.447,2.089\O,0,5.496,-5.639,2.662\C,0,6.6
55,-4.988,3.109\C,0,7.993,-5.096,2.459\O,0,6.525,-4.301,4.104\H,0,8.33
4,-6.147,2.445\H,0,7.937,-4.697,1.427\H,0,8.735,-4.493,3.022\C,0,5.902
,-6.224,0.362\C,0,6.884,-6.721,-0.398\H,0,5.272,-5.428,-0.02\H,0,7.51,
-7.526,-0.025\C,0,7.128,-6.191,-1.748\C,0,8.101,-6.68,-2.513\H,0,6.51,
-5.388,-2.14\H,0,8.267,-6.279,-3.506\H,0,8.745,-7.482,-2.173\Li,0,4.47
1,-4.908,4.375\\Version=x86-Linux-G98RevA.7\HF=-1293.1233283\RMSD=0.00
0e+00\Dipole=-0.7937799,0.3997814,0.1098703\PG=C01 [X(C20H29Li1N1O6)]\

\@

Single point energy B3-LYP/6-31+G(d) on the AM1 structure

N-N= 2.790070644440D+03 E-N=-8.568782926717D+03 KE= 1.280351997160D+03
1\1\GINC-MS3\SP\RB3LYP\6-31+G(d)\C20H29Li1N1O6(1+)\MARIE\28-Apr-2003\0
\\# B3LYP/6-31+G(D) SCF=(QC,MAXCYCLE=1024)\\5mer-2 CH3COOH after 2nd A
M1 opt. energy fromB3LYP\\1,1\C,0,-2.953111,-1.201804,1.012875\N,0,-2.
445543,-1.380104,2.043753\C,0,-5.011704,-0.402403,0.009244\C,0,-3.7354
93,-2.254363,-1.058461\C,0,-3.610503,-0.953803,-0.274749\H,0,-4.949556
,0.571342,0.55163\H,0,-5.546438,-0.242041,-0.958273\H,0,-5.599062,-1.1
26034,0.62336\H,0,-4.188296,-2.037471,-2.056676\H,0,-2.733469,-2.72253
4,-1.213918\H,0,-4.3938,-2.975688,-0.517206\C,0,-2.82387,0.10991,-1.04
9392\C,0,-1.478034,-0.294185,-1.64572\H,0,-2.683521,0.997814,-0.372696
\H,0,-3.467893,0.444015,-1.908872\H,0,-1.636957,-0.715194,-2.682345\O,
0,-0.902286,-1.334298,-0.829677\C,0,0.00098,-2.177737,-1.43037\C,0,0.3
64504,-3.342276,-0.576418\O,0,0.408847,-1.896182,-2.556441\H,0,1.17135
7,-3.931152,-1.078382\H,0,0.719994,-2.988919,0.423469\H,0,-0.533848,-3
.992526,-0.433413\C,0,-0.519703,0.889292,-1.751501\C,0,-0.193026,1.558
959,-0.418907\H,0,-0.978012,1.646457,-2.44337\H,0,0.427096,0.523635,-2
.232042\H,0,-0.650404,0.993936,0.440959\O,0,-0.719882,2.901483,-0.4882
34\C,0,-1.640057,3.31527,0.434118\C,0,-1.979489,4.758422,0.297351\O,0,
-2.088297,2.492606,1.237915\H,0,-1.561701,5.182168,-0.648056\H,0,-3.09
1048,4.875135,0.304037\H,0,-1.549521,5.310914,1.169912\C,0,1.305015,1.
725531,-0.176273\C,0,1.987868,0.419986,0.226821\H,0,1.454668,2.485295,
0.635716\H,0,1.806646,2.108065,-1.103223\H,0,1.765174,-0.38994,-0.5273
03\O,0,1.356286,0.029188,1.474123\C,0,1.726511,-1.133952,2.07074\C,0,2
.941493,-1.90174,1.690046\O,0,0.950676,-1.458076,2.991876\H,0,2.969578
,-2.066672,0.584314\H,0,3.853083,-1.320384,1.985442\H,0,2.952188,-2.88
8,2.217157\C,0,3.45087,0.643416,0.400675\C,0,4.341567,0.396593,-0.5708
08\H,0,3.746269,1.08224,1.367357\H,0,4.019644,-0.026977,-1.540287\C,0,
5.758515,0.666216,-0.429596\C,0,6.645168,0.427331,-1.399922\H,0,6.0790
21,1.0957,0.535803\H,0,7.715377,0.643502,-1.274914\H,0,6.365346,0.0068
11,-2.375825\Li,0,-1.29029,-1.417507,3.808783\\Version=x86-Linux-G98Re
vA.7\HF=-1293.0968957\RMSD=0.000e+00\Dipole=-1.0647099,-1.1924683,2.53
9742\PG=C01 [X(C20H29Li1N1O6)]\\@

Single point energy B3-LYP/6-31+G(d) on the DFT structure

N-N= 2.851430516194D+03 E-N=-8.689481650401D+03 KE= 1.280707000569D+03
1\1\GINC-MS3\SP\RB3LYP\6-31+G(d)\C20H29Li1N1O6(1+)\MARIE\29-Apr-2003\0
\\# B3LYP/6-31+G(D)\\5mer-2 CH3COOH after 2nd DFT opt. energy from DFT
\\1,1\C,0,-2.907567,-0.321594,0.885967\N,0,-2.144295,-0.190973,1.75431
9\C,0,-4.996235,0.619492,0.044406\C,0,-4.453621,-1.822715,-0.358453\C,
0,-3.849722,-0.399258,-0.237531\H,0,-4.602639,1.633945,0.161107\H,0,-5
.694458,0.605696,-0.798186\H,0,-5.538662,0.339498,0.951937\H,0,-5.1817

16,-1.81867,-1.176287\H,0,-3.671297,-2.548528,-0.570481\H,0,-4.972672,
-2.096211,0.565203\C,0,-3.110272,0.055571,-1.542753\C,0,-1.784207,-0.6
87179,-1.922281\H,0,-2.884697,1.11888,-1.441413\H,0,-3.83029,-0.060112
,-2.359537\H,0,-1.926524,-1.264129,-2.840079\O,0,-1.554841,-1.692724,-
0.838121\C,0,-0.386067,-2.391954,-0.607373\C,0,-0.638264,-3.430907,0.4
5968\O,0,0.691416,-2.146139,-1.152356\H,0,0.205849,-4.118296,0.509007\
H,0,-0.763403,-2.929933,1.427787\H,0,-1.558333,-3.978042,0.244451\C,0,
-0.598791,0.285418,-2.134757\C,0,-0.147404,1.005222,-0.860382\H,0,-0.8
9182,1.029098,-2.883406\H,0,0.245272,-0.288106,-2.51921\H,0,-0.33585,0
.378532,0.002876\O,0,-1.007857,2.235845,-0.708356\C,0,-1.124248,2.7838
36,0.541454\C,0,-1.854785,4.097233,0.513851\O,0,-0.660269,2.244856,1.5
60422\H,0,-2.3874,4.222033,-0.42788\H,0,-2.537652,4.153978,1.365338\H,
0,-1.125968,4.911001,0.61958\C,0,1.335003,1.437043,-0.854636\C,0,2.228
881,0.356883,-0.211971\H,0,1.445863,2.347709,-0.259458\H,0,1.692524,1.
640692,-1.868325\H,0,2.140041,-0.592741,-0.740487\O,0,1.564714,0.18520
4,1.148508\C,0,1.66539,-0.932804,1.943788\C,0,2.669641,-1.989105,1.608
714\O,0,0.836933,-0.952848,2.874572\H,0,2.382362,-2.451345,0.654679\H,
0,3.66126,-1.544754,1.483665\H,0,2.681875,-2.740954,2.397071\C,0,3.641
955,0.800016,-0.036237\C,0,4.677091,0.21356,-0.661505\H,0,3.791306,1.6
75924,0.59121\H,0,4.496749,-0.655443,-1.294614\C,0,6.059075,0.66599,-0
.568874\C,0,7.070821,0.068988,-1.212967\H,0,6.249148,1.532523,0.059779
\H,0,8.090662,0.425,-1.126516\H,0,6.910161,-0.79597,-1.85024\Li,0,-0.3
40151,0.576521,2.345334\\Version=x86-Linux-G98RevA.7\HF=-1293.1453673\
RMSD=6.291e-05\Dipole=-0.8070848,0.5015711,-0.6966581\PG=C01 [X(C20H29
Li1N1O6)]\\@

5mer – three acetic acids

Single point energy B3-LYP/6-31+G(d) on the MM/MD structure

N-N= 2.028412525266D+03 E-N=-6.509577880406D+03 KE= 1.053586758710D+03
1\1\GINC-MS5\SP\RB3LYP\6-31+G(d)\C18H25Li1N1O4(1+)\MARIE\17-Sep-2002\0
\\# B3LYP/6-31+G(D) SCF=(QC,MAXCYCLE=1024)\\5mer -3CH3COOH after MD, c
harge = 1.4284\\1,1\C,0,3.757,-8.377,7.658\N,0,2.883,-7.632,7.49\C,0,4
.462,-10.718,8.095\C,0,5.851,-8.816,8.95\C,0,4.939,-9.278,7.789\H,0,3.
879,-10.77,9.044\H,0,3.81,-11.118,7.283\H,0,5.323,-11.419,8.196\H,0,6.
169,-7.756,8.837\H,0,5.331,-8.896,9.933\H,0,6.771,-9.442,9.013\C,0,5.7
24,-9.292,6.439\C,0,6.318,-7.932,5.968\H,0,5.052,-9.687,5.647\H,0,6.56
2,-10.024,6.507\H,0,7.177,-7.72,6.644\O,0,5.316,-6.908,6.063\C,0,5.695
,-5.562,6.183\C,0,7.094,-5.086,6.371\O,0,4.786,-4.754,6.168\H,0,7.096,
-3.98,6.473\H,0,7.523,-5.517,7.296\H,0,7.712,-5.346,5.492\C,0,6.852,-8
.045,4.517\C,0,5.82,-7.732,3.417\H,0,7.266,-9.063,4.345\H,0,7.707,-7.3
49,4.393\H,0,5.439,-6.693,3.555\O,0,4.782,-8.717,3.432\C,0,3.464,-8.27
2,3.605\C,0,2.352,-9.118,3.121\O,0,3.211,-7.247,4.227\H,0,2.77,-10.005
,2.604\H,0,1.73,-9.445,3.977\H,0,1.736,-8.538,2.405\C,0,6.498,-7.821,2

.08\C,0,6.678,-6.757,1.289\H,0,6.834,-8.799,1.752\H,0,6.333,-5.776,1.6
01\C,0,7.343,-6.899,-0.017\C,0,7.535,-5.842,-0.809\H,0,7.681,-7.879,-0
.339\H,0,7.198,-4.859,-0.496\C,0,8.2,-5.991,-2.114\C,0,8.397,-4.941,-2
.909\H,0,8.537,-6.969,-2.445\H,0,8.888,-5.065,-3.868\H,0,8.074,-3.948,
-2.62\Li,0,3.23,-6.189,5.951\\Version=x86-Linux-G98RevA.7\HF=-1064.018
4916\RMSD=0.000e+00\Dipole=0.2127997,-0.6871073,1.7248948\PG=C01 [X(C1
8H25Li1N1O4)]\\@

Single point energy B3-LYP/6-31+G(d) on the AM1 structure

N-N= 2.000742288696D+03 E-N=-6.457036204074D+03 KE= 1.053395118890D+03
1\1\GINC-MS3\SP\RB3LYP\6-31+G(d)\C18H25Li1N1O4(1+)\MARIE\30-Sep-2002\0
\\# B3LYP/6-31+G(D) SCF=(QC,MAXCYCLE=1024)\\5mer - 3 CH3COOH, after AM
1 optimization, calcul of the B3LYP energy\\1,1\C,0,-3.491173,-1.08597
5,1.104774\N,0,-3.247578,-1.921179,1.87704\C,0,-4.591532,1.067433,0.81
4127\C,0,-4.608419,-0.624427,-1.015004\C,0,-3.784675,-0.035605,0.12595
1\H,0,-5.547197,0.656963,1.21955\H,0,-4.006495,1.522564,1.64918\H,0,-4
.833248,1.864136,0.069379\H,0,-4.087026,-1.492221,-1.483883\H,0,-5.604
472,-0.965111,-0.641169\H,0,-4.772269,0.160262,-1.793443\C,0,-2.472298
,0.573458,-0.385137\C,0,-1.498879,-0.388994,-1.063821\H,0,-1.942493,1.
072021,0.474968\H,0,-2.734398,1.366837,-1.13608\H,0,-2.015537,-0.95062
9,-1.892167\O,0,-1.109024,-1.326227,-0.037815\C,0,-0.639794,-2.568414,
-0.357377\C,0,-0.064606,-2.919124,-1.680235\O,0,-0.71663,-3.336895,0.6
19702\H,0,0.004113,-4.032306,-1.779162\H,0,-0.687547,-2.513682,-2.5142
34\H,0,0.96884,-2.491115,-1.754581\C,0,-0.292326,0.351482,-1.626689\C,
0,0.568319,1.046739,-0.568555\H,0,-0.65986,1.115649,-2.363526\H,0,0.34
7772,-0.378847,-2.188785\H,0,0.326765,0.65373,0.459399\O,0,0.274686,2.
458443,-0.650234\C,0,-0.115549,3.12249,0.482379\C,0,-0.108983,4.60085,
0.312375\O,0,-0.443696,2.46067,1.470553\H,0,0.826983,5.005766,0.773862
\H,0,-0.130328,4.88021,-0.768808\H,0,-0.993396,5.037779,0.83685\C,0,2.
020489,0.889021,-0.887016\C,0,2.884521,0.290061,-0.055477\H,0,2.336535
,1.323831,-1.848222\H,0,2.549424,-0.107327,0.919806\C,0,4.288256,0.128
,-0.365575\C,0,5.159288,-0.449328,0.482117\H,0,4.62429,0.514826,-1.343
269\H,0,4.825199,-0.828273,1.464408\C,0,6.566467,-0.606591,0.17881\C,0
,7.438642,-1.165098,1.022743\H,0,6.896683,-0.230891,-0.805845\H,0,8.50
2906,-1.271621,0.773105\H,0,7.151407,-1.547289,2.011524\Li,0,-2.067591
,-3.440268,2.731292\\Version=x86-Linux-G98RevA.7\HF=-1063.9888004\RMSD
=0.000e+00\Dipole=-2.9461953,-2.7564129,0.7525714\PG=C01 [X(C18H25Li1N
1O4)]\\@

Single point energy B3-LYP/6-31+G(d) on the DFT structure

N-N= 2.014383391336D+03 E-N=-6.482780151914D+03 KE= 1.053689295565D+03
1\1\GINC-MS5\SP\RB3LYP\6-31+G(d)\C18H25Li1N1O4(1+)\MARIE\27-Jan-2003\0
\\# B3LYP/6-31+G(D) SCF=(QC,MAXCYCLE=1024)\\3mer, calculation of energ
y after B3LYP/3-21G opt\\1,1\C,0,3.171867,-1.46479,-1.159323\N,0,2.682

44,-2.110574,-1.993532\C,0,4.905272,0.200939,-0.70274\C,0,4.363077,-1.
632875,0.980885\C,0,3.768857,-0.667589,-0.082831\H,0,5.662767,-0.43411
1,-1.17076\H,0,4.500488,0.892741,-1.446956\H,0,5.378188,0.777416,0.098
431\H,0,3.602298,-2.305396,1.388773\H,0,5.16186,-2.237565,0.54211\H,0,
4.78654,-1.036322,1.795116\C,0,2.695924,0.29785,0.520561\C,0,1.48693,-
0.34195,1.219635\H,0,2.329677,0.964842,-0.265998\H,0,3.219639,0.906519
,1.268008\H,0,1.795953,-1.005703,2.032125\O,0,0.872346,-1.198469,0.141
444\C,0,0.029425,-2.24943,0.286262\C,0,-0.670338,-2.495376,1.58794\O,0
,-0.135755,-2.947399,-0.740371\H,0,-1.150911,-3.472473,1.557467\H,0,0.
021786,-2.444608,2.433914\H,0,-1.437331,-1.721122,1.72296\C,0,0.467465
,0.699023,1.72337\C,0,-0.410199,1.309972,0.588965\H,0,1.007522,1.51319
9,2.216449\H,0,-0.184507,0.238132,2.47116\H,0,-0.157362,0.860423,-0.37
1607\O,0,-0.115203,2.777023,0.492903\C,0,0.674695,3.181574,-0.570414\C
,0,0.69414,4.685704,-0.653496\O,0,1.255909,2.386522,-1.312392\H,0,-0.3
05287,5.045399,-0.920954\H,0,0.945152,5.108251,0.323289\H,0,1.414868,5
.001424,-1.406815\C,0,-1.875309,1.193855,0.878145\C,0,-2.733917,0.5098
5,0.098714\H,0,-2.223516,1.70583,1.771983\H,0,-2.361822,0.037286,-0.81
1967\C,0,-4.150673,0.358842,0.365632\C,0,-4.994408,-0.328762,-0.436143
\H,0,-4.538519,0.840419,1.261069\H,0,-4.605019,-0.802858,-1.336832\C,0
,-6.416361,-0.482199,-0.186667\C,0,-7.243548,-1.164114,-0.993293\H,0,-
6.807487,-0.005302,0.709324\H,0,-8.301714,-1.256633,-0.778837\H,0,-6.8
86021,-1.648366,-1.89753\Li,0,0.919969,-2.850655,-2.22436\\Version=x86
-Linux-G98RevA.7\HF=-1064.0226754\RMSD=0.000e+00\Dipole=1.6222993,-1.8
098975,0.3954008\PG=C01 [X(C18H25Li1N1O4)]\\@

5mer – four acetic acids

Single point energy B3-LYP/6-31+G(d) on the MM/MD structure

N-N= 1.351768769229D+03 E-N=-4.623808916671D+03 KE= 8.266844418943D+02
1\1\GINC-MS5\SP\RB3LYP\6-31+G(d)\C16H21Li1N1O2(1+)\MARIE\08-Aug-2002\0
\\# B3LYP/6-31+G(D)\\5mer -4CH3COOH after MD charge = 1.4070\\1,1\C,0,
4.859,-6.801,8.861\N,0,4.899,-7.778,9.489\C,0,5.319,-4.361,8.782\C,0,3
.413,-5.315,7.467\C,0,4.846,-5.598,7.98\H,0,6.358,-4.489,9.165\H,0,5.3
16,-3.442,8.15\H,0,4.663,-4.159,9.66\H,0,2.958,-6.2,6.971\H,0,2.73,-5.
027,8.3\H,0,3.406,-4.474,6.735\C,0,5.831,-5.819,6.789\C,0,5.548,-7.046
,5.888\H,0,6.868,-5.917,7.187\H,0,5.837,-4.911,6.14\H,0,4.541,-6.915,5
.432\O,0,5.601,-8.241,6.682\C,0,5.137,-9.447,6.125\C,0,4.658,-9.612,4.
722\O,0,5.103,-10.404,6.877\H,0,4.299,-10.651,4.571\H,0,3.818,-8.922,4
.512\H,0,5.492,-9.439,4.015\C,0,6.612,-7.1,4.826\C,0,6.348,-6.83,3.544
\H,0,7.62,-7.364,5.125\H,0,5.343,-6.56,3.235\C,0,7.409,-6.909,2.528\C,
0,7.14,-6.684,1.241\H,0,8.422,-7.159,2.829\H,0,6.13,-6.435,0.931\C,0,8
.2,-6.773,0.224\C,0,7.929,-6.57,-1.066\H,0,9.215,-7.01,0.53\H,0,6.915,
-6.335,-1.376\C,0,8.988,-6.664,-2.081\C,0,8.721,-6.472,-3.37\H,0,10.00
8,-6.894,-1.788\H,0,9.513,-6.546,-4.105\H,0,7.722,-6.238,-3.718\Li,0,5

.61,-9.566,8.667\\Version=x86-Linux-G98RevA.7\HF=-834.9019045\RMSD=6.1
68e-05\Dipole=-0.8654199,-0.6299353,2.6834402\PG=C01 [X(C16H21Li1N1O2)
]\\@

Single point energy B3-LYP/6-31+G(d) on the AM1 structure

N-N= 1.349791641069D+03 E-N=-4.621411355726D+03 KE= 8.264844002025D+02
1\1\GINC-MS3\SP\RB3LYP\6-31+G(d)\C16H21Li1N1O2(1+)\MARIE\25-Sep-2002\0
\\# B3LYP/6-31+G(D) SCF=(QC,MAXCYCLE=1024)\\5mer - 4 CH3COOH, after AM
1 optimization, calcul of the B3LYP energy\\1,1\C,0,-4.250875,-0.68036
8,-0.190285\N,0,-5.012162,0.165195,-0.434098\C,0,-3.726858,-3.03203,-0
.556758\C,0,-3.213154,-1.941824,1.623267\C,0,-3.276802,-1.732783,0.113
523\H,0,-3.783803,-2.907248,-1.664502\H,0,-2.990594,-3.839558,-0.32437
8\H,0,-4.728558,-3.342444,-0.173824\H,0,-2.964748,-0.991087,2.151683\H
,0,-4.192443,-2.319068,2.006127\H,0,-2.426015,-2.699779,1.856737\C,0,-
1.904342,-1.343616,-0.454716\C,0,-1.311151,-0.027383,0.05742\H,0,-1.97
7067,-1.290072,-1.573617\H,0,-1.178352,-2.159355,-0.191982\H,0,-1.2722
43,-0.010935,1.182449\O,0,-2.240049,0.991351,-0.382277\C,0,-2.205727,2
.242408,0.160952\C,0,-1.052942,2.751845,0.943368\O,0,-3.246037,2.87330
3,-0.109416\H,0,-1.105219,3.867313,1.016205\H,0,-1.081485,2.319653,1.9
75478\H,0,-0.091368,2.45325,0.452065\C,0,0.032557,0.195248,-0.546595\C
,0,1.17678,-0.073123,0.102298\H,0,0.022817,0.569217,-1.582759\H,0,1.16
0857,-0.455225,1.139987\C,0,2.479029,0.107238,-0.49403\C,0,3.623574,-0
.170449,0.162358\H,0,2.501357,0.484551,-1.530708\H,0,3.599125,-0.55200
5,1.199532\C,0,4.928426,0.005308,-0.428366\C,0,6.068847,-0.275793,0.23
1356\H,0,4.955926,0.385681,-1.464177\H,0,6.042168,-0.657649,1.26793\C,
0,7.380508,-0.102786,-0.35565\C,0,8.514179,-0.38016,0.295254\H,0,7.404
077,0.277855,-1.392078\H,0,9.499968,-0.24196,-0.169186\H,0,8.533342,-0
.760516,1.325633\Li,0,-5.508735,2.181797,-0.838251\\Version=x86-Linux-
G98RevA.7\HF=-834.8931691\RMSD=0.000e+00\Dipole=-4.816,0.996554,-0.095
3566\PG=C01 [X(C16H21Li1N1O2)]\\@

Single point energy B3-LYP/6-31+G(d) on the DFT structure

N-N= 1.344944930654D+03 E-N=-4.610697677663D+03 KE= 8.267680827513D+02
1\1\GINC-MS5\SP\RB3LYP\6-31+G(d)\C16H21Li1N1O2(1+)\MARIE\29-Jan-2003\0
\\# B3LYP/6-31+G(D) SCF=QC\\5mer - 4 CH3COOH opt by B3LYP/3-21G\\1,1\C
,0,-4.378511,-0.457144,-0.240039\N,0,-5.034468,0.452533,-0.548501\C,0,
-4.16525,-2.891654,-0.404665\C,0,-3.520972,-1.653492,1.724768\C,0,-3.5
37025,-1.58692,0.171422\H,0,-4.184379,-2.865448,-1.498136\H,0,-3.55917
9,-3.743446,-0.081093\H,0,-5.184172,-3.02478,-0.030451\H,0,-3.144077,-
0.725318,2.164415\H,0,-4.529179,-1.835594,2.107588\H,0,-2.877196,-2.48
3367,2.03296\C,0,-2.093826,-1.431239,-0.418455\C,0,-1.260812,-0.223428
,0.054293\H,0,-2.157506,-1.394677,-1.511105\H,0,-1.541828,-2.337025,-0
.144742\H,0,-1.154611,-0.203752,1.142707\O,0,-2.159498,0.943041,-0.348
259\C,0,-2.090409,2.212723,0.106118\C,0,-0.914394,2.669842,0.914692\O,

0,-3.066713,2.945133,-0.184776\H,0,-0.969825,3.749444,1.048044\H,0,-0.
928964,2.188599,1.901637\H,0,0.017704,2.383835,0.419707\C,0,0.057273,-
0.135991,-0.631503\C,0,1.23762,-0.169493,0.02686\H,0,0.026418,-0.10598
1,-1.717678\H,0,1.230371,-0.219332,1.116897\C,0,2.535341,-0.15752,-0.5
97477\C,0,3.696734,-0.195933,0.107606\H,0,2.569653,-0.116941,-1.683673
\H,0,3.647859,-0.240908,1.195493\C,0,5.0094,-0.182331,-0.477347\C,0,6.
15168,-0.219186,0.25393\H,0,5.07308,-0.140357,-1.562656\H,0,6.083744,-
0.261793,1.34024\C,0,7.483878,-0.205936,-0.3134\C,0,8.60401,-0.242175,
0.42687\H,0,7.553999,-0.164381,-1.397927\H,0,9.588045,-0.231139,-0.026
808\H,0,8.567702,-0.284269,1.511557\Li,0,-4.655039,2.334256,-0.815076\
\Version=x86-Linux-G98RevA.7\HF=-834.9259864\RMSD=0.000e+00\Dipole=-2.
8415946,0.5541862,0.2263572\PG=C01 [X(C16H21Li1N1O2)]\\@

5mer – five acetic acids

Single point energy B3-LYP/6-31+G(d) on the MM/MD structure

N-N= 8.226423827855D+02 E-N=-3.035159882938D+03 KE= 5.996739026171D+02
1\1\GINC-MS5\SP\RB3LYP\6-31+G(d)\C14H17Li1N1(1+)\MARIE\07-Aug-2002\0\\
B3LYP/6-31+G(D)\\5mer -5CH3COOH after molecular dynamic charge = -1.
3836\\1,1\C,0,5.119,-5.982,8.474\N,0,6.079,-6.139,9.116\C,0,3.067,-4.5
99,8.191\C,0,3.006,-7.039,7.626\C,0,3.9,-5.777,7.636\H,0,2.158,-4.426,
7.568\H,0,2.722,-4.786,9.234\H,0,3.648,-3.648,8.184\H,0,2.612,-7.279,8
.639\H,0,2.13,-6.894,6.951\H,0,3.55,-7.934,7.249\C,0,4.321,-5.449,6.21
8\C,0,5.111,-6.258,5.501\H,0,3.957,-4.535,5.752\H,0,5.471,-7.189,5.924
\C,0,5.51,-5.901,4.131\C,0,6.305,-6.702,3.418\H,0,5.155,-4.972,3.694\H
,0,6.658,-7.636,3.842\C,0,6.713,-6.336,2.052\C,0,7.514,-7.131,1.34\H,0
,6.357,-5.406,1.62\H,0,7.87,-8.064,1.766\C,0,7.926,-6.761,-0.023\C,0,8
.731,-7.552,-0.735\H,0,7.567,-5.83,-0.454\H,0,9.09,-8.484,-0.309\C,0,9
.142,-7.178,-2.097\C,0,9.944,-7.965,-2.811\H,0,8.789,-6.252,-2.541\H,0
,10.235,-7.675,-3.813\H,0,10.315,-8.905,-2.422\Li,0,7.969,-6.263,9.897
\\Version=x86-Linux-G98RevA.7\HF=-605.7675659\RMSD=9.625e-05\Dipole=1.
5883796,0.3589433,7.8730265\PG=C01 [X(C14H17Li1N1)]\\@

Single point energy B3-LYP/6-31+G(d) on the AM1 structure

N-N= 8.192583314038D+02 E-N=-3.028508790806D+03 KE= 5.995654649488D+02
1\1\GINC-MS3\SP\RB3LYP\6-31+G(d)\C14H17Li1N1(1+)\MARIE\26-Sep-2002\0\\
B3LYP/6-31+G(D)\\5mer - 5 CH3COOH, after AM1 optimization, calcul of
the B3LYP energy\\1,1\C,0,-4.890998,0.782792,0.114673\N,0,-5.442273,1
.804057,0.206436\C,0,-4.961489,-1.39875,-0.974152\C,0,-4.139403,-1.164
277,1.36784\C,0,-4.181361,-0.503585,-0.007539\H,0,-4.414717,-2.367494,
-1.083567\H,0,-5.984647,-1.606794,-0.580287\H,0,-5.043631,-0.922382,-1
.979921\H,0,-5.171521,-1.419014,1.709835\H,0,-3.545178,-2.108537,1.297
824\H,0,-3.662924,-0.495151,2.12332\C,0,-2.82433,-0.224999,-0.577504\C

,0,-1.669947,-0.312952,0.101775\H,0,-2.831063,0.034031,-1.649552\H,0,-
1.651052,-0.588237,1.1724\C,0,-0.38647,-0.067407,-0.513259\C,0,0.77511
7,-0.178135,0.163185\H,0,-0.391606,0.21142,-1.580673\H,0,0.778537,-0.4
64287,1.230981\C,0,2.061437,0.059458,-0.443815\C,0,3.219994,-0.062759,
0.23553\H,0,2.061808,0.347263,-1.509232\H,0,3.218471,-0.354051,1.30162
9\C,0,4.510725,0.170081,-0.366866\C,0,5.665424,0.041155,0.314411\H,0,4
.514388,0.462228,-1.431319\H,0,5.662676,-0.252795,1.379373\C,0,6.96281
,0.271438,-0.284854\C,0,8.11116,0.142098,0.385957\H,0,6.962051,0.56547
,-1.349344\H,0,9.085311,0.320868,-0.088586\H,0,8.154466,-0.149088,1.44
4144\Li,0,-6.387161,3.611069,0.351875\\Version=x86-Linux-G98RevA.7\HF=
-605.7774833\RMSD=7.799e-05\Dipole=-8.4778361,4.0678304,0.5923394\PG=C
01 [X(C14H17Li1N1)]\\@

Single point energy B3-LYP/6-31+G(d) on the DFT structure

N-N= 8.170335962822D+02 E-N=-3.023847710689D+03 KE= 5.997599989496D+02
1\1\GINC-MS5\SP\RB3LYP\6-31+G(d)\C14H17Li1N1(1+)\MARIE\27-Feb-2003\0\\
B3LYP/6-31+G(D)\\%mer - 5 CH3COOH after DFT opt\\1,1\C,0,-4.887727,0
.806038,0.141022\N,0,-5.373411,1.862194,0.218436\C,0,-5.092743,-1.4055
64,-0.91692\C,0,-4.16878,-1.14139,1.444781\C,0,-4.236463,-0.50741,0.02
7133\H,0,-4.585267,-2.370405,-1.002775\H,0,-6.094607,-1.561629,-0.5053
71\H,0,-5.171118,-0.961752,-1.913715\H,0,-5.178262,-1.32367,1.824148\H
,0,-3.643844,-2.09707,1.360659\H,0,-3.631754,-0.500636,2.149159\C,0,-2
.869489,-0.238382,-0.603077\C,0,-1.685711,-0.293455,0.042221\H,0,-2.90
1543,-0.004961,-1.664837\H,0,-1.659427,-0.536782,1.102203\C,0,-0.40771
4,-0.070459,-0.585615\C,0,0.77469,-0.163952,0.080914\H,0,-0.404512,0.1
76309,-1.64498\H,0,0.758236,-0.419174,1.140425\C,0,2.064118,0.047856,-
0.509388\C,0,3.232077,-0.057208,0.182089\H,0,2.095225,0.302149,-1.5668
96\H,0,3.192997,-0.315404,1.23981\C,0,4.534828,0.147455,-0.386545\C,0,
5.688631,0.034186,0.319293\H,0,4.582654,0.405656,-1.442745\H,0,5.63979
5,-0.225996,1.375742\C,0,7.008426,0.236761,-0.240831\C,0,8.143463,0.12
04,0.468126\H,0,7.056076,0.495859,-1.296279\H,0,9.116443,0.277923,0.01
7753\H,0,8.130226,-0.137887,1.522997\Li,0,-6.091026,3.55762,0.332146\\
Version=x86-Linux-G98RevA.7\HF=-605.7867998\RMSD=6.906e-05\Dipole=-7.7
467599,3.7853769,0.5831252\PG=C01 [X(C14H17Li1N1)]\\@

5mer – three acetic acids – one lithium acetate

Single point energy B3-LYP/6-31+G(d) on the MM/MD structure

N-N= 1.355181608714D+03 E-N=-4.613835639203D+03 KE= 8.193886240651D+02
1\1\GINC-MS5\SP\RB3LYP\6-31+G(d)\C16H22N1O2(1+)\MARIE\31-Jul-2002\0\\#
B3LYP/6-31+G(D)\\5mer - 3CH3COOH -CH3COO-Li+ after molecular dynamic\
\1,1\C,0,8.029,-8.541,4.884\N,0,8.078,-8.243,3.766\C,0,9.259,-8.699,7.
035\C,0,7.442,-10.327,6.517\C,0,7.887,-8.852,6.334\H,0,9.185,-8.916,8.

127\H,0,10.019,-9.403,6.618\H,0,9.678,-7.672,6.933\H,0,6.46,-10.545,6.
045\H,0,8.179,-11.037,6.073\H,0,7.353,-10.596,7.596\C,0,6.856,-7.879,7
.013\C,0,5.602,-7.464,6.186\H,0,7.37,-6.949,7.349\H,0,6.499,-8.349,7.9
6\H,0,4.842,-7.13,6.941\O,0,5.114,-8.592,5.453\C,0,3.717,-8.704,5.371\
C,0,3.086,-10.041,5.359\O,0,3.046,-7.7,5.192\H,0,1.986,-9.946,5.252\H,
0,3.49,-10.634,4.514\H,0,3.311,-10.558,6.314\C,0,5.882,-6.269,5.238\H,
0,6.97,-6.104,5.096\H,0,5.478,-5.349,5.714\H,0,5.68,-7.301,3.303\C,0,5
.28,-5.272,3.083\C,0,4.113,-4.637,2.648\H,0,6.252,-4.891,2.789\H,0,3.1
42,-5.038,2.932\C,0,4.173,-3.496,1.842\C,0,3.015,-2.857,1.384\H,0,5.14
1,-3.094,1.553\H,0,2.039,-3.248,1.66\C,0,3.093,-1.724,0.572\C,0,1.954,
-1.073,0.099\H,0,4.06,-1.32,0.285\H,0,2.056,-0.197,-0.53\H,0,0.952,-1.
414,0.337\C,0,5.223,-6.457,3.864\\Version=x86-Linux-G98RevA.7\HF=-827.
752836\RMSD=3.578e-05\Dipole=-1.4446466,2.2244888,-0.6257054\PG=C01 [X
(C16H22N1O2)]\\@

Single point energy B3-LYP/6-31+G(d) on the AM1 structure

N-N= 1.346701517962D+03 E-N=-4.597089331405D+03 KE= 8.195181832551D+02
1\1\GINC-MS3\SP\RB3LYP\6-31+G(d)\C16H22N1O2(1+)\MARIE\26-Sep-2002\0\\#
B3LYP/6-31+G(D)\\5mer - 3 CH3COOH - CH3COOLi, after AM1 optimization,
calcul of the B3LYP energy\\1,1\C,0,-4.128391,0.604478,0.594505\N,0,-
4.151396,1.724221,0.904509\C,0,-5.371643,-1.142856,-0.560408\C,0,-3.99
1772,-1.677728,1.439193\C,0,-4.08882,-0.798154,0.195943\H,0,-5.493508,
-0.480617,-1.450575\H,0,-5.33095,-2.204844,-0.90183\H,0,-6.257608,-1.0
13198,0.106523\H,0,-3.98847,-2.753315,1.139464\H,0,-3.060568,-1.458845
,2.013247\H,0,-4.869397,-1.497486,2.106422\C,0,-2.893186,-1.041579,-0.
735705\C,0,-1.588615,-0.426182,-0.231063\H,0,-3.124277,-0.611436,-1.74
7515\H,0,-2.763079,-2.148953,-0.851121\H,0,-1.567862,-0.372815,0.89341
3\O,0,-1.569789,0.908124,-0.768011\C,0,-0.800448,1.85509,-0.142917\C,0
,-1.0939,3.239329,-0.593921\O,0,0.029278,1.457884,0.683534\H,0,-1.3560
12,3.253815,-1.680031\H,0,-1.970284,3.623659,-0.009406\H,0,-0.206536,3
.89035,-0.40372\C,0,-0.377327,-1.211364,-0.746057\H,0,-0.237036,-0.999
64,-1.841267\H,0,-0.588317,-2.316125,-0.642859\H,0,0.711111,-0.70422,1
.102915\C,0,2.094232,-0.918803,-0.539322\C,0,3.239755,-0.600737,0.2125
63\H,0,2.218135,-1.144068,-1.615023\H,0,3.113084,-0.357227,1.28886\C,0
,4.52395,-0.563585,-0.343489\C,0,5.633552,-0.223795,0.398077\H,0,4.642
302,-0.811965,-1.41537\H,0,5.523903,0.030374,1.472447\C,0,6.949239,-0.
178736,-0.159289\C,0,8.033252,0.158722,0.565494\H,0,7.050882,-0.435264
,-1.230801\H,0,9.0397,0.18823,0.11747\H,0,7.983982,0.422501,1.633532\C
,0,0.845901,-0.92352,0.022974\\Version=x86-Linux-G98RevA.7\HF=-827.876
5168\RMSD=4.917e-05\Dipole=5.2401432,-1.7968601,-0.6477805\PG=C01 [X(C
16H22N1O2)]\\@

Single point energy B3-LYP/6-31+G(d) on the DFT structure

N-N= 1.349996472088D+03 E-N=-4.603224983527D+03 KE= 8.197684714197D+02

1\1\GINC-MS5\SP\RB3LYP\6-31+G(d)\C16H22N1O2(1+)\MARIE\27-Feb-2003\0\\#
B3LYP/6-31+G(D)\\5mer - 3 CH3COOH - CH3COOLi after DFT optimization\\
1,1\C,0,-4.219278,0.78187,0.271867\N,0,-4.203004,1.937209,0.414941\C,0
,-5.472774,-1.076685,-0.745732\C,0,-4.368925,-1.328275,1.524086\C,0,-4
.242027,-0.680289,0.11705\H,0,-5.419287,-0.610171,-1.733871\H,0,-5.495
652,-2.165344,-0.863966\H,0,-6.395888,-0.75802,-0.253787\H,0,-4.427123
,-2.416428,1.415557\H,0,-3.51686,-1.076676,2.163853\H,0,-5.279882,-0.9
76718,2.016436\C,0,-2.946854,-1.183773,-0.604779\C,0,-1.645635,-0.6173
48,-0.034941\H,0,-2.99182,-0.91085,-1.664012\H,0,-2.936082,-2.277096,-
0.527246\H,0,-1.660404,-0.57809,1.058963\O,0,-1.630104,0.790606,-0.534
681\C,0,-0.652949,1.605335,-0.074807\C,0,-0.944258,3.047565,-0.338612\
O,0,0.350725,1.146072,0.523874\H,0,-0.924429,3.233985,-1.419054\H,0,-1
.963788,3.251217,0.010532\H,0,-0.212176,3.680014,0.161156\C,0,-0.36386
6,-1.322009,-0.517008\H,0,-0.276235,-1.204493,-1.601515\H,0,-0.453418,
-2.395436,-0.293823\H,0,0.891913,-0.926149,1.262417\C,0,2.098294,-0.70
0634,-0.489009\C,0,3.287513,-0.520887,0.192688\H,0,2.105162,-0.738204,
-1.574413\H,0,3.251812,-0.465143,1.280141\C,0,4.558019,-0.408812,-0.42
093\C,0,5.705714,-0.239497,0.308132\H,0,4.61523,-0.457581,-1.504929\H,
0,5.63484,-0.191399,1.393976\C,0,7.017839,-0.116759,-0.264809\C,0,8.12
1833,0.051338,0.491076\H,0,7.100417,-0.163843,-1.346941\H,0,9.106072,0
.142454,0.046789\H,0,8.068014,0.102044,1.574631\C,0,0.873291,-0.816466
,0.182557\\Version=x86-Linux-G98RevA.7\HF=-827.8841278\RMSD=4.539e-05\
Dipole=3.4152412,-1.6312713,-0.2237719\PG=C01 [X(C16H22N1O2)]\\@

5mer – four acetic acids – one lithium acetate

Single point energy B3-LYP/6-31+G(d) on the MM/MD structure

N-N= 8.445309564041D+02 E-N=-3.058587962765D+03 KE= 5.926206033139D+02
1\1\GINC-MS5\SP\RB3LYP\6-31+G(d)\C14H18N1(1+)\MARIE\07-Aug-2002\0\\# B
3LYP/6-31+G(D)\\5mer -4CH3COOH -CH3COOLi after MD, overall charge = 1.
5508\\1,1\C,0,2.314,-10.162,3.565\N,0,1.448,-9.406,3.63\C,0,4.515,-10.
658,2.497\C,0,2.967,-12.516,3.124\C,0,3.471,-11.113,3.55\H,0,4.092,-10
.71,1.463\H,0,4.846,-9.603,2.622\H,0,5.42,-11.311,2.494\H,0,2.182,-12.
914,3.811\H,0,2.51,-12.502,2.104\H,0,3.794,-13.265,3.094\C,0,4.118,-11
.223,4.979\H,0,5.083,-11.776,4.923\H,0,3.455,-11.849,5.621\H,0,4.537,-
10.115,6.84\C,0,5.381,-9.118,5.237\C,0,5.145,-7.835,4.746\H,0,6.388,-9
.524,5.242\H,0,4.14,-7.411,4.756\C,0,6.189,-7.073,4.231\C,0,5.96,-5.79
1,3.737\H,0,7.202,-7.468,4.218\H,0,4.956,-5.375,3.749\C,0,7.006,-5.022
,3.234\C,0,6.781,-3.734,2.752\H,0,8.015,-5.424,3.221\H,0,5.776,-3.322,
2.765\C,0,7.83,-2.963,2.259\C,0,7.615,-1.676,1.787\H,0,8.841,-3.359,2.
241\H,0,8.445,-1.09,1.411\H,0,6.628,-1.227,1.788\C,0,4.328,-9.9,5.769\
\Version=x86-Linux-G98RevA.7\HF=-598.655757\RMSD=8.139e-06\Dipole=2.85
09983,1.2885619,0.3134967\PG=C01 [X(C14H18N1)]\\@

Single point energy B3-LYP/6-31+G(d) on the AM1 structure

N-N= 8.139996436148D+02 E-N=-2.997770945824D+03 KE= 5.926142448732D+02
1\1\GINC-MS3\SP\RB3LYP\6-31+G(d)\C14H18N1(1+)\MARIE\26-Sep-2002\0\\# B
3LYP/6-31+G(D)\\5mer - 4 CH3COOH - CH3COOLi, after AM1 optimization, c
alcul of the B3LYP energy\\1,1\C,0,4.040348,1.283178,-0.436358\N,0,3.7
81049,2.351289,-0.814183\C,0,4.779005,0.008071,1.507154\C,0,5.532986,-
0.613948,-0.78348\C,0,4.372745,-0.05645,0.038067\H,0,5.64552,0.701239,
1.636251\H,0,3.934509,0.373038,2.138551\H,0,5.081162,-1.007814,1.85924
3\H,0,5.278616,-0.62509,-1.870255\H,0,6.443553,0.015598,-0.635951\H,0,
5.759428,-1.656047,-0.453008\C,0,3.153087,-0.974459,-0.142122\H,0,3.32
9029,-1.919012,0.449079\H,0,3.072917,-1.27628,-1.223547\H,0,1.976083,0
.465785,1.040124\C,0,0.673352,-0.775911,-0.132355\C,0,-0.535996,-0.165
543,0.297487\H,0,0.598289,-1.603305,-0.862211\H,0,-0.463311,0.666694,1
.02749\C,0,-1.776796,-0.560982,-0.164389\C,0,-2.957186,0.059803,0.2478
61\H,0,-1.842114,-1.393629,-0.890027\H,0,-2.897508,0.896613,0.97419\C,
0,-4.223538,-0.329703,-0.222566\C,0,-5.378761,0.291675,0.181519\H,0,-4
.277914,-1.166041,-0.94484\H,0,-5.334246,1.131293,0.904267\C,0,-6.6724
29,-0.097023,-0.294597\C,0,-7.804515,0.514175,0.098645\H,0,-6.710005,-
0.936251,-1.014193\H,0,-8.79054,0.200795,-0.279589\H,0,-7.818108,1.352
93,0.811478\C,0,1.888913,-0.362805,0.310505\\Version=x86-Linux-G98RevA
.7\HF=-598.7806191\RMSD=6.544e-05\Dipole=-3.8737105,-1.505445,0.734427
4\PG=C01 [X(C14H18N1)]\\@

Single point energy B3-LYP/6-31+G(d) on the DFT structure

N-N= 8.279653584987D+02 E-N=-3.025933662748D+03 KE= 5.928445950345D+02
1\1\GINC-MS5\SP\RB3LYP\6-31+G(d)\C14H18N1(1+)\MARIE\28-Feb-2003\0\\# B
3LYP/6-31+G(D)\\5mer - 4 CH3COOH - CH3COOLi after DFT optimization\\1,
1\C,0,3.296376,1.351319,0.125378\N,0,2.617983,2.294981,0.047692\C,0,4.
204106,-0.345201,1.673116\C,0,5.537376,0.439526,-0.346646\C,0,4.118294
,0.140705,0.203982\H,0,4.703442,0.411784,2.28451\H,0,3.209566,-0.52747
7,2.09101\H,0,4.789798,-1.269655,1.71536\H,0,5.49045,0.787327,-1.38282
1\H,0,6.015381,1.211574,0.263381\H,0,6.143631,-0.470985,-0.300453\C,0,
3.446405,-0.961812,-0.72112\H,0,4.086742,-1.847781,-0.671347\H,0,3.448
286,-0.575305,-1.746027\H,0,1.928701,-2.112166,0.416809\C,0,0.956127,-
0.589825,-0.685861\C,0,-0.344131,-0.886293,-0.200602\H,0,1.070204,0.24
5097,-1.370479\H,0,-0.450005,-1.73248,0.47726\C,0,-1.477126,-0.158753,
-0.53053\C,0,-2.736446,-0.477545,-0.017884\H,0,-1.381196,0.692588,-1.1
98421\H,0,-2.815837,-1.333955,0.650607\C,0,-3.909985,0.238976,-0.30672
2\C,0,-5.130662,-0.113466,0.227849\H,0,-3.847056,1.097537,-0.969492\H,
0,-5.18191,-0.975736,0.891267\C,0,-6.351875,0.585644,-0.031703\C,0,-7.
527031,0.20264,0.516754\H,0,-6.313038,1.447671,-0.691043\H,0,-8.447887
,0.737757,0.315867\H,0,-7.593429,-0.655324,1.179467\C,0,2.054951,-1.29
1806,-0.287561\\Version=x86-Linux-G98RevA.7\HF=-598.7895151\RMSD=2.193
e-05\Dipole=-3.0032826,-1.8440121,0.1097124\PG=C01 [X(C14H18N1)]\\@

5mer – four acetic acids – one lithium acetate – isobutyronitrile (polyene)

Single point energy B3-LYP/6-31+G(d) on the MM/MD structure

N-N= 4.082500508984D+02 E-N=-1.700330740221D+03 KE= 3.835202554116D+02
1\1\GINC-MS5\SP\RB3LYP\6-31+G(d)\C10H11(1+)\MARIE\04-Aug-2002\0\\# B3L
YP/6-31+G(D)\\5mer - 4CH3COOH, AIBN-H, CH3COOLi charge of 1.0707 after
MD\\1,1\C,0,5227.418,-565.238,159.78\H,0,5227.782,-564.398,160.356\H,
0,5227.761,-566.226,160.048\C,0,5226.012,-565.985,157.939\C,0,5226.249
,-567.365,158.016\H,0,5225.341,-565.616,157.172\H,0,5226.91,-567.796,1
58.761\C,0,5225.628,-568.231,157.121\C,0,5225.851,-569.605,157.182\H,0
,5224.958,-567.842,156.358\H,0,5226.517,-570.014,157.936\C,0,5225.229,
-570.47,156.285\C,0,5225.451,-571.843,156.345\H,0,5224.562,-570.071,15
5.527\H,0,5226.118,-572.249,157.1\C,0,5224.828,-572.706,155.447\C,0,52
25.045,-574.075,155.502\H,0,5224.16,-572.314,154.687\H,0,5224.552,-574
.731,154.796\H,0,5225.704,-574.513,156.242\C,0,5226.572,-565.013,158.7
76\\Version=x86-Linux-G98RevA.7\HF=-387.2390046\RMSD=3.492e-05\Dipole=
0.322742,-0.0598674,0.2495819\PG=C01 [X(C10H11)]\\@

Single point energy B3-LYP/6-31+G(d) on the AM1 structure

N-N= 4.023161501590D+02 E-N=-1.688515752339D+03 KE= 3.833059426362D+02
1\1\GINC-MS3\SP\RB3LYP\6-31+G(d)\C10H11(1+)\MARIE\27-Sep-2002\0\\# B3L
YP/6-31+G(D)\\5mer -4CH3COOH -CH3COOLi -IH, after AM1 optimization, ca
lcul of the B3LYP energy\\1,1\C,0,5.49282,-0.52252,0.00013\H,0,6.03656
4,-0.762617,-0.931741\H,0,6.036367,-0.76236,0.932189\C,0,3.125215,0.58
8469,-0.000106\C,0,1.904519,-0.142021,-0.000061\H,0,3.069075,1.696004,
-0.000259\H,0,1.963308,-1.249257,0.000026\C,0,0.670298,0.480134,-0.000
101\C,0,-0.525807,-0.238739,-0.000025\H,0,0.623641,1.58568,-0.00016\H,
0,-0.485424,-1.347619,0.000053\C,0,-1.785757,0.385753,-0.000004\C,0,-2
.958049,-0.327735,0.000125\H,0,-1.820229,1.491644,-0.000083\H,0,-2.933
828,-1.436164,0.000219\C,0,-4.245106,0.300912,0.000231\C,0,-5.394505,-
0.398009,-0.000164\H,0,-4.262227,1.406923,0.000626\H,0,-6.374959,0.104
192,-0.000144\H,0,-5.428694,-1.498282,-0.000603\C,0,4.31244,0.002396,-
0.000046\\Version=x86-Linux-G98RevA.7\HF=-387.3501158\RMSD=4.256e-05\D
ipole=-0.0694574,-0.3400237,0.0000191\PG=C01 [X(C10H11)]\\@

Single point energy B3-LYP/6-31+G(d) on the DFT structure

N-N= 4.025361052148D+02 E-N=-1.684185951667D+03 KE= 3.816295434333D+02
1\1\GINC-MS5\FOpt\RB3LYP\3-21G\C10H11(1+)\MARIE\15-Nov-2002\0\\# B3LYP
/3-21G OPT\\5mer - 4 CH3COOH - CH3COOLi - IH,b3lyp/3-21G optimization
after AM1 optimization\\1,1\C,5.4425002346,-0.6752237612,0.0001176135\

H,5.9410323208,-0.952008518,-0.9278501938\H,5.9408220895,-0.9520330652
,0.9281916577\C,3.158549469,0.6227288611,-0.0000447134\C,1.9077768407,
-0.056724136,-0.0000474085\H,3.166450523,1.7108493999,0.0000304877\H,1
.9326658307,-1.1443039823,-0.0000666702\C,0.679153767,0.5832615227,-0.
0000299804\C,-0.520829337,-0.132386727,-0.0000381994\H,0.6450218237,1.
6690444799,-0.000008289\H,-0.46632009,-1.2203740529,-0.0000572919\C,-1
.7946928973,0.4588953222,-0.0000152387\C,-2.9482408801,-0.2964867476,-
0.0000181121\H,-1.8680729732,1.5428192635,0.000006557\H,-2.8616717704,
-1.3822627893,-0.0000411926\C,-4.2685395906,0.2539282843,0.0000078151\
C,-5.3707270975,-0.5298461264,0.000015584\H,-4.3686513403,1.3352820318
,0.0000259554\H,-6.3681128909,-0.1055971019,0.000044703\H,-5.299390440
9,-1.6136530367,-0.0000007168\C,4.3160873108,-0.042773597,0.0000068056
\\Version=x86-Linux-G98RevA.7\HF=-385.2155602\RMSD=2.879e-09\RMSF=2.56
5e-05\Dipole=-0.077011,-0.4113623,0.0000716\PG=C01 [X(C10H11)]\\@

Acetic acid

Single point energy B3-LYP/6-31+G(d) on the MM/MD structure

N-N= 1.195606152702D+02 E-N=-7.754356125388D+02 KE= 2.268178251635D
1\1\GINC-MS5\SP\RB3LYP\6-31+G(d)\C2H4O2\MARIE\30-Jul-2002\0\\# B3LYP
-31+G(D)\\acetic acid after molecular dynamic\\0,1\H,0,3.154,-5.653,
205\O,0,3.712,-5.191,5.913\C,0,4.949,-4.776,5.428\C,0,5.33,-5.022,4.
2\O,0,5.727,-4.204,6.17\H,0,6.344,-4.617,3.826\H,0,5.322,-6.112,3.82
H,0,4.599,-4.516,3.353\\Version=x86-Linux-G98RevA.7\HF=-229.0810108\
SD=9.222e-05\Dipole=-0.638774,-0.7489354,-1.5538442\PG=C01 [X(C2H4O2
\\@

Single point energy B3-LYP/6-31+G(d) on the AM1 structure

N-N= 1.200052954582D+02 E-N=-7.763301718768D+02 KE= 2.268689782252D+02
1\1\GINC-MS3\SP\RB3LYP\6-31+G(d)\C2H4O2\MARIE\27-Sep-2002\0\\# B3LYP/6
-31+G(D)\\CH3COOH, after AM1 optimization, calcul of the B3LYP energy\
\0,1\H,0,-0.344038,-1.780185,0.000058\O,0,-0.888879,-0.982154,-0.00000
2\C,0,-0.086077,0.127299,-0.000032\C,0,1.393033,-0.053166,0.000001\O,0
,-0.712488,1.185986,0.000011\H,0,1.896703,0.944315,-0.000433\H,0,1.708
279,-0.619393,0.910298\H,0,1.70826,-0.620189,-0.909803\\Version=x86-Li
nux-G98RevA.7\HF=-229.0819132\RMSD=9.905e-05\Dipole=1.4792219,-1.25150
05,0.0000422\PG=C01 [X(C2H4O2)]\\@

Single point energy B3-LYP/6-31+G(d) on the DFT structure

N-N= 1.191994599350D+02 E-N=-7.746638213132D+02 KE= 2.268304083998D+02
1\1\GINC-MS5\SP\RB3LYP\6-31+G(d)\C2H4O2\MARIE\28-Feb-2003\0\\# B3LYP/6
-31+G(D)\\acetic acid after DFT optimization\\0,1\H,0,0.213363,1.83339

4,0.000218\O,0,0.831259,1.055705,0.000113\C,0,0.131661,-0.145787,-0.00
0118\C,0,-1.385086,0.008899,0.000003\O,0,0.740844,-1.199537,-0.000067\
H,0,-1.841111,-0.980314,-0.000247\H,0,-1.714227,0.559194,0.889237\H,0,
-1.714302,0.559702,-0.888883\\Version=x86-Linux-G98RevA.7\HF=-229.0851
25\RMSD=8.730e-05\Dipole=-1.4504679,1.1430135,0.0000584\PG=C01 [X(C2H4
O2)]\\@

Lithium acetate

Single point energy B3-LYP/6-31+G(d) on the MM/MD structure

N-N= 1.334120065580D+02 E-N=-8.215726128482D+02 KE= 2.339816667409D
1\1\GINC-MS5\SP\RB3LYP\6-31+G(d)\C2H3Li1O2\MARIE\30-Jul-2002\0\\# B3
P/6-31+G(D)\\CH3COO-Li+ after molecular dynamic\\0,1\C,0,1595.122,-9
.905,1459.14\C,0,1595.464,-927.521,1458.794\O,0,1594.468,-929.19,146
184\H,0,1596.032,-927.525,1457.844\H,0,1594.533,-926.935,1458.672\H,
1596.086,-927.089,1459.601\O,0,1595.476,-929.866,1458.395\Li,0,1594.
6,-931.216,1459.368\\Version=x86-Linux-G98RevA.7\HF=-236.0859702\RMS
2.531e-05\Dipole=-0.1567426,-1.670632,-0.0212341\PG=C01 [X(C2H3Li1O2
\\@

Single point energy B3-LYP/6-31+G(d) on the AM1 structure

N-N= 1.294195457576D+02 E-N=-8.135834436269D+02 KE= 2.336273328683D+02
1\1\GINC-MS3\SP\RB3LYP\6-31+G(d)\C2H3Li1O2\MARIE\09-Apr-2003\0\\# B3LY
P/6-31+G(D)\\CH3COOLi, after AM1 optimization, calcul of the B3LYP ene
rgy\\0,1\C\O,1,1.286027\O,1,1.285316,2,116.81471\Li,3,2.241584,1,92.39
9222,2,-0.006795,0\C,1,1.496277,2,121.494892,3,179.989455,0\H,5,1.1155
93,1,110.52586,2,-179.484945,0\H,5,1.116543,1,109.3295,2,-58.725363,0\
H,5,1.116954,1,109.304334,2,59.795624,0\\Version=x86-Linux-G98RevA.7\H
F=-236.0725722\RMSD=6.530e-05\Dipole=1.7967094,0.0005847,1.1104361\PG=
C01 [X(C2H3Li1O2)]\\@

Single point energy B3-LYP/6-31+G(d) on the DFT structure

N-N= 1.321661095991D+02 E-N=-8.186207665173D+02 KE= 2.337985527157D+02
1\1\GINC-MS3\SP\RB3LYP\6-31+G(d)\C2H3Li1O2\MARIE\08-Apr-2003\0\\# B3LY
P/6-31+G(D)\\CH3COOLi after the 3rd DFt opt.\\0,1\C\O,1,1.30159006\O,1
,1.3015773,2,119.4058243\Li,3,1.85103257,1,82.91260581,2,0.0758927,0\C
,1,1.51464755,2,120.2812664,4,178.2506593,0\H,5,1.09114718,1,109.90011
34,2,152.4476106,0\H,5,1.09749255,1,108.8959627,2,-88.92768545,0\H,5,1
.09118787,1,109.8942461,2,29.66399737,0\\Version=x86-Linux-G98RevA.7\H
F=-236.0959988\RMSD=4.202e-05\Dipole=1.0421059,-0.0323247,0.609416\PG=
C01 [X(C2H3Li1O2)]\\@

Isobutyronitrile

Single point energy B3-LYP/6-31+G(d) on the MM/MD structure

N-N= 1.577824001413D+02 E-N=-8.045193062595D+02 KE= 2.0910
1\1\GINC-MS5\SP\RB3LYP\6-31+G(d)\C4H7N1\MARIE\30-Jul-2002\0
-31+G(D)\\1/2 initiator + H after molecular dynamic\\0,1\C,
932,1.795\N,0,5.782,-4.533,2.402\C,0,3.763,-6.985,0.923\C,0
37,-0.405\C,0,3.734,-5.446,1.011\H,0,3.749,-7.442,1.94\H,0,
,0.378\H,0,4.676,-7.349,0.397\H,0,4.623,-5.115,-0.985\H,0,2
-0.973\H,0,3.66,-3.724,-0.36\H,0,2.813,-5.132,1.554\\Versio
-G98RevA.7\HF=-211.3897761\RMSD=5.875e-05\Dipole=-1.2378932
,-0.9017584\PG=C01 [X(C4H7N1)]\\@

Single point energy B3-LYP/6-31+G(d) on the AM1 structure

N-N= 1.593527754128D+02 E-N=-8.076963176455D+02 KE= 2.091856363231D+02
1\1\GINC-MS3\SP\RB3LYP\6-31+G(d)\C4H7N1\MARIE\27-Sep-2002\0\\# B3LYP/6
-31+G(D)\\I-H, after AM1 optimization, calcul of the B3LYP energy\\0,1
\C,0,1.069742,-0.001306,-0.093918\N,0,2.206107,-0.000638,0.151306\C,0,
-1.013513,1.250902,0.14559\C,0,-1.016003,-1.249617,0.145767\C,0,-0.350
266,-0.000054,-0.402446\H,0,-0.528607,2.166098,-0.270409\H,0,-2.093214
,1.255692,-0.138955\H,0,-0.938427,1.281701,1.258936\H,0,-0.940945,-1.2
80422,1.259121\H,0,-2.095711,-1.252266,-0.13872\H,0,-0.532947,-2.16584
2,-0.270142\H,0,-0.452662,-0.000042,-1.528932\\Version=x86-Linux-G98Re
vA.7\HF=-211.3886047\RMSD=6.512e-05\Dipole=-1.5999087,0.0004889,-0.295
9191\PG=C01 [X(C4H7N1)]\\@

Single point energy B3-LYP/6-31+G(d) on the DFT structure

N-N= 1.584143942891D+02 E-N=-8.058875758451D+02 KE= 2.092456560344D+02
1\1\GINC-MS5\SP\RB3LYP\6-31+G(d)\C4H7N1\MARIE\28-Feb-2003\0\\# B3LYP/6
-31+G(D)\\isobutyronitrile after DFT optimization\\0,1\C,0,-1.080435,-
0.001271,0.103349\N,0,-2.214814,-0.000744,-0.159696\C,0,1.022062,1.279
409,-0.149144\C,0,1.024677,-1.278048,-0.149326\C,0,0.350326,-0.000063,
0.41744\H,0,0.555492,2.180339,0.25983\H,0,2.084143,1.278921,0.116685\H
,0,0.930866,1.297689,-1.239572\H,0,0.933575,-1.296348,-1.239764\H,0,2.
086746,-1.275471,0.116537\H,0,0.559938,-2.180008,0.259472\H,0,0.453161
,-0.000072,1.510772\\Version=x86-Linux-G98RevA.7\HF=-211.3916476\RMSD=
5.703e-05\Dipole=1.6245526,0.0005507,0.3017126\PG=C01 [X(C4H7N1)]\\@

Claims to Original Research

1. The dissociation of gas-phase synthetic poly(butyl acrylate) and poly(vinyl acetate) were investigated by ESI-MS/MS [1,2].

2. The Dissociation of poly(vinyl acetate) ionized with lithium was investigated by molecular mechanics/molecular dynamics, semi-empirical and density functional theory calculation [1].

3. The monomer sequence of three copolymers produced by free radical polymerization (PBA/PVAc, PBA/PMMA and PMMA/PVAc) was investigate using tandem mass spectrometry [2].

[1] Giguère, M.-S. and Mayer, P. M., Climbing the internal energy ladder: energy deposition & the unimolecular decomposition of ionized poly (vinyl acetate). *Manuscript in preparation,* **2003**

[2] Giguère, M.-S.; Dubé, M. A. and Mayer, P. M., Sequencing synthetic copolymers using electrospray ionization tandem mass spectrometry. *Manuscript in preparation,* **2003**